5-2004

Contributions of Q67 and Y69 Residues to Ligand Binding and Catalysis in R67 Dihydrofolate Reductase

Lori Gail Stinnett
University of Tennessee - Knoxville

To the Graduate Council:

I am submitting herewith a dissertation written by Lori Gail Stinnett entitled "Contributions of Q67 and Y69 Residues to Ligand Binding and Catalysis in R67 Dihydrofolate Reductase." I have examined the final electronic copy of this dissertation for form and content and recommend that it be accepted in partial fulfillment of the requirements for the degree of Doctor of Philosophy, with a major in Biochemistry and Cellular and Molecular Biology.

Elizabeth E. Howell, Major Professor

We have read this dissertation and recommend its acceptance:

Richard Pagni, Cynthia Peterson, Daniel Roberts, Engin Serpersu

Accepted for the Council:

Carolyn R. Hodges

Vice Provost and Dean of the Graduate School

(Original signatures are on file with official student records.)

To the Graduate Council:

I am submitting herewith a dissertation written by Lori Gail Stinnett entitled "Contributions of Q67 and Y69 Residues to Ligand Binding and Catalysis in R67 Dihydrofolate Reductase." I have examined the final electronic copy of this dissertation for form and content and recommend that it be accepted in partial fulfillment of the requirements for the degree of Doctor of Philosophy, with a major in Biochemistry and Cellular and Molecular Biology.

Elizabeth E. Howell
Major Professor

We have read this dissertation
and recommend its acceptance:

Richard Pagni

Cynthia Peterson

Daniel Roberts

Engin Serpersu

Accepted for the Council:

Anne Mayhew
Vice Chancellor and Dean of
Graduate Studies

(Original signatures are on file with official student records.)

CONTRIBUTIONS OF Q67 AND Y69 RESIDUES TO LIGAND BINDING AND CATALYSIS IN R67 DIHYDROFOLATE REDUCTASE

A Dissertation
Presented for the
Doctor of Philosophy
Degree
The University of Tennessee, Knoxville

Lori Gail Stinnett
May 2004

Dedication

This dissertation is dedicated to several people who hold a special place in my heart. First, I would like to dedicate this dissertation to my parents who have supported me, prayed for me, and encouraged me throughout my life. I would also like to dedicate this dissertation to Chris West who also supported and prayed for me in addition to listening to me vent when things were not going well. This dissertation is also dedicated to my brothers (Tony, Chris, and Gary), my sister-in-laws (Jamie, Carrie, and Megan), and my nephew (Ethan) and niece (Lily) and soon-to-be nephew (Caleb). Finally, I would like to dedicate this dissertation in memory of my grandparents (Gentry Stinnett, Elsie Stinnett, Andy King, and Betty King) who are with the Lord.

Acknowledgments

I would like to acknowledge my major professor, Dr. Elizabeth Howell, for allowing me to complete my graduate research in her lab. Being a graduate student in her lab has provided me with valuable skills and knowledge that will be important as I continue to pursue my career as a scientist. I would also like to thank my committee for encouraging me to understand and defend my research. I admire each of my committee members as scientists and hope to someday reach such a level of understanding. I would also like to thank other faculty members who have served as professors and teaching and/or research mentors through my graduate career.

I would also like to acknowledge my lab and fellow BCMB graduate students. I want to thank Smiley for being patient with me (sometimes!!) when I would forget how to do an experiment, was afraid to use a new piece of equipment, or would drop an entire protein prep on the floor. I also want to thank him for discussing with me concepts on a level that even I could understand. I would like to thank Stephanie for spending countless hours with me helping me to understand my research and letting me vent when nothing was going right. I also want to thank both Smiley and Stephanie for helping me with my experiments. I owe so much to the both of you! I would also like to thank Sally and Michael for listening to my presentations and providing helpful suggestions. I would also like to thank my BCMB friends. I really appreciate their help, support, and friendship over these years.

Finally, I would like to thank my family and friends for supporting me, praying for me, and listening to me over these last five years. I could not have made it without their support.

Abstract

Dihydrofolate reductase (DHFR) serves an important role in metabolism by reducing dihydrofolate (DHF) to the product tetrahydrofolate via hydride transfer from NADPH. R67 DHFR, a plasmid encoded form of the enzyme which provides resistance to trimethoprim, functions as a homotetramer with D_2 symmetry. Both ligands, DHF and NADPH, interact within a 25Å active site pore. Mutagenesis of one active site residue results in four-symmetry related mutations causing large effects on binding and catalysis. A construct containing four copies of the DNA for R67 DHFR ligated in-frame and flanked by unique restriction sites was engineered and asymmetric mutants were built using this construct. Q67H asymmetric mutants were built with the goal of preserving tight binding without inhibition, as Q67H R67 DHFR binds both DHF and NADPH with greater affinity than the wild-type enzyme, but also yields severe DHF and NADPH inhibition [Park, H., Bradrick, T. D., and Howell, E. E. (1997) *Protein Eng. 10*, 1415-1424]. Although many of the Q67H asymmetric mutants bind NADPH with greater affinity than the control, inhibition is often observed. From these studies, a role for Q67 in selecting for the productive ternary complex over inhibitory complexes was proposed. Asymmetric Y69F mutants were also generated, as the k_{cat} for Y69F R67 DHFR is increased 2 fold compared to the wild-type enzyme, while the K_m values are increased [Strader, M. B., Smiley, R. D., Stinnett, L. G., VerBerkmoes, N. C., and Howell, E. E. (2001) *Biochemistry 40*, 11344-11352]. These asymmetric mutants were constructed with the goal of increasing k_{cat} while maintaining high affinity. Although this goal was not accomplished, these asymmetric mutants provided insight into ligand binding and catalysis in R67 DHFR as they support a model where *two* Y69 residues interact with

NADPH, while mutations along the dimer-dimer interface increasing k_{cat}. Thus, generating asymmetric mutants of R67 DHFR has provided a means by which to understand ligand binding and catalysis in a homotetrameric enzyme where only a single active site pore is available.

Table of Contents

Part **Page**

I. A Background to R67 Dihydrofolate Reductase.....1
Antibiotic Resistance and R-plasmid DHFRs.....2
DHFR: Metabolic Function.....3
DHFR: Ligand Structures.....3
R67 DHFR: Stereochemistry of Hydride Transfer.....6
R67 DHFR: Structure.....7
R67 DHFR: Ligand Binding in the Active Site.....7
R67 DHFR: Ligand Interactions in the Active Site.....10
R67 DHFR: Stereochemistry of the Transition State.....11
R67 DHFR: No Proton Donor.....11
R67 DHFR: Catalytic Mechanism.....13
R67 DHFR: Inhibitor Studies.....16
R67 DHFR: Residues Comprising the Active Site Pore.....16
R67 DHFR: "Hot Spot" Binding.....22
R67 DHFR: Electrostatic Interactions.....23
R67 DHFR: Other Catalytic Functions.....24
R67 DHFR: Generation of the Quad Construct.....24
Goal of Research Project.....31
References.....33

II. Breaking Symmetry: Mutations Engineered into R67 Dihydrofolate Reductase, a D_2 Symmetric Homotetramer Possessing a Single Active Site Pore.....36
Abstract.....37
Introduction.....38
Materials and Methods.....43
Results.....47
Discussion.....70
Acknowledgement.....80
Supporting Information Available.....80
References.....82
Appendix.....86

III. Determining the Role of Symmetry Related Y69 Residues in Ligand Binding and Catalysis in R67 Dihydrofolate Reductase.....90
Abstract.....91
Introduction.....92
Materials and Methods.....98
Results.....101
Discussion.....114
Acknowledgement.....123
References.....124

IV. R67 DHFR and Quad 3 DHFR, A Global Perspective.....….127
Catalytic Efficiency.....…128
Ligand Specificity.....….....…137
Selection of the Productive Ternary Complex.....….....…140
Quad 3 as a Template for Understanding Ligand Binding and Catalysis in R67 DHFR.....….....……142
R67 DHFR as a Template for "Evolving" an Enzyme Active Site.....….....….142
References.....151
Vita.....153

List of Tables

Part II **Page**

Table

1 A comparison of steady state kinetic values at pH 7.0 for numerous R67 DHFR constructs.....53

2 A comparison of wt R67 DHFR with Quad 3 using isothermal titration calorimetry to monitor ligand binding.....54

3 Binding of $NADP^+$ to the various DHFR species as monitored by ITC at pH 8.0.....57

4 Results of binding studies at pH 8.0 using isothermal titration calorimetry.....59

5 Ternary complex formation monitored by ITC.....63

6 A comparison of pK_a values describing titration of Quad 3 variants from a "closed" to an "open" form as monitored by fluorescence……...89

Part III **Page**

Table

1 A comparison of kinetic parameters for wild-type R67 DHFR, Quad 3 DHFR, Y69F asymmetric mutants, Y69L R67 DFFR, and Y69F R67 DHFR at pH 7.0.....……...103

2 Comparison of NADPH binding constants for Y69F asymmetric mutants and Y69L R67 DHFR as determined by isothermal titration calorimetry.....105

3 Comparison of pK_a values for Y69F asymmetric mutants……..112

Part IV **Page**

Table

1 Comparison of catalytic efficiencies for Q67H, Y69F, and K32M asymmetric mutants of Quad 3 DHFR…….....130

List of Figures

Part I **Page**

Figure

1 Metabolic pathway involving dihydrofolate reductase....4
2 Chemical structures of ligands recognized by DHFR including folate and NADPH…….....5
3 Front view of R67 DHFR crystal structure (protein data bank 1 VIE).....8
4 Proposed binding scheme for R67 DHFR.....15
5 Conolly surface map of R67 DHFR.....17
6 Proposed contacts between R67 DHFR active site residues and ligands.....18
7 Comparison of Quad gene constructs of R67 DHFR.....26
8 Schematic of "topology-switching" phenomenom.....28
9 Schematic of unique Q67H asymmetric mutants.....30

Part II **Page**

Figure

1 Top left: the ribbon structure of homotetrameric R67 DHFR (1VIE in the protein data bank).....42
2 Flowchart for construction of the quadrupled R67 DHFR genes.....48
3 Isothermal titration calorimetry analysis of DHF binding to Q67H:1+4 DHFR.....55
4 Steady state kinetic data for various R67 DHFRs.....65
5 A bar graph comparing cooperativity ratios for the various protein constructs.....73
6 A plot of entropy ($T\Delta S$) vs enthalpy (ΔH) for various mutants and ligands....79
7 Steady state kinetic data for Q67H:1+3 (top panel) and Q67H:1+4 R67 DHFRs (bottom panel)….....87
8 A series of fluorescence titration curves monitoring the equilibrium between "open" and "closed" forms of Quad 3 and its mutants.....88

Part III **Page**

Figure

1 A ribbon structure of R67 DHFR (protein data bank file 1VIE).....…...93
2 Isotherms for DHF binding to Y69F asymmetric mutants generated by isothermal titration calorimetry.....108
3 Comparison of CD spectra for Y69 mutants.....110
4 pH titrations for select Y69F asymmetric mutants.....111

Part IV **Page**

Figure

1 Ribbon diagram of R67 DHFR (protein data bank 1VIE) with Y69 residues shown as purple balls-and-sticks, while Q67 residues are shown as white balls-and-sticks.....131

Part I: A Background to R67 Dihydrofolate Reductase

Antibiotic Resistance and R-plasmid DHFRs

For several decades, drug companies have focused much attention on synthesis of antibiotics which specifically target microbial cells (*1*). Antibiotics have been designed to target several pathways in the microbial cell, ranging from pathways involved in generation of the cell wall to pathways involved in metabolism of folate (*2*). Along with the increase in use of the antibiotics came the realization that bacteria were able to acquire resistance mechanisms which rendered the antibiotics ineffective (*1*). Although several such resistance mechanisms have since been discovered, one particularly interesting mechanism was identified in the 1970s in patients with bacterial infections whose treatment involved use of the antibiotic trimethoprim (TMP) (*3-7*). In these studies, chromosomal (bacterial) dihydrofolate reductase (DHFR), an enzyme involved in folate metabolism, was the antibiotic target (*3-7*). Bacterial cells resistant to TMP were found to contain an R-plasmid (or resistance plasmid) which afforded the resistance mechanism. Interestingly, the R-plasmid contains the gene for a form of DHFR which was not susceptible to TMP. Since the plasmid-encoded enzyme catalyzed the same reaction as the chromosomal enzyme, bacterial cells were able to survive in the presence of TMP even though their own DHFR was inhibited (*5*, *6*).

Subsequent studies have determined that several distinct R-plasmid encoded DHFRs exist. These R-plasmids have been categorized based on amino acid sequence comparisons into 5 groups designated A-E. Of these five groups, one group, C, is particularly interesting in that the amino acid sequences of members of this group are rather dissimilar from those of the other groups ((*8*) and references therein). Group C

consists of R-plasmid DHFRs classified as Type II DHFRs (*8*). Type II DHFRs are also interesting from a clinical perspective due to their lack of sensitivity to TMP (*9, 10*).

One R-plasmid DHFR of particular interest in our laboratory is R67 DHFR. R67 DHFR is classified as a Type II R-plasmid encoded enzyme, distinguished along with other Type II enzymes by its lack of sensitivity to TMP (*9*). Surprising to researchers at the time of its discovery is that the enzyme shares no genetic homology with any dihydrofolate reductases (*10*). Interestingly, studies also indicated that R67 DHFR exists as a homotetramer (*7*).

DHFR: Metabolic Function

What functional role does DHFR play in metabolism? Dihydrofolate reductase catalyzes the transfer of a hydride ion from the cofactor, NADPH, to the substrate, 7,8-dihydrofolate, forming 5,6,7,8-tetrahydrofolate. This reaction is illustrated in Figure 1. It plays an important role in single-carbon metabolism, a pathway important in generation of purine nucleotides as well as other metabolites. As such, the enzyme's function is important to the survival of the cell. Thus, dihydrofolate reductases have been the target of both antibiotic as well as anti-cancer drugs (*11*).

DHFR: Ligand Structures

Chemical structures for the ligands, NADPH and folate, are shown in Figure 2. Both NADPH and NADH are composed of the following moieties: an adenine ring, two ribose rings connected by a pyrophosphate bridge, and a nicotinamide ring. The chemical reaction, or hydride transfer, occurs at the C4 (carbon four) position of the nicotinamide ring. NADH and NADPH are distinguished by the presence of a phosphate group at the 2′ position of the ribose ring (adjacent to the adenine ring) in NADPH that is

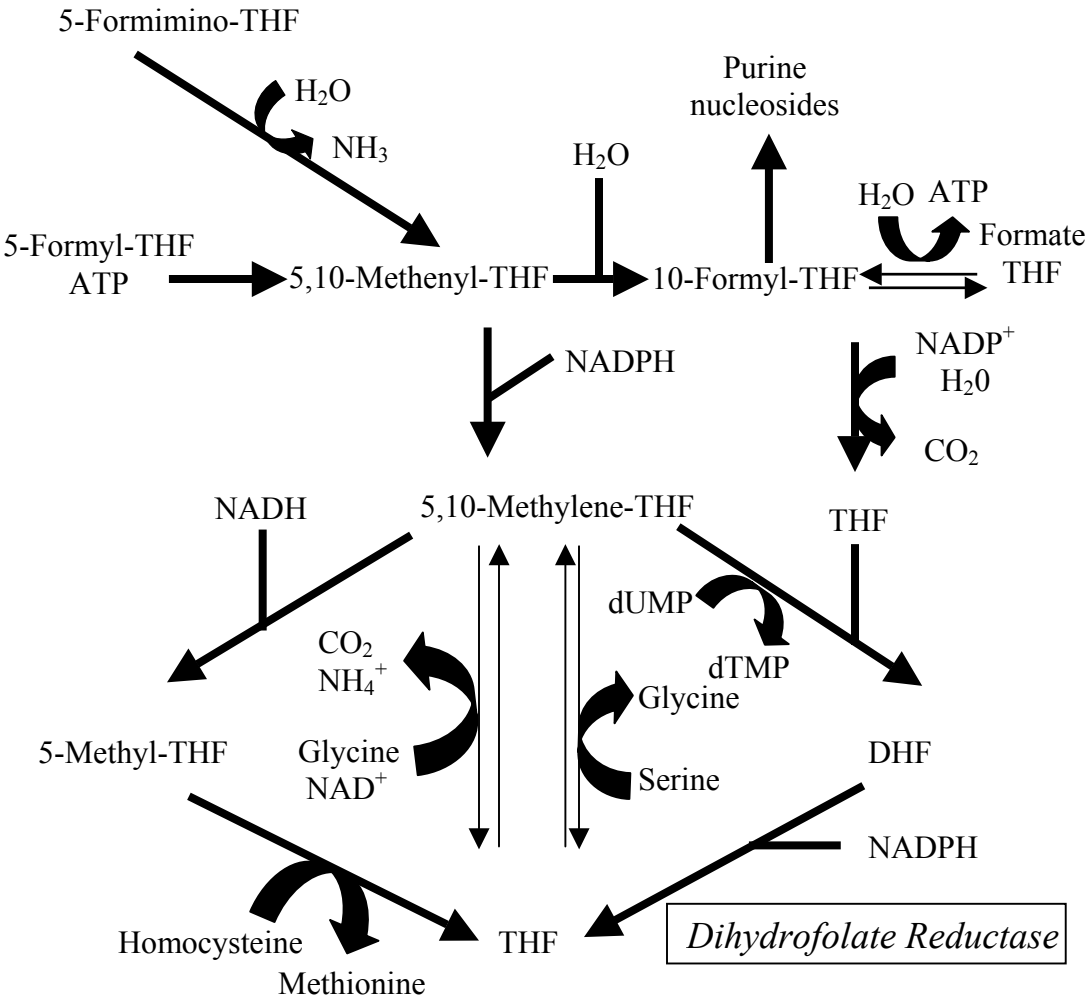

Figure 1. Metabolic pathway involving dihydrofolate reductase. Modified from (*11*).

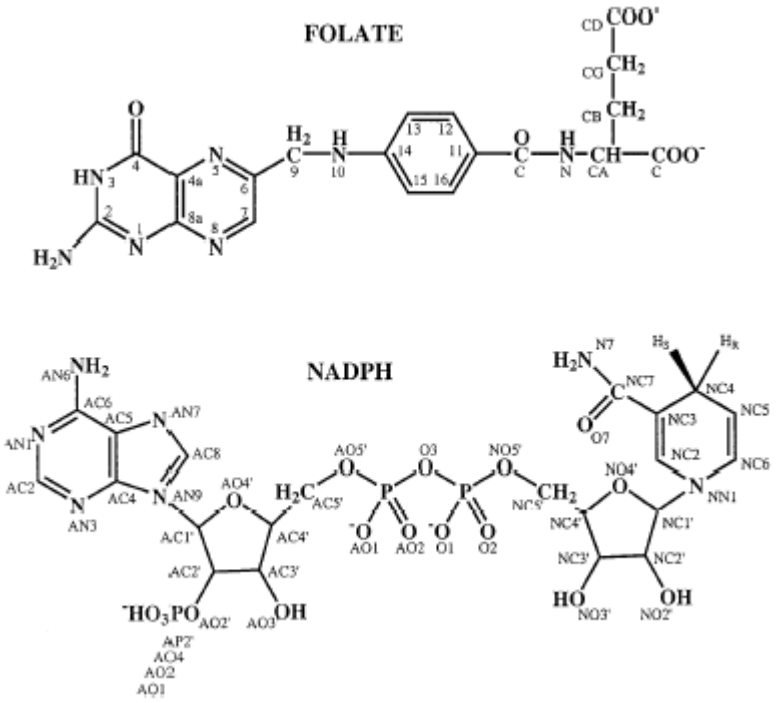

Figure 2. Chemical structures of ligands recognized by DHFR including folate and NADPH. Taken from (*12*).

not present in NADH. Instead, the ribose ring of NADH is unmodified, containing a hydroxyl group at its 2′ position (*11*). DHF and folate are composed of a pteridine ring, a *para*-aminobenzoic acid moiety (pABA), and a glutamic acid moiety (*12*). For both DHF and folate, the chemical reaction occurs on the pteridine ring. DHF and folate are distinguished by a reduction of folate's C7-N8 (carbon seven-nitrogen 8) double bond generating DHF. DHFR catalyzes the reduction of both folate to 7,8-DHF as well as the reduction of 7,8-DHF to 5,6,7,8-tetrahydrofolate (*11*). However, in R67 DHFR, the efficiency of the former is greatly reduced in comparison to the latter (Howell, personal communication). For comparative purposes, the pyrophosphate-ribose-adenine moieties of NADPH will be referred to as the NADPH tail while the ribose-nicotinamide moieties will be referred to as the NADPH head. Similarly, the pteridine ring of DHF will be referred to as the DHF head and the pABA-glutamic acid moieties will be referred to as the pABA-glu tail (*12*).

R67 DHFR: Stereochemistry of Hydride Transfer

In oxidoreductase reactions, hydride transfer from NADPH or NADH to the ligand is stereospecific. Dehydrogenases are often categorized as being either A-specific or B-specific based on the stereochemistry of the transfer. A-specific dehydrogenases catalyze the transfer of the pro-R hydrogen at carbon-4 of NADPH (or NADH) to the ligand. In contrast, B-specific dehydrogenases catalyze the transfer of the pro-S hydrogen at carbon-4 of NADPH (or NADH). The two classes of enzymes are also distinguished in respect to the orientation of the cofactor within the active site. In A-specific dehydrogenases, the ribonicotinamide bond is located in an orientation anti to the carbon-3 amide substituent of the nicotinamide moiety. This orientation is syn for B-

specific dehydrogenases ((*13*) and references therein). For R67 DHFR, isotope studies where the kinetics of hydride transfer are monitored when NADPD is substituted for NADPH indicate that the pro-R hydrogen is transferred during the reaction (*14, 15*). However, in contrast to other dehydrogenases, NMR studies suggest that the ribonicotinamide bond is in a syn conformation in the active site (*16*).

R67 DHFR: Structure

The first crystal structure solved for the R67 DHFR was that of the dimer (*17*). Chymotrypsin cleavage of the first 16 amino acids of each monomer (*18*) facilitated crystallization of the active form of the enzyme, the homotetramer (*19*). This structure, illustrated in Figure 3, indicates that R67 DHFR is a D_2 symmetric enzyme possessing 222 symmetry. Structural evidence also indicates that the enzyme is a β-barrel protein where each monomer is composed of five β-strands in an antiparallel orientation. Assembly of each of the four monomers yields a 25Å pore that extends through the center of the enzyme. Two pairs of symmetry-related glutamine 67 residues hydrogen-bond generating a "floor" and "ceiling" to the pore (*19*).

R67 DHFR: Ligand Binding in the Active Site

In addition to the crystal structure for the apoenzyme, a crystal structure has also been solved for an enzyme-folate complex. In this structure, the pteridine ring of one folate molecule (designated FolI) interacts near the pore's center such that its *si* face is available for hydride transfer. A second folate molecule (designated FolII) binds further out from the pore's center in an orientation that prevents access to its *si* face for hydride transfer. In contrast to the electron density observed for the pteridine rings for FolI and FolII, diffuse electron density is observed for the pABA-glu tails of the two molecules.

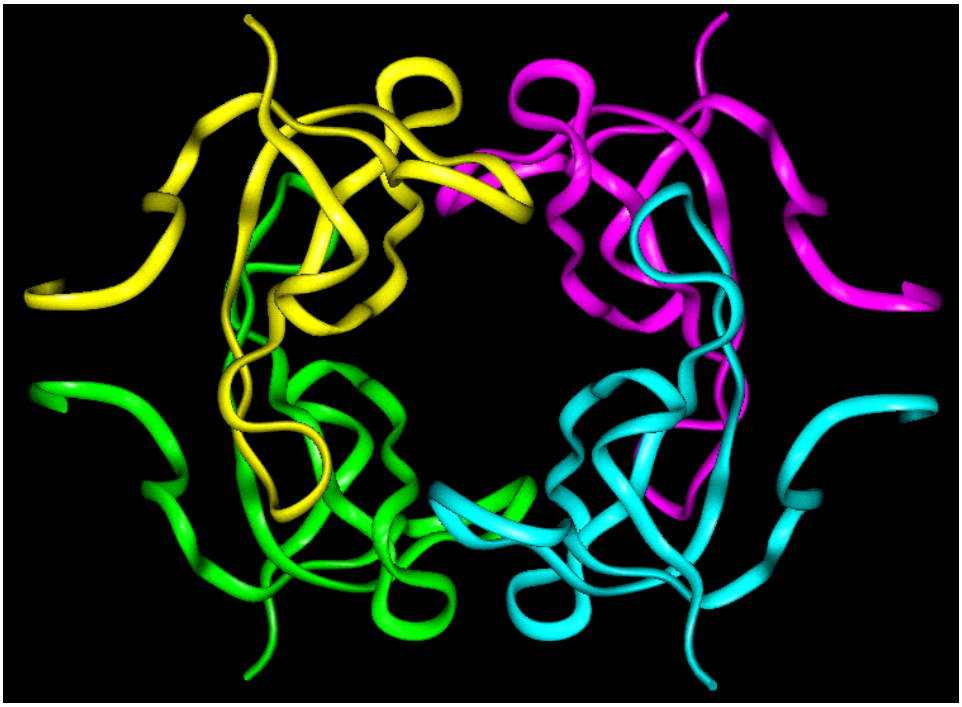

Figure 3. Front view of R67 DHFR crystal structure (protein data bank 1VIE). Monomers were originally labeled clockwise as ABDC and have been relabeled 1234, where monomer 1 is green, monomer 2 is yellow, monomer 3 is magenta, and monomer 4 is cyan.

This density orients the two pABA-glu tails in opposite directions away from the pore's center. The lack of a strong electron density for the tails suggests that the tails lack specific contacts with the enzyme's active site (*19*). These data are supported by docking studies using the computer programs DOCK version 4.0 and SLIDE version 1.1 (*12*). In these studies, the substrate, folate, was docked into the highest scoring enzyme·NMN (nicotimamide mononucleotide) complex where the stereochemistry of hydride transfer from NMN was A-side. (NMN contains the nicotinamide ring, ribose ring, and one phosphate group of the NADPH pyrophosphate bridge.) In most high scoring predictions using this software, FolI docked in an orientation similar to that observed in the crystal structure. However, the docked location of the pABA-glu tail was not consistent within the highest scoring conformers corresponding to the observed diffuse electron density in the crystal structure. These data suggest that the pABA-glu tail displays some degree of mobility within the active site (*12, 19*). Li et al. (*16*) propose that positive transferred nuclear Overhauser interactions observed only for the glutamate tail of folate support such a model.

In contrast to folate, no crystal structure has been determined for NADPH or an NADPH moiety (such as NMN) bound to R67 DHFR. However, NMR studies have provided some insight into NADPH binding in the active site of R67 DHFR. Although no specific bonding interactions between the enzyme and cofactor were identified, shifts in protein amide resonances upon cofactor ($NADP^+$) binding implicate several amino acids as being involved in ligand binding. Residues proposed by other studies to line the active site (*12, 19, 20*) were most often associated with the greatest chemical shift changes upon ligand binding (*21*).

R67 DHFR: Ligand Interactions in the Active Site

NMR studies have provided information regarding how the ligands bind within the active site. In these studies, intraligand interactions are determined by transferred nuclear Overhauser effects (NOE's). Positive transferred NOE's for the glutamic acid tails of two folate molecules bound within the active site are observed. Interestingly, in the same complex, negative tNOE's for the pABA and pteridine moieties of folate are noted. Combined, these data suggest that the tail mobile within the active site. In contrast, transferred NOE studies suggest that NADPH binds where the bond between the ribose and nicotinamide rings is syn while the bond between the ribose and adenine rings is anti (*16*).

NMR studies have also revealed information regarding interactions between NADPH and DHF, or interligand interactions, in the active site. These interactions are distinguished by studies involving interligand Overhauser effects (ILOE's) (*16*). Based on the enzyme-folate complex determined by x-ray crystallography, Narayana et al. (*19*) originally hypothesized that NADPH's nicotinamide ring would interact between glutamine 67 residues comprising the "ceiling" of the enzyme and FolI bound in close proximity to the "floor" of the enzyme. Thus, both DHF and NADPH would bind in a single half of the active site pore (*16, 19*). In such an orientation, strong interligand interactions should occur between the pABA moiety of DHF and the nicotinamide ring of NADPH. These interligand interactions were not observed by NMR studies suggesting that such an arrangement of ligands within the active site is unlikely. In contrast, the ILOE data suggest that the nicotinamide and pteridine rings bind near the pore's center

allowing the tail moieties of NADPH and DHF to project away from one another toward opposite halves of the active site pore (*16*).

R67 DHFR: Stereochemistry of the Transition State

Quantum-mechanical/molecular-mechanical studies have been employed to predict the orientation of the pteridine ring of DHF and the nicotinamide ring of NADPH during catalysis. In vacuo studies suggest that two transition state stereochemistries are possible, an *endo* transition state and an *exo* transition state (*22*). Of the two possible transition states, an *endo* transition state yields the greatest overlap of the highest occupied molecular orbitals and lowest unoccupied molecular orbitals (*23*). As a result, the *endo* transition state is proposed to be 2-8 kcal/mole more stable than the *exo* transition state (*22*). Addition of the active site environment to the calculations for *E. coli* DHFR, however, suggests that in this enzyme catalyzed reaction, the *exo* transition state is favored. Thus, active site interactions allow a transition state, less thermodynamically favored in vacuo, to be approached in the enzyme active site (*22*). In contrast to *E. coli* DHFR, ILOEs for a folate-$NADP^+$-enzyme complex for R67 DHFR support the use of an *endo* transition state for this enzyme (*16*).

R67 DHFR: No Proton Donor

Originally, it was proposed that an ionizable moiety is involved in the catalytic mechanism for R67 DHFR as a non-linear pH versus rate profile was observed for the enzyme. The pK associated with the pH versus velocity plot was determined to be 5.8 (*18*). It was therefore proposed that ionization of symmetry-related histidine 62 residues, located along the dimer-dimer interface of R67 DHFR, may be involved in catalysis. However, gel filtration studies indicated that at pH 5, the elution profile of the enzyme

represented that of a dimer, whereas at pH 8, the elution profile represented that of a tetramer (*24*). In addition, steady-state kinetic analysis of dimeric H62C R67 DHFR treated with DEPC indicated that the catalytic efficiency of the dimer is affected 200-600 fold. These studies indicate that the "bell-shape" nature of the pH versus activity plot is therefore due to a disruption of the active tetrameric protein into a less active or inactive dimeric protein at acidic pH values (around pH 6) (*24*).

What causes the > 100 fold increase in catalytic activity as pH is decreased from ~10 to ~7 in R67 DHFR (*18*)? Comparisons with *E. coli* DHFR led to the suggestion that a proton donor other than histidine 62 may be involved in catalysis. In *E. coli* DHFR, aspartic acid 27 is proposed to provide a proton to dihydrofolate during catalysis. Mutagenesis studies where this residue is replaced with a serine result in a decrease in k_{cat} for the reaction (*25*).

Does R67, like *E. coli* DHFR, have a proton donor (*26*)? For R67 DHFR, symmetry-related tyrosine 69 residues are the only amino acid residues with dissociable side chains within the proposed active site that may provide a proton to DHF during catalysis. However, pH versus rate profiles for R67 DHFR indicated that no ionization effects are observed around pH 9.5-10, the solution pK of tyrosine (*26*). Titration of a non-dissociable R67 DHFR mutant (H62C R67 DHFR) with acid yielded a linear pH versus rate profile, where k_{cat} increases as pH decreases. Based on these studies, it was determined that, in contrast to *E. coli* DHFR, there is no proton donor in R67 DHFR, and the substrate must be pre-protonated for the reaction to occur (*26*).

R67 DHFR: Catalytic Mechanism

Prior to ligand binding and x-ray crystallography studies, it was proposed that due to the symmetry of R67 DHFR, four ligands could potentially bind within the large active site pore (*27, 19*). However, x-ray crystallography studies suggest that a total of two folate molecules associate with the enzyme, where steric effects prevent four from binding (*19*). In addition, ligand binding studies using isothermal titration calorimetry and fluorescence anisotropy suggest that steric effects allow a limit of two ligands to bind within the active site. This includes two non-productive complexes where two NADPH or two DHF molecules interact with the enzyme. A single productive, ternary complex forms when one NADPH and one DHF molecule interact in the active site (*19*).

In addition to the stoichiometric data obtained from these studies, isothermal titration calorimetry studies also provided information regarding interaction between ligands within the active site, in particular, their *cooperative* behavior (*27*). When the binding of one ligand in the active site affects the binding of a second ligand within the active site, the two ligands are said to be cooperative. Two types of cooperativity are possible based on the nature of the interactions within the active site. If one molecule binds in a manner that requires the second ligand to display a weaker affinity to the enzyme, the *interligand interaction* is negatively cooperative. In contrast, if the binding of the first ligand allows the second ligand to bind more tightly, the interaction is positively cooperative. Cooperativity patterns between two ligands can be determined by dividing the dissociation constant for the second ligand binding event by the dissociation constant for the first ligand binding event (i.e. K_{d2}/K_{d1}) (*20*, *27*). When the K_{d2}/K_{d1} value is greater than one, the pattern reflects positive cooperativity. However, when the value

is less than one, the pattern of ligand binding suggests negative cooperativity. If no inter-ligand cooperativity occurs (i.e. the ligands bind independently of one another), a value of one is expected (*20*, *27*).

Comparison of the K_d values for the first and second NADPH binding events in R67 DHFR yielded a K_{d2}/K_{d1} value less than one, suggesting that the two NADPH molecules interact in a negatively cooperative fashion within the active site (*27*). To explain this pattern of cooperativity, it was suggested that the first NADPH molecule interacts with the enzyme close to the pore's center. This binding was proposed to prevent tight binding of a second NADPH molecule in a symmetry related site through steric or electrostatic interactions. In contrast, comparisons of the binding affinities for two DHF/folate molecules within the active site indicated that these ligands display positive cooperativity. It was therefore suggested that the first DHF/folate molecule binds with weak affinity within the active site. However, the second DHF molecule interacts with both the enzyme and the already bound DHF/folate molecule resulting in an increased binding affinity. In addition, interactions are also proposed to occur between NADPH and DHF, bound in the productive, ternary complex. Specifically, it is proposed that positive cooperativity occurs between NADPH and DHF that allows DHF to bind with a greater affinity in the productive complex (*27*). These studies, in addition to steady-state kinetic studies for wild-type R67 DHFR (*18*), have allowed a mechanism for catalysis to be proposed. A diagram of this mechanism is shown in Figure 4. Based on these studies, it is proposed that R67 DHFR can follow a random bi-substrate mechanism, but favors a pathway where NADPH interacts with the enzyme first followed by DHF (based on the K_d values and cooperativity patterns). Cooperativity patterns

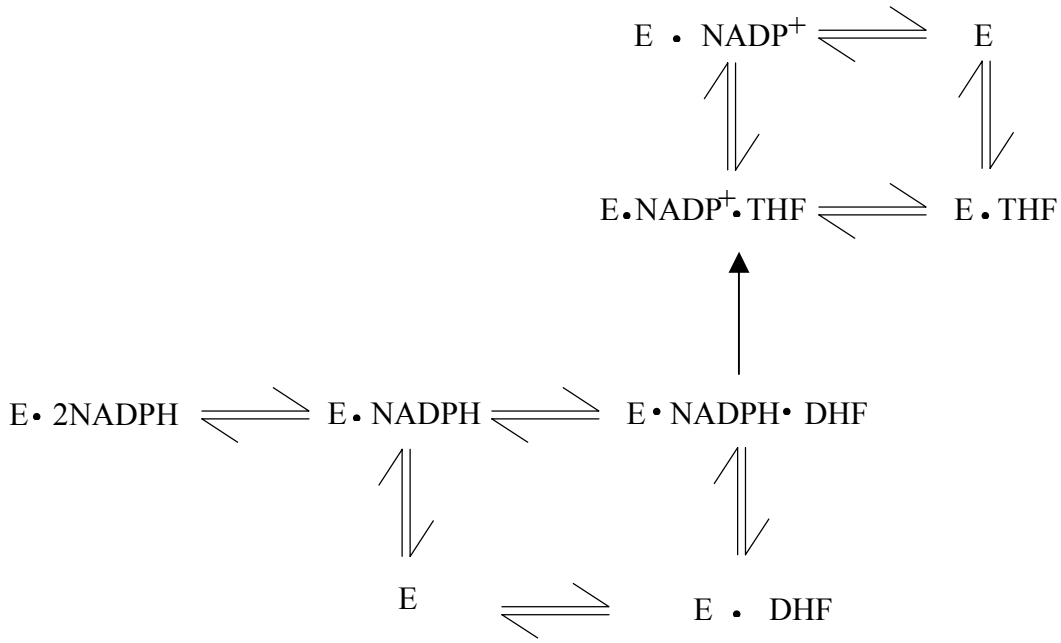

Figure 4. Proposed binding scheme for R67 DHFR. Double arrows represent events in equilibrium while the single arrow represents the rate-determining step for the enzyme catalyzed reaction. Taken from (*27*).

between two bound NADPH molecules and two bound DHF molecules disfavor their formation in comparison to the active ternary complex. Thus, substrate and cofactor inhibition are not detected for R67 DHFR (*18, 27*). Kinetic isotope studies using NADPD also show an isotope effect of 3 indicating that the hydride transfer step is rate-limiting (*14*).

R67 DHFR: Inhibitor Studies

In order to better understand the mechanism of R67 DHFR, inhibition studies were performed. In these studies, no inhibition by DHF or NADPH was detected while only minor inhibition by tetrahydrofolate was detected. The substrate, folate, displayed competitive inhibition with respect to DHF and noncompetitive inhibition with respect to NADPH. $NADP^+$ was competitive with respect to NADPH and para-uncompetitive with respect to DHF. Based on these inhibitor studies as well as isotope effects indicating that hydride transfer is the rate-limiting step for the reaction, it was proposed by Morrison and Sneddon that R67 DHFR follows a "Bi-Bi rapid equilibrium, random mechanism" (*15*).

R67 DHFR: Residues Comprising the Active Site Pore

Docking studies predict that several residues near the active site pore may be involved in binding DHF and/or NADPH. These include lysine 32, serine 65, valine 66, glutamine 67, isoleucine 68, and tyrosine 69 (*12*). The crystal structure for R67 DHFR where the active site residues are highlighted is shown in Figure 5. The proposed contacts between the active site residues and specific moieties of the substrate and cofactor based on docking predictions are illustrated in Figure 6. In attempts to better understand how these active site residues are involved in ligand binding and catalysis, site-directed mutagenesis studies have been performed, and the mutants have been

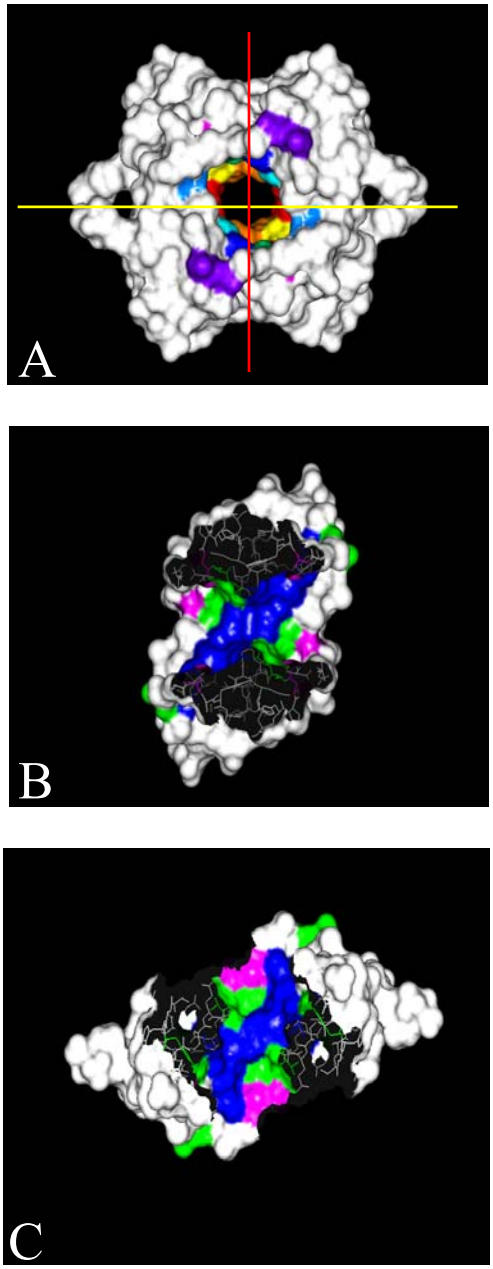

Figure 5. Conolly surface map of R67 DHFR. Active site residues affecting ligand binding and/or catalysis are highlighted in blue. Residues in green have minimal affects on ligand binding and catalysis, while magneta residues are important for dimer-dimer interactions. Panel A shows a front view of the Conolly surface map. Panel B shows a view of a single dimer interface generated by dissecting the tetramer in half along the dimer-dimer interface. Panel C is a view of a single monomer interface generated by dissecting the tetramer in half along the monomer-monomer interface. Taken from (*30*).

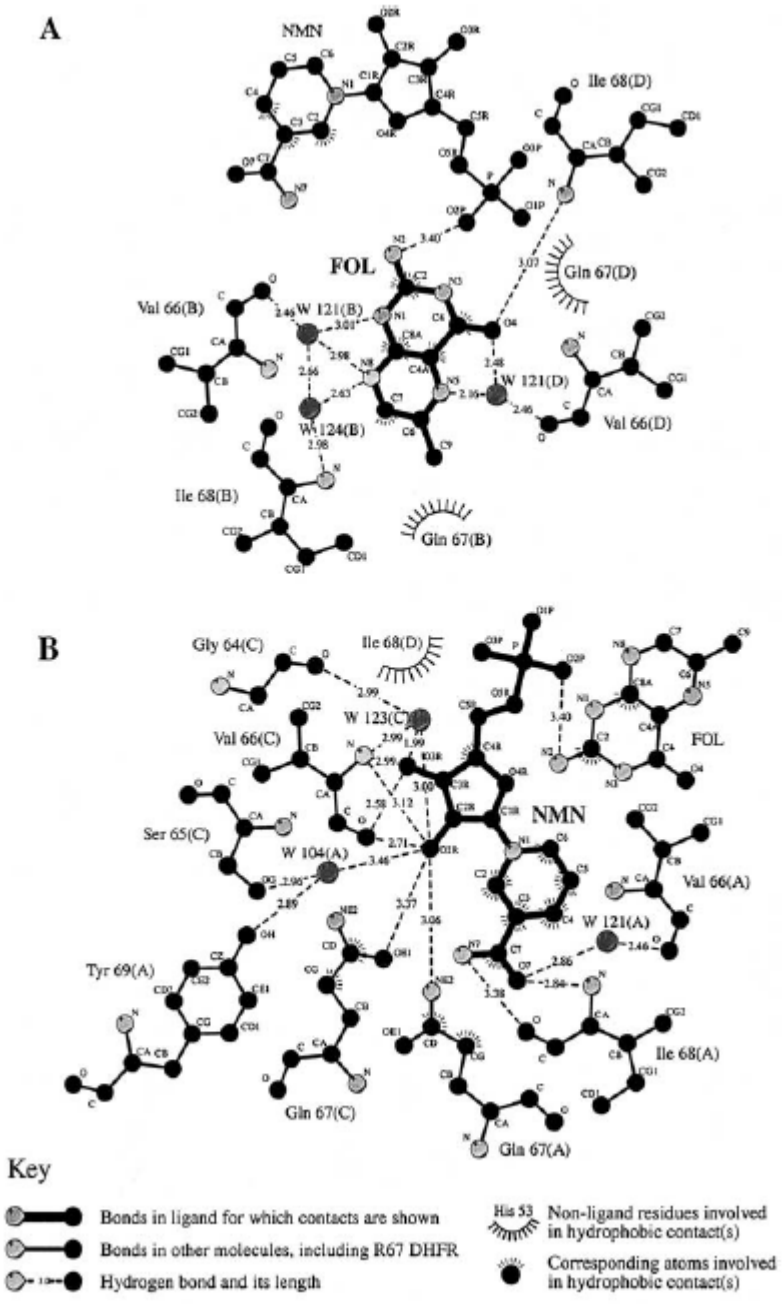

Figure 6. Proposed contacts between R67 DHFR active site residues and ligands. Taken from (*12*).

characterized (*20, 28, 29*). For clarity, the proposed interactions for each of these residues will be described followed by the effects of mutagenesis on ligand binding and catalysis.

Lysine 32

Docking studies suggest that lysine 32 may provide contacts to the glutamate moiety of DHF. In addition, these studies indicate that a symmetry-related lysine 32 may also provide binding contacts to the 2′ phosphate moiety of the cofactor (*12*). Lysine 32 was therefore mutated to methionine. However, K32M R67 DHFR was unable to be characterized kinetically and thermodynamically since the mutations resulted in a dimer (*28*). This residue will be considered later as the electrostatic potential of the enzyme is discussed.

Serine 65

No direct interactions are predicted between serine 65 and either NADPH or DHF. However, docking studies do predict that the –OH group of serine 65 may interact via a water mediated hydrogen bond with a ribose hydroxyl group and with a phosphate oxygen of NMN (*12, 20*). No specific interactions between serine 65 and folate were predicted by docking studies. However, since the hydroxyl group of the residue is directed toward the active site, a potential role in hydrogen bonding interactions with the ligand was also proposed (*12, 20*). Serine 65 was mutated to alanine residue to remove its potential for hydrogen bond formation through its side chain. S65A displayed similar kinetic and thermodynamic characteristics to that of the wild-type enzyme. These data suggest that either the serine hydroxyl group is not involved in binding DHF and NADPH or that the interactions are not direct (*12*, *20*).

Glutamine 67

Symmetry-related glutamine 67 residues are proposed to play an important role in definition of the active site architecture as x-ray crystallographic data indicate that they contribute the "floor" and "ceiling" to the active site (*19*). Docking studies also indicate that these residues play an important role in binding interactions with both NADPH and DHF. Specifically, it is proposed that hydrogen bonding interactions between a glutamine 67 side chain and a ribose hydroxyl group of NMN occur. In addition, it is predicted that van der Waals contacts between glutamine 67 and the nicotinamide moiety of NMN occur. Similar interactions are proposed between symmetry-related glutamine 67 residues and the folate's pteridine ring (*12, 20*). Symmetry-related glutamine 67 residues were mutated to histidine residues to generate Q67H R67 DHFR (*29*) and to cysteine residues to generate Q67C R67 DHFR (*20*). These mutations both resulted in a slower k_{cat} for the reaction. However, the two mutations had opposite effects on $K_{m(DHF)}$ and $K_{m(NADPH)}$. For Q67H R67 DHFR, $K_{m(DHF)}$ is ~ 25 fold tighter than the wild-type value while the $K_{m(NADPH)}$ is ~ 100 fold tighter than R67 DHFR. In contrast, the $K_{m(DHF)}$ for Q67C R67 DHFR increased ~ 9.5 fold while the $K_{m(NADPH)}$ increased ~ 9 fold. These studies suggest that symmetry-related glutamine 67 residues play a role in binding NADPH and DHF (*12*, *20*, *29*).

Isoleucine 68

Docking studies predict that backbone amide and carboxyl moieties of isoleucine 68 interact with the nicotinamide ring of NMN while van der Waals contacts are also predicted between the residue and NMN. In addition, the backbone amide of I68 is also predicted to interact via a hydrogen bond with the pteridine ring of folate. A water

mediated interaction between the backbone amide of another isoleucine 68 and the pteridine ring of folate is proposed as well (*12, 20*). Therefore, symmetry-related I68 residues were mutated in two different experiments to leucine and methionine generating I68L R67 DHFR and I68M R67 DHFR, respectively (*20*). In both mutants, the $K_{m(DHF)}$ values were increased ~ 4 fold while the $K_{m(NADPH)}$ values were increased ~ 7-9 fold. Both mutations also resulted in a decrease in k_{cat} for the reaction, with the I68M mutant having the most dramatic effect. Ligand binding studies were also conducted for I68L R67 DHFR to determine the effects of the mutations on binding of NADPH to the enzyme using isothermal titration calorimetry. In these studies, the binding of the first NADPH is increased ~ 10 fold while the binding of the second NADPH is increased ~ 5 fold. These data suggest that symmetry-related I68 residues comprise the binding sites for both NADPH and DHF (*12*, *20*).

Tyrosine 69

Docking studies predict formation of two types of interactions between Y69 and NMN. These include a water mediated hydrogen bond between the hydroxyl of the residue and a phosphate oxygen of NMN as well as van der Waals contacts between the ring edge of the residue and ribose hydroxyl groups of NMN. A possible interaction between tyrosine 69 and folate has also been proposed from docking studies. Specifically, a hydrogen bonding interaction is predicted between the hydroxyl of the amino acid and the glutamate tail of the ligand (*12, 20*). Thus, symmetry-related Y69 residues were mutated to either phenylalanine residues to generate Y69F R67 DHFR or to histidine residues to generate Y69H R67 DHFR (*20*). Both mutations increased the $K_{m(DHF)}$ to a similar extent, ~ 8 fold. However, the histidine mutations had a more

dramatic effect on the $K_{m(NADPH)}$ value, with a value ~ 59 fold greater than the wild-type enzyme versus the 22 fold greater value observed for Y69F R67 DHFR. Interestingly, the effects on k_{cat} were also unique. For Y69F R67 DHFR, the k_{cat} was increased > 2 fold while the reaction rate for Y69H R67 DHFR was ~ 100 fold slower than the wild-type enzyme. Again, these data suggest that Y69 residues comprise a portion of the binding sites for both DHF and NADPH (*12*, *20*).

R67 DHFR: "Hot Spot" Binding

Site-directed mutagenesis studies of homotetrameric R67 DHFR as well as docking studies suggest that R67 DHFR may display a "hot spot" binding mode (*12, 20*). "Hot spot" or "consensus" binding modes are often observed in proteins which recognize more that one unique ligand or "partner" (*31*). For example, immunoglobulin G (IgG) recognizes several unique protein scaffolds. Comparing the interactions between IgG and each of the protein partners reveals that several IgG residues are involved in interactions with each of the scaffolds. In particular, a surface is formed by those residues commonly involved in the interactions. In the IgG surface, the residues comprising the surface have a large degree of hydrophobicity (*31*). However, other "hot spots" are recognized by their amphipathic character (*12, 20*). Such is the case for R67 DHFR. In this enzyme, several of the residues proposed to comprise the active site also display some amphipathic character. For example, the side chain of tyrosine 69 is composed of a hydrophobic ring as well as a polar hydroxyl group. Although the R-chains of valine 66 and isoleucine 68 are non-polar, their amide and carbonyl backbone moieties provide polar character since they are also appropriately positioned for interactions with the ligands. In addition, the symmetry of R67 DHFR is important for this "hot spot" binding

mode as docking studies indicate that symmetry related residues may play a role in binding both ligands. These studies also suggest that the binding sites for the two ligands share some degree of overlap. Based on these characteristics, R67 DHFR is proposed to have a "hot spot" binding mode (*12*).

R67 DHFR: Electrostatic Interactions

An electrostatic potential map for R67 DHFR was constructed with the program, DELPHI. These studies indicate that the active site of R67 DHFR is positively charged (*12*). Since both NADPH and DHF are negatively charged, it was suggested the positive charge character of the enzyme draws the ligands towards the active site (*12, 28*). A large portion of the positive potential is generated by two adjacent residues, lysine 32 and lysine 33. In addition to generating a positive electrostatic potential, docking studies also suggest that symmetry-related lysine 32 residues facilitate binding of both DHF and NADPH by participating in electrostatic contacts (*12*). In order to assess the involvement lysine 32 in ligand binding and catalysis, this residue was mutated to both polar and nonpolar residues. Unfortunately, each of the cells expressing these mutants was TMP sensitive. K32A and K32M were further characterized and both decreased the stability of the tetramer resulting in inactive dimers. Studies involving K33M indicate that it is active and tetrameric. In fact, this mutant is similar to wild-type R67 DHFR both kinetically and thermodynamically. It was therefore proposed that this residue contributes only weakly to ligand binding and catalysis (*28*).

To indirectly address the role of K32 residues in ligand binding and catalysis, salt studies were performed on R67 DHFR as well as the K33M mutant. In these studies, increasing concentrations of salt in the buffer medium should interfere with ionic contacts

formed between K32 and the ligands. In these experiments, K_m values for both ligands increased linearly as the amount of salt in the buffer was increased. The same trend was observed for the k_{cat} for the reaction. In addition, ligand binding for both folate and NADPH was affected by increasing salt concentrations. Based on these studies, it was suggested that K32 forms contacts with the pyrophosphate bridge and 2′ phosphate of NADPH. In addition, these studies indicate that an ionic interaction must be disrupted in order to approach the transition state for the reaction (*28*).

R67 DHFR: Other Catalytic Functions

In addition to catalyzing the reduction of DHF to tetrahydrofolate, NMR studies suggest that R67 DHFR may catalyze two other reactions. One alternate activity of R67 DHFR is that of a phosphatase. Specifically, it has been indicated that R67 DHFR catalyzes the conversion of $NADP^+$ to NAD^+ over time. This side reaction is however slow (on the order of hours) compared to the catalytic activity of other enzymes (*21*).

In addition to its phosphatase activity, NMR studies also indicate the ability of R67 DHFR to catalyze a transhydrogenase reaction. This reactivity stems from the enzyme's ability to bind NADPH and $NADP^+$ simultaneously in a non-productive complex (in respect to the enzyme's dehydrogenase activity). These studies indicate that the enzyme is able to facilitate the transfer of a hydride from the reduced cofactor to the oxidized cofactor to an extent (*21*).

R67 DHFR: Generation of the Quad Construct

Since R67 DHFR is a tetramer formed by the interaction of four identical monomers, site-directed mutagenesis of the gene coding for the monomer results in four symmetry-related mutations in the tetramer. This often has large effects on both ligand

binding and catalysis. Specifically, binding affinities of both DHF and NADPH are often both affected by the mutations (*20, 28*). Bradrick et al. (*27*) approached this problem by generating the Quad 1 construct which contains four copies of the DNA for the monomer associated in-frame. A schematic of this construct is shown in Figure 7. The linker region between each of the gene copies is the DNA coding for the first 17 amino acids of the monomer (*32*). These residues are not ordered in the crystal structure for the dimeric enzyme and were cleaved facilitating crystallization of the tetramer (*17, 19*). In addition, chymotrypsin cleavage of the first 16 residues does not alter enzyme activity (*18*). Quad 1 was characterized and compared to wild-type R67 DHFR to ensure that linking the genes had not affected protein structure and/or enzyme activity. Steady-state kinetic parameters for the two enzymes were similar suggesting that linking the genes had not affected enzyme activity. In contrast to wild-type R67 DHFR, Quad 1 was unable to regain full activity upon refolding following unfolding with guanidine hydrochloride at pH 8. Quad 1, since it is monomeric, is also unable to dissociate into dimers following titration with hydrochloric acid. However, titration can cause the subunits of the monomer to "splay out" as symmetry-related histidine 62 residues are protonated. Interestingly, these titrations yield a pKa value for symmetry-related histidine 62 residues in Quad 1 which is decreased (~ 5.5) with respect to that for R67 DHFR (~ 6.8). Although these differences between Quad 1 and R67 DHFR were noted, Quad 1 was still considered a good mimic of the homotetrameric enzyme (*32*).

One concern regarding Quad 1 was that of its final topology. In these studies, it was predicted that several different topologies were possible for the enzyme. However, in only two of the topologies (ABCD and ABDC) does a linker span the dimer-dimer

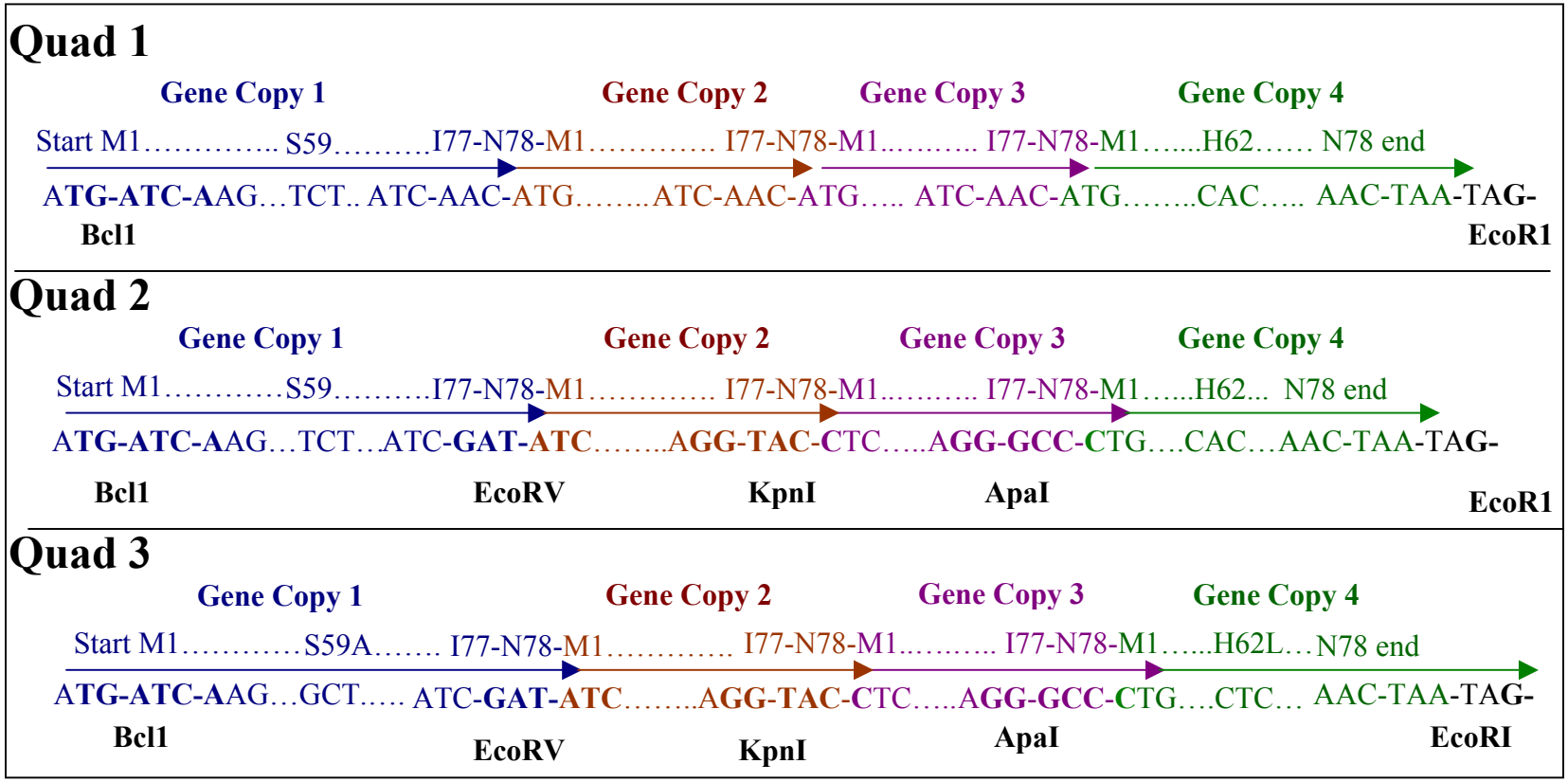

Figure 7. Comparison of Quad gene constructs of R67 DHFR. The gene copy number is listed above the amino acid sequence which is above the nucleotide sequence. Each gene copy corresponds to a monomer of R67 DHFR. Quad 1 contains the DNA encoding the monomers associated in-frame while Quad 2 incorporates unique restriction enzyme sites which are highlighted. Quad 3 contains a S59A and H62L mutation in domains 1 and 4, respectively. Modified from (*33*).

interface a single time. Of these two topologies, the ABCD topology requires the shortest span of the linker region across the dimer-dimer interface suggesting that this topology may be favored (*32*). A schematic of this is shown in Figure 8 where monomers ABCD are renamed as domains 1234 (*33*).

Quad 1 was originally constructed as a first step in the goal of generating asymmetric mutation. Since each gene, linked in-frame in Quad 1, is identical, primers designed for site-directed mutagenesis studies recognize the same region in every gene. Unfortunately, this approach yields four symmetry-related mutations. As a solution to this problem, a new construct was generated. This construct, named Quad 2, is shown in Figure 7. Quad 2 is similar to Quad 1 in that it also contains four copies of the DNA for the R67 DHFR monomer associated in-frame. Again, the linker region between the genes is the DNA coding for the first 17 amino acids of the monomer. However, each of the genes is flanked by unique restriction enzyme sites. In addition to the Quad 2 construct, four additional constructs were generated. These constructs contain a single copy of the gene flanked by unique restriction enzyme sites. An asymmetric mutation can be generated by performing site-directed mutagenesis on one of the single copy genes. The plasmid containing the gene is then digested by the appropriate restriction enzymes. At the same time, Quad 2 is also digested with the same restriction enzymes. The single gene copy containing the appropriate mutation is then ligated into the Quad 2 construct (*33,* Hicks et al., manuscript in preparation).

Asymmetric mutations of glutamine 67 residues were generated using this system. Two of these mutants were characterized kinetically: Q67H: 1+3 and Q67H: 1+4. Before proceeding, it is necessary to explain the nomenclature that will be used to

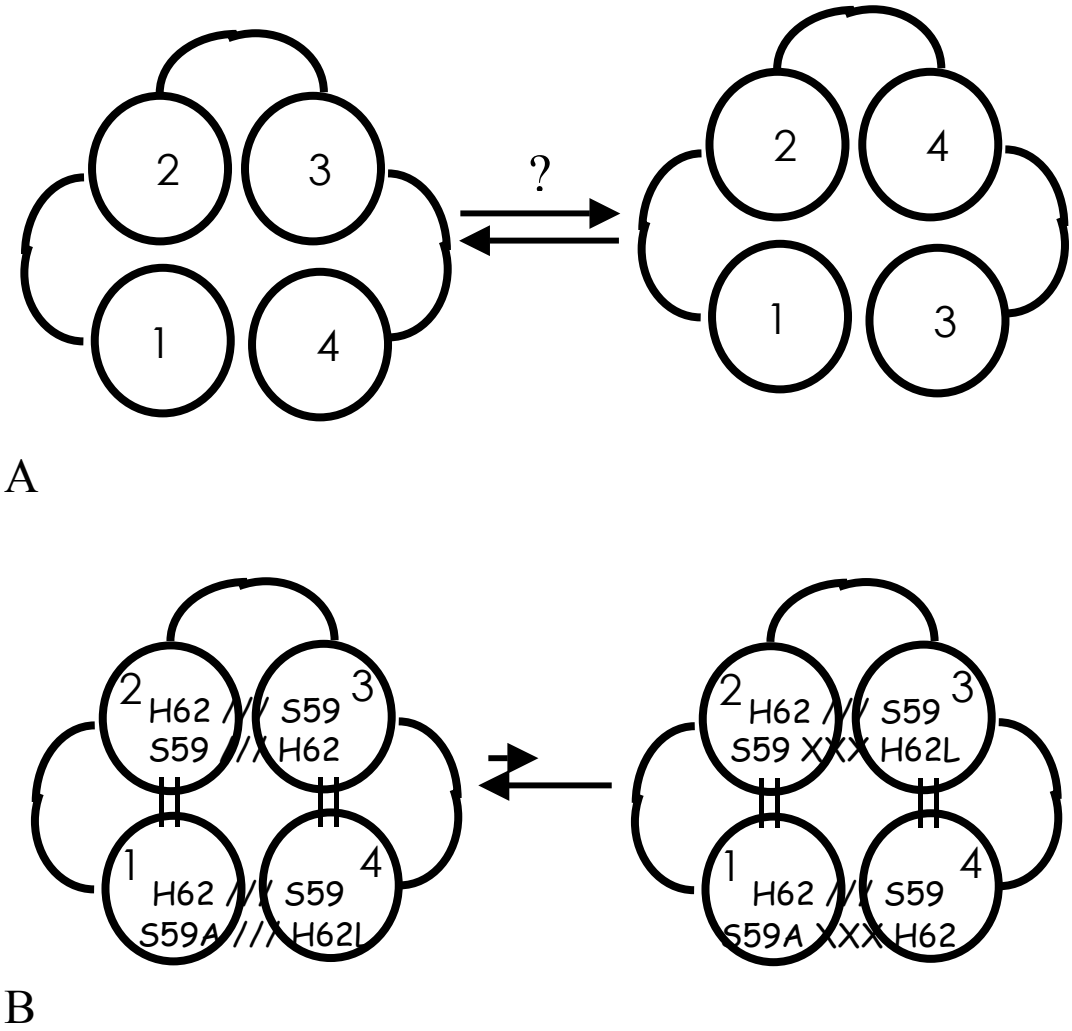

Figure 8. Schematic of "topology switching" phenomenon. Panel A illustrates the equilibrium proposed between the two topologies of the Quad 2 protein. Panel B shows the shift in equilibrium proposed to occur upon introduction of a S59A mutation in domain 1 and an H62L mutation in domain 4.

describe the asymmetric mutants throughout this dissertation. We will identify the wild-type residue and its position in the monomeric amino acid sequence first. This will be followed by the single letter code for the residue to which it is being mutated. We will then identify the asymmetric location of the mutations. As shown in Figure 3, we have identified each domain of the monomeric Quad 2 construct numerically where domain 1 occurs in the bottom-left region and the numbering continues in a clock-wise manner. Therefore, Q67H: 1+3 contains two glutamine 67 residues mutated to histidine residues. The Q67H mutations are located in domain 1 and in domain 3. Six unique asymmetric mutants can be generated using this system, one single mutant, three double mutants, one triple mutant, and one quadruple mutant. These are: Q67H: 1, Q67H 1+2, Q67H: 1+3, Q67H: 1+4, Q67H: 1+2+3, and Q67H: 1+2+3+4. A schematic of these asymmetric mutations is shown in Figure 9 (*33*). The same pattern of asymmetric mutations applies regardless of the residue mutated.

Originally, it was proposed that by generating asymmetric mutations, it might be possible to provide unique binding sites for NADPH and DHF (*27*, *29*). In addition, it was proposed that each asymmetric mutant would be unique since each mutant would provide a slightly different active site to the ligands. Therefore, it was proposed that the kinetic properties of Q67H: 1+3 and Q67H: 1+4 would be different. However, initial steady- state kinetic evaluation of the mutants indicated that the two were similar kinetically. This led to the conclusion that the Quad constructs may not exist in a single topology. Instead, it was suggested that a "topology-switching" phenomenon may occur. If this topology-switching does occur, Q67H: 1+3 and Q67H: 1+4 are no longer unique (*33*). This is illustrated in Figure 8.

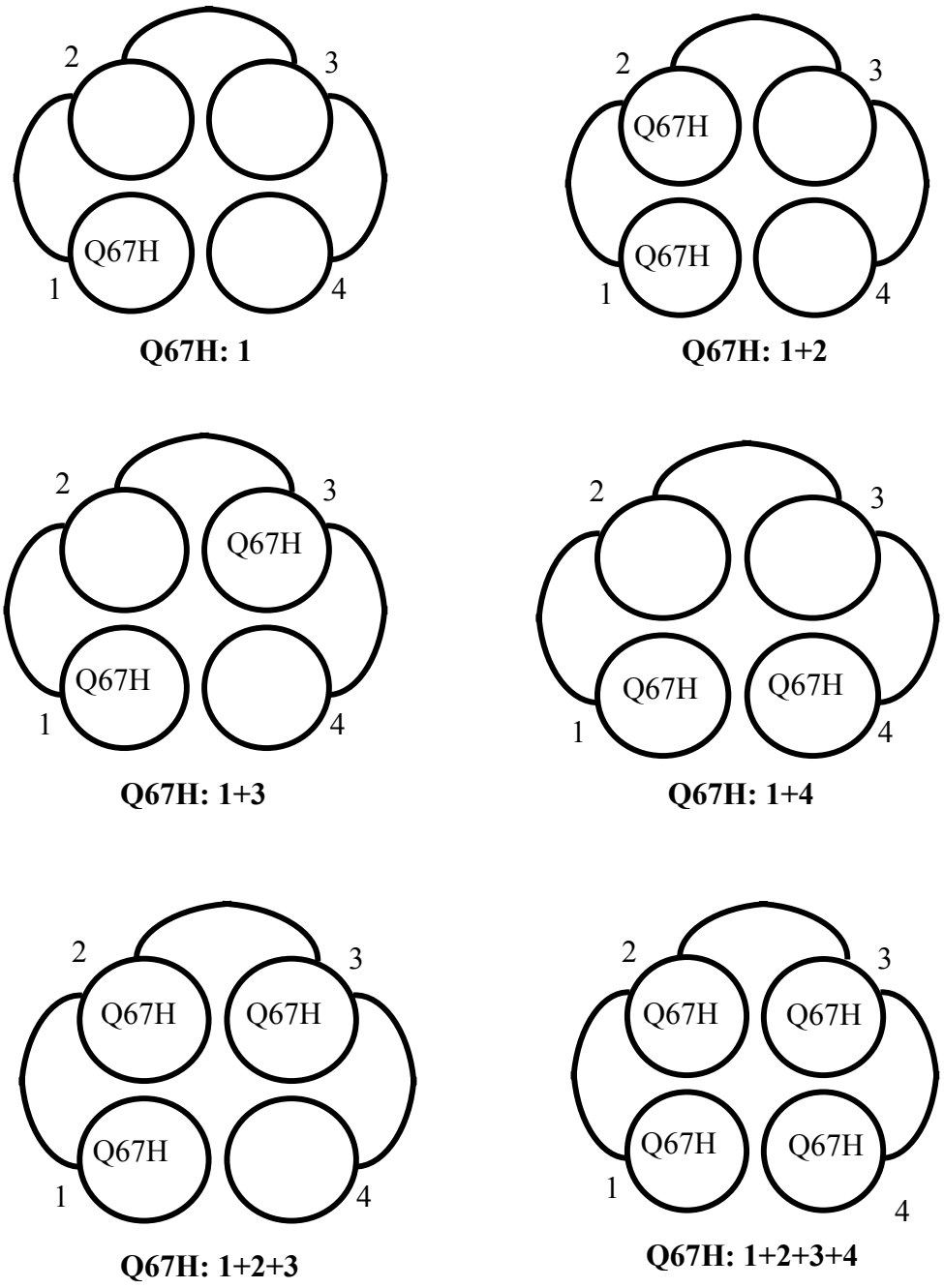

Figure 9. Schematic of unique Q67H asymmetric mutants. Each sphere represents a domain of Quad 3 where each domain is numbered clockwise. One unique single mutant (Q67H: 1), three unique double mutants (Q67H: 1+2, Q67H: 1+3, and Q67H: 1+4), one unique triple mutant (Q67H: 1+2+3), and one unique quadruple mutant (Q67H: 1+2+3+4) are possible using the Quad 3 construct. Modified from (*33*).

Studies by Dam et al. (*34*) provided a solution to the "topology-switching" problem. These researchers generated several mutations at serine 59 and histidine 62 in homotetrameric R67 DHFR. These two residues were considered important as they form a hydrogen bond that is lost upon protonation of histidine 62 (*19, 24*). Protonation of symmetry-related 62 residues causes the homotetramer to dissociate resulting in dimers (*24*). Mutation of symmetry-related serine 59 residues to alanine residues yielded dimers that were unable to self-associate as did mutation of symmetry-related histidine 62 residues to leucine residues. Interestingly, combining these dimeric mutants in a 1:1 ratio generated a heterotetramer with kinetic characteristics similar to that of the wild-type protein (*33*, *34*).

Based on the findings of Dam et al. (*34*), a final Quad construct was generated, Quad 3. The Quad 3 construct is shown in Figure 7. Quad 3 is a modified version of Quad 2 which contains two additional mutations: a S59A mutation in domain 1 and a H62L mutation in domain 4. The Quad 3 construct was used to generate each of the asymmetric mutations described in this dissertation. Characterization of Q67H asymmetric mutants generated in the Quad 3 construct suggest that a shift in the equilibrium towards a single topology occurs in this construct as illustrated in Figure 8.

Goal of Research Project

The goal of this research project is to asymmetrically mutate R67 DHFR such that unique binding sites are provided to the substrate and cofactor. By doing so, we propose to gain an understanding of the contacts occurring between residues located in specific domains of the active site and the ligands. For this project, we have chosen to focus on

two active site residues, glutamine 67 and tyrosine 69, both of which are proposed to interact with both DHF and NADPH.

References

1. Chu, D. T. W., Plattner, J. J., and Katz, L. (1996) *J Med Chem 39*, 3853-3874.
2. Neu, H. C. (1992) *Science 257*, 1064-1073.
3. Fleming, M. P., Datta, N., and Greneberg, R. N. (1972) *British Medical Journal 1*, 726-728.
4. Datta, N., and Hedges, R. W. (1972) *J Gen Microbiol 72*, 349-355.
5. Amyes, S. G., and Smith, J. T. (1974) *Biochem Biophys Res Commun 58*, 412-418.
6. Skold, O., and Widh, A. (1974) *J Biol Chem 249*, 4324-4325.
7. Smith, S. L., Stone, D., Novak, P., Baccanari, D. P., and Burchall, J. J. (1979) *J Biol Chem 254*, 6222-6225.
8. Barg, N. L., Register, S., Thomson, C., and Amyes, S. (1995) *Antimicrob Agents Chemother 39*, 112-116.
9. Pattishall, K. H., Acar, J., Burchall, J. J., Goldstein, F. W., and Harvey, R. J. (1977) *J Biol Chem 252*, 2319-2323.
10. Stone, D., and Smith, S. L. (1979) *J Biol Chem 254*, 10857-10861.
11. Matthews, C. K., and van Holde, K. E. (1996) *Biochemistry*, The Benjamin/Cummings Publishing Company, Inc., New York.
12. Howell, E. E., Shukla, U., Hicks, S. N., Smiley, R. D., Kuhn, L. A., and Zavodszky, M. I. (2001) *J Comput Aided Mol Des 15*, 1035-1052.
13. Wu, Y., and Houk, K. N. (1991) *J Am Chem Soc 113*, 2353-2358.
14. Morrison, J. F. (1989) *A Study of Enzymes*, Vol. 2, CRC Press Inc., New York.

15. Morrison, J. F., and Sneddon, M. K. (1989) in *Chemistry and Biology of Pteridines*, Walter de Gruyter and Co., New York.

16. Li, D., Levy, L. A., Gabel, S. A., Lebetkin, M. S., DeRose, E. F., Wall, M. J., Howell, E. E., and London, R. E. (2001) *Biochemistry 40*, 4242-4252.

17. Matthews, D. A., Smith, S. L., Baccanari, D. P., Burchall, J. J., Oatley, S. J., and Kraut, J. (1986) *Biochemistry 25*, 4194-4204.

18. Reece, L. J., Nichols, R., Ogden, R. C., and Howell, E. E. (1991) *Biochemistry 30*, 10895-10904.

19. Narayana, N., Matthews, D. A., Howell, E. E., and Nguyen-huu, X. (1995) *Nat Struct Biol 2*, 1018-1025.

20. Strader, M. B., Smiley, R. D., Stinnett, L. G., VerBerkmoes, N. C., and Howell, E. E. (2001) *Biochemistry 40*, 11344-11352.

21. Pitcher, W. H., 3rd, DeRose, E. F., Mueller, G. A., Howell, E. E., and London, R. E. (2003) *Biochemistry 42*, 11150-11160.

22. Castillo, R., Andres, J., and Moliner, V. (1999) *J Am Chem Soc 121*, 12140-12147.

23. Andres, J., Moliner, V., Safont, V. S., Domingo, L. R., Picher, M. T., and Kretchl, J. (1996) *Bioorg Chem 24*, 10-18.

24. Nichols, R., Weaver, C. D., Eisenstein, E., Blakley, R. L., Appleman, J., Huang, T. H., Huang, F. Y., and Howell, E. E. (1993) *Biochemistry 32*, 1695-1706.

25. Howell, E. E., Villafranca, J. E., Warren, M. S., Oatley, S. J., and Kraut, J. (1986) *Science 231*, 1123-1128.

26. Park, H., Zhuang, P., Nichols, R., and Howell, E. E. (1997) *J Biol Chem 272*, 2252-2258.

27. Bradrick, T. D., Beechem, J. M., and Howell, E. E. (1996) *Biochemistry 35*, 11414-11424.

28. Hicks, S. N., Smiley, R. D., Hamilton, J. B., and Howell, E. E. (2003) *Biochemistry 42*, 10569-10578.

29. Park, H., Bradrick, T. D., and Howell, E. E. (1997) *Protein Eng 10*, 1415-1424.

30. Strader, M. B., Stinnett, L. G., Hicks, S. N., Smiley, R. D., and Howell, E. E. (2003) in *18th Annual Enzyme Mechanisms Conference*, Galveston Island, TX.

31. DeLano, W. L., Ultsch, M. H., de Vos, A. M., and Wells, J. A. (2000) *Science 287*, 1279-1283.

32. Bradrick, T. D., Shattuck, C., Strader, M. B., Wicker, C., Eisenstein, E., and Howell, E. E. (1996) *J Biol Chem 271*, 28031-28037.

33. Smiley, R. D., Stinnett, L. G., Saxton, A. M., and Howell, E. E. (2002) *Biochemistry 41*, 15664-15675.

34. Dam, J., Rose, T., Goldberg, M. E., and Blondel, A. (2000) *J Mol Biol 302*, 235-250.

Part II: Breaking Symmetry: Mutations Engineered into R67 Dihydrofolate Reductase, a D_2 Symmetric Homotetramer Possessing a Single Active Site Pore

The section is a slightly revised version of a manuscript published by R. Derike Smiley, Lori G. Stinnett, Arnold M. Saxton, and Elizabeth E. Howell in 2001 in *Biochemistry*:

R. Derike Smiley, Lori G. Stinnett, Arnold M. Saxton, and Elizabeth E. Howell (2001). **Breaking Symmetry: Mutations Engineered into R67 Dihydrofolate Reductase, a D_2 Symmetric Homotetramer Possessing a Single Active Site Pore**. *Biochemistry 41:* 15664-15675.

This author contributed the following to this manuscript: (1) some protein expression and purification, (2) protein extinction coefficients, (3) steady-state kinetic data, (4) pH titration data, (5) circular dichroism spectroscopy data, and (6) some assistance with writing the manuscript. This research was supported by NSF grant MCB-9808302 (to E.E.H.).

Abstract

R67 dihydrofolate reductase (DHFR) is an R-plasmid encoded enzyme that confers resistance to the antibacterial agent, trimethoprim. This homotetramer possesses a single active site pore and exact 222 symmetry. The symmetry imposes constraints on the ability of the enzyme to optimize binding of the substrate, dihydrofolate (DHF), and the cofactor, NADPH, resulting in a "one site fits both ligands" approach. This approach allows formation of either a NADPH•NADPH, a dihydrofolate•dihydrofolate or a NADPH •dihydrofolate complex. The first two complexes are non-productive while the third is the productive catalytic species. To break the symmetry of the active site, a tandem array of four R67 DHFR genes has been linked in frame, allowing individual manipulation of each gene copy. Various numbers and combinations of asymmetric Q67H mutations have been engineered into the tandem gene array. The Q67H mutation was chosen for investigation as it was previously found to tighten binding to both dihydrofolate and NADPH by ~ 100 fold in homotetrameric R67 DHFR (*1*). Non-additive effects on ligand binding are observed when 1 to 4 mutations are inserted, indicating either conformational changes in the protein or different cooperativity patterns

in the ligand•ligand interactions. From steady state kinetics, addition of Q67H mutations does not drastically affect formation of the NADPH•dihydrofolate complex, however a large energy difference between the productive and non-productive complexes is no longer maintained. A role for Q67 in discriminating between these various states is proposed. Since theories of protein evolution suggest gene duplication followed by accumulation of mutations can lead to divergence of activity, this study is a first step towards asking if introduction of asymmetric mutations in the quadruplicated R67 DHFR gene can lead to optimization of ligand binding sites.

Introduction

Dihydrofolate reductase (DHFR)[1] reduces dihydrofolate (DHF) to tetrahydrofolate using the cofactor NADPH in a hydride transfer reaction. Tetrahydrofolate is essential for cell survival as it is a precursor for formation of thymidylate, methionine, purine nucleosides, as well as other intermediates in metabolism. The antibiotic trimethoprim has been used clinically as an inhibitor against *E. coli* chromosomal DHFR. However, R-plasmid encoded R67 DHFR confers resistance to this antibiotic. This DHFR variant is not homologous either in genetic composition or structure to the chromosomally encoded enzyme (*2,3*).

[1] Abbreviations: DHFR, dihydrofolate reductase; wt, wild type; TMP, trimethoprim; DHF, dihydrofolate, NADP(+/H), nicotinamide adenine dinucleotide phosphate (oxidized/reduced); NMNH, reduced nicotinamide mononucleotide; MTH buffer, 50 mM MES + 100 mM Tris, + 50 mM acetic acid polybuffer; ITC, isothermal titration calorimetry; CD, circular dichroism. Mutant enzymes containing amino acid substitutions are described by the wild type residue and numbered position in the sequence, followed by the amino acid substitution. For example, Q67H R67 DHFR describes the gln67 $\rightarrow$ his mutant.

Numerous observations lead to the hypothesis that R67 DHFR is a primitive enzyme. First, the active species is a homotetramer that possesses 222 symmetry as shown in Figure 1 (protein data bank file 1VIE, ref 3). The single active site is a 25 Å pore that extends the length of the protein. As a consequence of the 222 symmetry, binding of DHF and NADPH to the pore results in formation of three different complexes (DHF•DHF, NADPH•NADPH or DHF•NADPH; ref 4). Only the ternary complex (DHF•NADPH) results in catalysis. For the latter complex, DHF occupies half the pore and cofactor the other half; the pteridine ring of DHF and the nicotinamide ring of NADPH encounter each other at the center of the pore where the reaction occurs (*5*). A drawback of the 222 symmetry is that binding to NADPH and DHF cannot be independently optimized. The enzyme appears to possess a binding "hot spot" that can accommodate (with some degree of overlap) both DHF and NADPH (*6,7*).

A second observation suggesting R67 DHFR is a primitive enzyme is that mutations typically have a large cumulative effect since one mutation per gene results in four mutations per active site. Mutations that tighten binding do not necessarily lead to enhanced catalytic efficiency as binding is concurrently tightened in all symmetry related sites. This leads to substantial substrate and cofactor inhibition because of formation of the nonproductive complexes, DHF•DHF and NADPH•NADPH (*1,4*).

A third observation is that R67 DHFR does not possess a general acid in its active site pore. Instead it requires the substrate be activated by protonation (*1,8-9*). In other words, catalysis increases as the pH approaches the pK_a of N5 on DHF (2.59; ref 10).

Introduction of asymmetric mutations should break the constraints imposed on R67 DHFR due to its 222 symmetry, leading to addition of functional groups or building substrate specificity. For the latter, mutations may be added to one half the pore leading to more specific binding of NADPH. Conversely, specificity may be built in the other half of the pore, allowing more precise binding of DHF. Construction of asymmetric mutations by mixing populations (e.g. wildtype and mutant R67 DHFRs) is limited by the pH dependent dissociation of tetrameric R67 DHFR into dimers (*11*). Thus any heterotetramers formed and isolated will readily dissociate and reassociate to a mixture of homo- and heterotetramers upon titration of His62 and its symmetry related residues[2] at pH values ≤8.

To construct asymmetric mutations in R67 DHFR, a gene oligomerization strategy is necessary. Therefore, Bradrick et al. (*12*) linked in-frame four copies of the gene coding for the 78 amino acid monomer. The protein product of this tandem gene array is an active monomer with four times the mass of the wildtype (wt) monomer and that possesses the essential tertiary structure of the wt homotetramer. The linker between gene copies corresponds to the natural N-terminus. In this protein, residues are not numbered consecutively. Instead residues 1-78 describe the 1st (A) domain, residues 101-178 describe the 2nd (B) domain, residues 201-278, the 3rd (C) domain and residues 301-378, the 4th (D) domain. The domains correspond to the monomers in wt R67 DHFR.

[2] The amino acids in the first monomer (A) are labeled 1-78; those in the second monomer (B), 101-178; those in the third monomer (C), 201-278; and those in the fourth monomer (D), 301-378. For brevity, when a single residue is mentioned, all four symmetry related residues are implied. The monomer arrangement going clockwise in the crystal structure 1VIF is ABDC (3). To minimize confusion in the quadruplicated gene construct, we have re-labeled the monomers ABCD going clockwise.

This paper describes the addition of asymmetric mutations to the tandem gene array. The Q67H substitution was initially chosen for analysis as it tightens binding to both NADPH and DHF in the context of the wt homotetramer (*1*). Glutamine 67 and its symmetry related residues occur at the center of the active site pore. They form the "ceiling" and "floor" of the pore (Figure 1). Each Q67 residue hydrogen bonds with a symmetry related Q67 residue at both dimer-dimer interfaces. Both of the hydrogen-bonded pairs extend into the active site causing the pore radius to decrease near the middle. From the folate co-crystal structure, Q67 forms extensive van der Waals interactions with the pteridine ring of folate (*3*). Our recent computational docking studies using DOCK (docking based on van der Waals interactions) and SLIDE (docking based on hydrogen bond formation) predict interactions between Q67 and NMNH (reduced nicotinamide-ribose-P_i moiety of NADPH) (*6*). In these predicted interactions, Q67 may form a hydrogen bond to one of the ribose OHs (O2′) through its NE2 group as well as form van der Waals interactions with several atoms of the nicotinamide ring through its sidechain. This ternary complex model proposes that Q67 serves a dual role in binding both folate/DHF and NADPH. The previously constructed Q67H mutant also supports this notion as it tightens binding to both NADPH and DHF by factors of 100 and 6000 fold respectively (*1*). Binding affinity may be strengthened due to ring stacking interactions between the imidazole ring of histidine and the nicotinamide and/or pteridine rings of NADPH and DHF respectively (*13-15*).

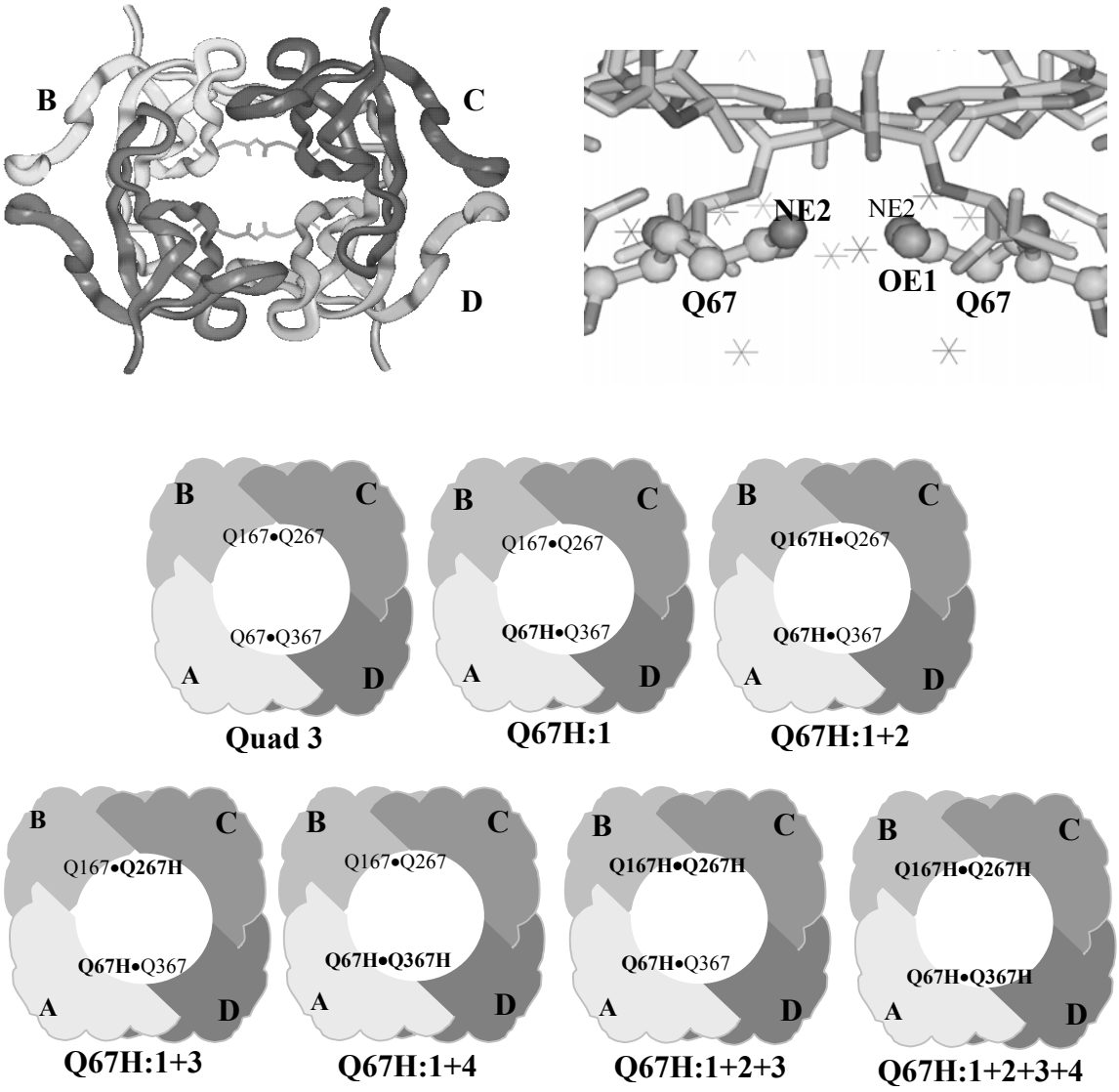

Figure 1. Top left: the ribbon structure of homotetrameric R67 DHFR (1VIE in the protein data bank). Each monomer is shaded differently and labeled A, B, C or D. While 1VIE assigns the monomer topology as ABDC going clockwise, we have revised this to ABCD to minimize confusion in the four gene copy construct. The single active site pore occurs in the center of the structure. The Q67 sidechains are highlighted; they appear at the top and bottom surfaces of the active site pore. Top right: An enlarged view of a pair of symmetry related Q67 residues from the B and C subunits. The Q67s are in the center of the image in ball and stick format and the NE2 and OE1 atoms labeled. Water molecules are given as stars. The active site pore is directly below the 2 glutamines. The rest of the figure: a cartoon representing the topologies of various asymmetric Q67H mutations. Quad 3 is the parent structure that possesses covalent linkers between each monomer in homotetrameric (wt) R67 DHFR.

Materials and Methods

Site-directed mutagenesis

A synthetic R67 DHFR gene, carried in pUC8, has been previously described (*16*). A tandem array of 4 R67 DHFR genes was previously constructed where the genes are linked in-frame (*12*). The resulting protein, named Quad 1, possesses four times the mass of the native R67 DHFR monomer. Mutations were introduced using the PCR based protocol outlined in the Quickchange kit from Stratagene. DNA sequencing was performed by the University of TN sequencing facility to confirm all constructs.

Protein purification

E. coli STBLII cells (*F¯mcrA Δ(mcrB-hsdRMS-mrr) recA1 endA1 gyrA96 thi supE44 relA1 λ¯Δ(lac-proAB);* Gibco BRL) were used to maintain the tandem gene arrays as well as express the monomeric R67 DHFR and mutants (*17*). Cells were grown at 30°C with shaking for approximately 60 hours. The cells were lysed by sonication and the crude protein extract was clarified with streptomycin sulfate and concentrated with 55% ammonium sulfate. The proteins were purified using the following chromatography columns: G-75 Sephadex size exclusion column, DEAE Fractogel column, Biorad HighQ column, and FPLC HighQ column (*7,16*). The purity of the proteins was determined by SDS-PAGE.

Isothermal titration calorimetry

Binding affinities and the enthalpy associated with binding were monitored using isothermal titration calorimetry (ITC) as previously described (*1,4*). Briefly, measurements were carried out on a Microcal Omega Ultrasensitive Isothermal Titration

Calorimeter equipped with a nanovoltmeter for improved sensitivity and connected to a circulating water bath for temperature control. The data were automatically collected by an IBM PC running DSCITC data acquisition software and were analyzed using Origin version 2.9 software provided by the manufacturer. The design and operation of this instrument have been described by Wiseman et al. (*18*). Samples typically consisted of ~90-100 μM protein in MTH buffer (50mM MES, 100mM Tris, 50mM acetic acid, and 10mM β-mercaptoethanol), pH 8. This buffer maintains constant ionic strength from pH 4.5 to 9.5 (*19*). Measurements were performed at 28°C. Ligand concentrations in the syringe were typically 20 times the protein concentration. Addition of ligand to buffer only was performed to allow baseline corrections. Data describing NADPH or DHF binding were fit to an interacting sites model where the stoichiometry of ligand binding was set equal to two. Data describing binding of $NADP^+$ were fit to a single site model. Ternary complex data were obtained by titrating DHF into a 1:1 mixture of R67 DHFR:$NADP^+$ and were fit to a single site model.

Steady state kinetics

The kinetic behavior of each protein was monitored using a Perkin-Elmer λ3a spectrophotometer controlled by an IBM PS2 (*20*). The data were collected using the program UVSL3. Each experiment was conducted at 30°C in MTH buffer. Four to five subsaturating concentrations of both DHF and NADPH were utilized to monitor activity. To calculate k_{cat} and K_m values for those variants displaying no to minimal substrate or cofactor inhibition, the data were fit globally to the nonlinear Michaelis-Menton equation describing bisubstrate kinetics using SAS v8.2 (*21*; Smiley et al., manuscript in

preparation). These values agree with the more traditional data analysis approach (*22, 23*) where primary linear 1/[substrate] vs 1/velocity plots are followed by secondary plots, yielding kinetic parameters. To calculate k_{cat} and K_m values for those variants displaying substantial substrate/cofactor inhibition, the data were fit globally using SAS to a rate equation describing the R67 DHFR mechanism (*4*). The mechanism is shown in Scheme I and the corresponding rate equation is:

$$v = \frac{k_{cat} \bullet [E_{total}] \bullet [DHF] \bullet [NADPH]}{\{[DHF][NADPH] + K_{m\,(DHF)} \bullet [NADPH] + K_{m\,(DHF)} \bullet K_{d1\,(NADPH)} + K_{m\,(NADPH)} \bullet [DHF] + (K_{m\,(DHF)} \bullet [NADPH]^2 / K_{d2\,(NADPH)}) + (K_{m\,(NADPH)} \bullet [DHF]^2 / K_{d2\,(DHF)})\}} \quad (1)$$

where v is the velocity of the reaction; $[E_{total}]$, [DHF], [NADPH] are the concentrations of enzyme, substrate and cofactor; and K_{d1} and K_{d2} are the first and second binding constants for the specified ligands as measured by isothermal titration calorimetry (ITC). In fitting these data sets, the K_d values obtained by isothermal titration calorimetry were used as constraints. Since three K_d values are entered explicitly with bounds allowing some minor variation, the fourth K_d is solved using a closed thermodynamic loop relationship ($K_{m\,(NADPH)} = K_{d1\,(NADPH)} \bullet K_{m\,(DHF)} / K_{d1\,(DHF)}$). To keep any variation from funnelling to the fourth K_d, a ratio of $K_{d1\,(NADPH)}$ to $K_{d1\,(DHF)}$ was sometimes used as a fixed parameter (again with bounds allowing some minor variation). In the fitting process, the inputted K_d values and the K_{d1} ratio were allowed to vary by 2-3 fold. If the 2-3 fold changes in K_d values gave better fits to the steady state kinetic data, then these

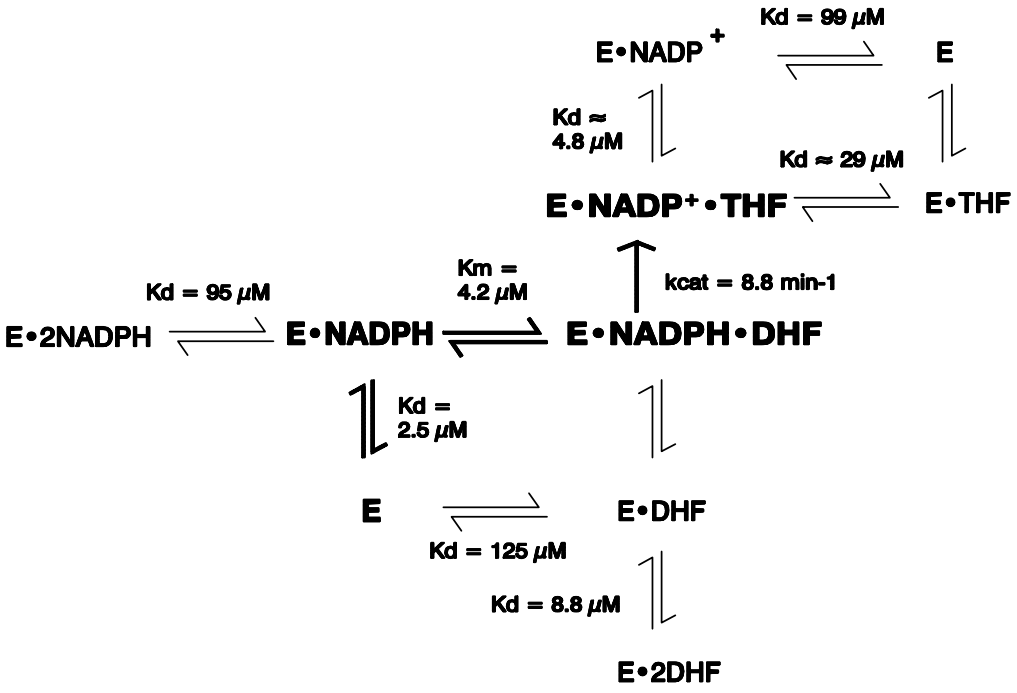

Scheme 1. Binding scheme for R67 DHFR proposed from steady-state kinetics (*16*) and isothermal titration calorimetry (*4*) studies.

K_d values were used to re-assess the ITC fits. All ITC refits remained within 90% confidence intervals.

Protein and ligand concentrations were determined spectrophotometrically. For all mutants, extinction coefficients were determined using the biuret assay (*24*). Ligand concentrations were determined using the following extinction coefficients: 28,000 l/mol•cm at 282 nm for DHF (*25*) and 6230 l/mol•cm at 340 nm for NADPH (*26*). The molar extinction coefficient used to assess DHFR reduction of DHF was 12,300 l $mol^{-1}cm^{-1}$ (*27*).

Results

Construction of an altered tandem array

Direct mutagenesis of the quadruplicated gene construct described in Bradrick et al. (*12*) did not allow control of either the number of mutations or their placement since each of the gene copies was identical. Therefore a different mutagenesis strategy was devised. In this alternate approach, unique restriction sites were designed between the gene copies by mutagenesis of the 5′ and 3′ ends of each of the single copy genes. This process resulted in 4 different single R67 DHFR gene constructs. Introduction of an asymmetric mutation into the desired gene copy was next performed and ligation of the resulting constructs allowed reconstruction of the quadruplicated gene containing the desired asymmetric mutation(s).

The tandem array containing the restriction sites but no asymmetric mutations is named Quad 2. Figure 2 shows a Bcl1 site at the 5′ end of gene copy 1; an EcoRV site separates gene copies 1 and 2; a KpnI site occurs between copies 2 and 3; an ApaI site

Figure 2. Flowchart for construction of the quadruplicated R67 DHFR genes. The complete R67 DHFR gene sequence is given in reference 16. Construction of the initial quadruplicated gene, Quad 1, is described in reference 12. Each gene copy coding for a 78 amino acid monomer is denoted by a horizontal arrow. Partial DNA sequences with engineered unique restriction sites (in bold) are shown below the line while the corresponding amino acids are given above the line. For Quad 3, two additional mutations were added; gene copy 1 contains a S59A mutation while gene copy 4 contains a H362L mutation (*29*).

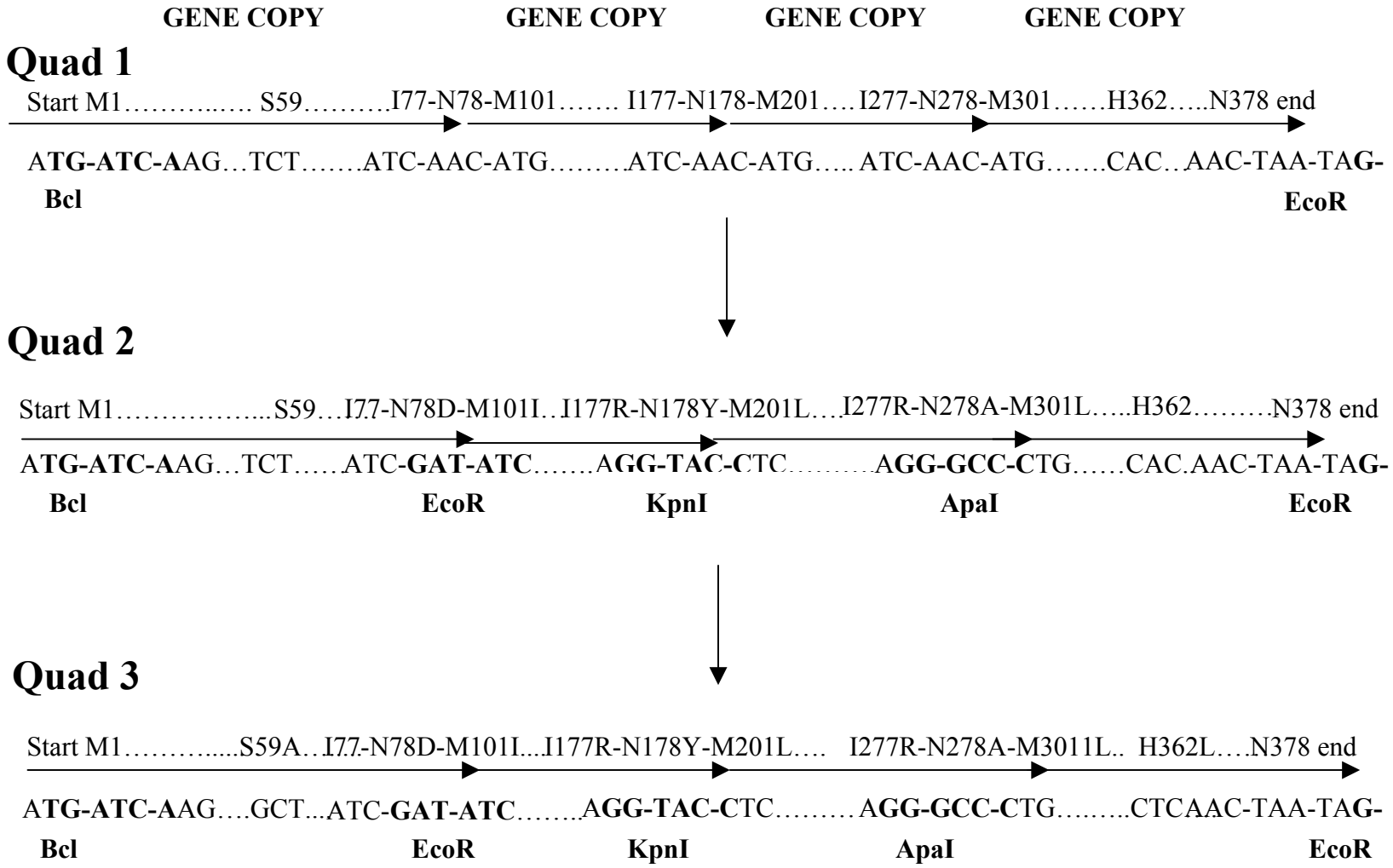
GENE COPY
GENE COPY
GENE COPY
GENE COPY
Quad 1
Start M1……..…. S59…….I77-N78-M101……. I177-N178-M201….I277-N278-M301……H362…..N378 end
ATG-ATC-AAG…TCT…….ATC-AAC-ATG……ATC-AAC-ATG….. ATC-AAC-ATG…….CAC…AAC-TAA-TAG-
Bcl
EcoR
Quad 2
Start M1……...S59…I77-N78D-M101I…I177R-N178Y-M201L….I277R-N278A-M301L…..H362……N378 end
ATG-ATC-AAG…TCT……ATC-GAT-ATC…….AGG-TAC-CTC……AGG-GCC-CTG……CAC.AAC-TAA-TAG-
Bcl
EcoR
KpnI
ApaI
EcoR
Quad 3
Start M1…….....S59A…I77-N78D-M101I...I177R-N178Y-M201L…. I277R-N278A-M3011L.. H362L….N378 end
ATG-ATC-AAG….GCT...ATC-GAT-ATC……..AGG-TAC-CTC…… AGG-GCC-CTG…..…..CTCAAC-TAA-TAG-
Bcl
EcoR
KpnI
ApaI
EcoR

divides genes copies 3 and 4; and an EcoR1 site is positioned at the 3′ end of gene copy 4. Introduction of the restriction sites in the gene creates several amino acid changes. The C-terminal wt R67 DHFR sequence is Ile77-Asn78; for direct connection to the second gene copy, the next residue would be Met101. However for the construct that contains the EcoRV site, N78D+M101I mutations are present. For the construct that introduces the KpnI site, I177R+N178Y+M201L mutations occur. Lastly, for the Apa I restriction site, I277R+N278A+M301L mutations are introduced. While these changes are not always conservative, a comparison of type II DHFR sequences indicates the N-terminal 26 residues and the C-terminal 2 residues are not well conserved (*28*). Further, removal of the N-terminal 16 amino acids by chymotrypsin treatment does not affect enzyme activity (*16*).

From an examination of the homotetramer structure, it appears feasible to form either an ABCD or an ABDC topology or a mixture of the two species in the quadruplicated gene product. This option arises as the N-terminal Pro19 residues from the C and D monomers are equidistant (>45Å) from the C-terminal N78 residue in the B monomer in the R67 DHFR crystal structure. These two symmetry related Pro19 residues are ~15 Å apart[3]. To constrain the various potential folding topologies to a single ABCD domain arrangement, we introduced a S59A mutation in gene copy 1 and a H362L mutation into gene copy 4. Individually, the S59A and H62L mutations destabilize the homotetramer, forming inactive dimers. However 1:1 mixtures restore almost full activity, indicating they complement each other and form heterotetramers

[3] The N-terminal 17-18 amino acids are disordered in the dimer structure (30) and when 16 N-terminal amino acids were cleaved off, the truncated protein crystallized as a tetramer (3).

(29). The quadruple variant containing these mutations is named Quad 3. All subsequent mutants described below use this as a "parent".

The final step in this process introduced Q67H mutations into Quad 3. A single Q67H mutation was constructed in gene copy 1; single mutations in other gene copies were not constructed as the 222 symmetry of R67 DHFR predicts they will be equivalent. For double Q67H mutants, 3 non-equivalent constructs are possible. The first contains mutations in gene copies 1&2 (=Q67H:1+2); the second contains Q67H mutations in gene copies 1&3 (= Q67H:1+3); and the third contains Q67H mutations in gene copies 1&4 (=Q67H:1+4). In the 1+2 construct, Q67H lies next to a wt Q67 residue at the "floor" as well as the "ceiling" of the pore and the mutations occur on the "left hand" side of the pore. In the 1+3 construct, Q67H again lies next to a wt Q67 residue at the "floor" of the pore, however the second Q67H mutation occurs "diagonally" across the pore on the "ceiling." In the Q67H:1+4 construct, a Q67H pair should form at the "floor" of the active site pore while a wt Q67 pair should occur at the "ceiling". From the symmetry, the 1+2 construct should be equivalent to a 3+4 construct; the 1+3 and 2+4 constructs should be equivalent as are the 1+4 and 2+3 constructs. Only one triple mutant, Q67H:1+2+3, was constructed as was a single quadruple mutant, Q67H:1+2+3+4. Figure 1 shows a cartoon of the mutant configurations.

Does the Quad 3 protein mimic WT R67 DHFR?

Prior to construction and evaluation of any asymmetric mutants, it was necessary to assess the effect of the mutations that added the unique restriction sites between gene copies, as well as the S59A and H362L mutations used to constrain possible folding topologies to the quadruplicated gene product. To determine whether the Quad 3 protein

mimics wt R67 DHFR, steady state kinetics and isothermal titration calorimetry were utilized. Table 1 gives the k_{cat} and K_m values for wt R67 DHFR, the original Quad 1 protein (*12*) as well as the Quad 3 protein derived from this work. The k_{cat} and K_m values for Quad 3 are similar to those of Quad 1 and are within a factor of 2 of wt R67 DHFR, indicating the effects of the mutations are minor.

A comparison of ITC binding data for NADPH, DHF and $NADP^+$ is given in Table 2. Again, the Quad 3 protein mimics wt R67 DHFR reasonably well. The largest difference is an approximately 5 fold weaker binding of the first DHF molecule. However the previously reported K_d values for DHF binding to wt DH→sFR were fit including the first data point (*4*). In contrast, the values reported in this study do not use the first data point due to its variability associated with the first mixing event in the calorimeter. This difference in fitting explains an approximately 2 fold change in K_d. Any additional variance arises from differences between the Quad 3 and wild type proteins.

What are the effects of the asymmetric Q67H mutations?

To assess the effects of the Q67H mutations on ligand binding, ITC was used to monitor binding to DHF, NADPH, and $NADP^+$ in various combinations. A representative titration is given in Figure 3. Data for all mutants were obtained except for the Q67H:1+2+3+4 variant. We find the data for this species are not readily reproducible as the protein solution often is turbid after the titration, indicating aggregation at high protein concentrations.

Table 1. A comparison of steady state kinetic values at pH 7.0 for numerous R67 DHFR constructs.

Enzyme Variant	k_{cat} (sec^{-1})	$K_{m\ (NADPH)}$ (μM)	$K_{m\ (DHF)}$ (μM)	R^2 (SAS)
WT R67 DHFR[a]	1.3	3.0	5.8	-
Quad 1[b]	0.75	4.5	8.0	-
Quad 3[c]	0.81 ± 0.02	4.4 ± 0.4	6.7 ± 0.4	90%
Q67H:1[c]	0.23 ± 0.01	1.3 ± 0.1	3.6 ± 0.2	90%
Q67H:1+2[d]	0.21 ± 0.01	0.28 ± 0.02	3.6 ± 0.3	89%
Q67H:1+3[d]	0.23 ± 0.01	1.8 ± 0.1	11 ± 0.6	97%
Q67H:1+4[d]	0.15 ± 0.01	0.95 ± 0.14	2.6 ± 0.5	84%
Q67H:1+2+3[d]	0.090 ± 0.01	0.45 ± 0.06	7.5 ± 2.3	85%
Q67H:1+2+3+4[d]	0.10 ± 0.01	0.026 ± 0.004	0.13 ± 0.02	86%
Q67H R67 DHFR (pH 8)[e]	0.022 ± 0.001	0.03 (calculated)	0.16 ± 0.005	-
Q67H R67 DHFR (pH 8)[f]	0.025 ± 0.001	0.014 ± 0.002	0.14 ± 0.01	91%

[a] Values from reference 16.
[b] Values from reference 12.
[c] Global non-linear fit to the Michaelis-Menton equation describing bisubstrate kinetics using SAS.
[d] Global non-linear fit (SAS) to a rate equation describing the R67 DHFR mechanism (eq 1) using ITC values as constraints.
[e] Fit values from reference 1 using FITSIM.
[f] Global non-linear fit (SAS) to a rate equation describing the R67 DHFR mechanism (eq 1) using ITC values as constraints.

Table 2. A comparison of wt R67 DHFR with Quad 3 using isothermal titration calorimetry to monitor ligand binding.

Complex	K_d (μM)	ΔH (cal/mol)	Stoichiometry
Wt R67 DHFR with NADPH[a]	5.0 ± 0.3 48 ± 2	-8600 ± 200 -5800 ± 2500	1.56 ± 0.14
Quad 3 with NADPH	4.0 ± 0.3 37.1 ± 3.0	-3000 ± 26 -9400 ± 83	2[b]
Wt R67 DHFR with DHF[a]	250 ± 50 4.4 ± 0.7	-7900 ± 900 -1400 ± 60	1.88 ± 0.1
Quad 3 with DHF	46 ± 0.7 2.0 ± 0.02	-8420 ± 110 -3750 ± 39	2[b]
Wt R67 DHFR with $NADP^+$[a]	99 ± 3	-7700 ± 500	0.99 ± 0.03
Quad 3 with $NADP^+$	31.3 ± 1.3	-7000 ± 450	0.95 ± 0.02
Wt R67 DHFR • $NADP^+$ with DHF[a]	4.8 ± 1.0	-11700 ± 300	1.22 ± 0.01
Quad 3 • $NADP^+$ with DHF	4.9 ± 0.1	-11500 ± 800	0.99 ± 0.01

[a] Results from reference 12. Microscopic values (k_{d1}, k_{d2}) are reported. The statistical relationship between microscopic and macroscopic constants is $K_{d1} = ½ k_{d1}$ and $K_{d2} = 2 k_{d2}$ (52).

[b] The stoichiometry is set at 2 by choosing the two interacting sites model in Origin, the software used by the ITC for fitting the data. Since the value is set, it is presented with no error.

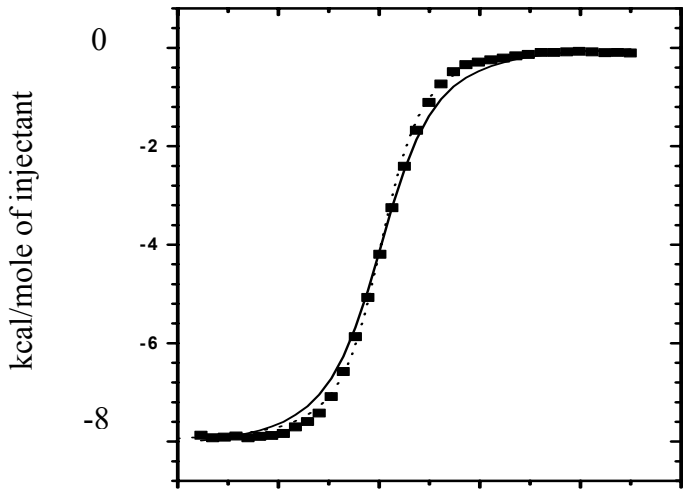

Figure 3. Isothermal titration calorimetry analysis of DHF binding to Q67H:1+4 DHFR. The protein concentration was 100 μM and the data were fit using the 2 interacting sites model (dotted line). Best fit values are given in Table 4. To fit the steady state kinetic data (table 1), the ITC values were allowed to vary up to 3 fold from the best fit values. In fitting of the kinetic data, the (microscopic) K_d values for DHF binding to Q67H:1+4 shifted to K_{d1} = 2.12 and K_{d2} =106 μM. These involve a 2.3 fold increase and a 3 fold decrease from the K_d values given in Table 4. The refit is shown by the solid line.

Table 3 gives the K_d and ΔH values associated with binding of $NADP^+$. Only one $NADP^+$ binds per R67 DHFR as compared to 2 NADPH molecules. This different stoichiometry is likely due to charge-charge repulsion between the positively charged nicotinamide rings in $NADP^+$. A trend noted is introduction of each successive Q67H mutation results in tighter binding of $NADP^+$ over a 7-fold range (with some variability for the different topologies of the double mutants). A generally linear relationship between the number of mutations and the K_d is consistent with no conformational changes upon binding and additive (independent) interactions between the Q67H residues (*30*). While a model does not exist for bound $NADP^+$, a model for bound, reduced NMN has recently been generated by docking NMNH into R67 DHFR•FolI, where Fol1 is the productively bound pteridine ring in the crystal structure (*6*). In this model, the reduced nicotinamide moiety of NMN interacts with one pair of symmetry related Q67 residues, while the pteridine ring of FolI interacts with the other pair of Q67 residues. One interpretation of the above ITC results suggests that bound $NADP^+$ interacts with at least three of the Q67 residues since successive addition of up to 3 mutations continues to tighten binding. This scenario would require $NADP^+$ to bridge between both pairs of Q67 residues, a distance of ~11A (between carboxamide atoms). This interpretation suggests some alteration of the binding mode for $NADP^+$ with respect to that proposed for reduced NMN in a ternary complex. An alternate hypothesis is that when $NADP^+$ binds to either wt or Q67H R67 DHFRs, the binding constant reflects the statistical average of binding at each symmetry related site. Since the sites are equivalent in the homotetramer, statistical averaging has no effect. However when $NADP^+$ binds to an

Table 3. Binding of $NADP^+$ to the various DHFR species as monitored by ITC at pH 8.0.

Complex	K_d (μM)	ΔH (cal/mol)	stoichiometry
Quad 3 titrated with $NADP^+$	31.3 ± 1.3	-7000 ± 450	0.95 ± 0.02
Q67H:1 with $NADP^+$	19.3 ± 1.9	-6500 ± 250	1.1 ± 0.03
Q67H:1+2 with $NADP^+$	13.1 ± 1.0	-7600 ± 240	1.1 ± 0.02
Q67H:1+3 with $NADP^+$	15.3 ± 1.4	-6300 ± 340	1.1 ± 0.01
Q67H:1+4 with $NADP^+$	11.2 ± 1.0	-13,900 ± 520	1.0 ± 0.04
Q67H:1+2+3 with $NADP^+$	4.23 ± 0.3	-12,200 ± 220	1.1 ± 0.05
Q67H R67 DHFR with $NADP^+$[a]	3.4 ± 0.9	-9900 ± 500	0.70 ± 0.05

[a] Results from reference 1.

asymmetric mutant, for example Q67H:1, there are several possible binding orientations, i.e. one symmetry pair of orientations would place the nicotinamide ring near a wt Q167-Q267 homo-pair while a second pair of orientations would juxtapose the nicotinamide ring near the Q67H-Q367 hetero-pair. If the contribution of the Q67H residue to the overall binding constant is minor, the observed K_d may be an average value reflecting the contributions associated with binding at non-equivalent sites. As the number of Q67H mutations increases, this would lead to an overall decrease in the apparent K_d. This explanation seems more likely than the model where $NADP^+$ interacts with ≥ 3 Q67H residues, although that cannot be ruled out.

A more complex relationship arises when the effects of the Q67H mutations on binding NADPH or DHF (binary conditions) are assessed. Table 4 gives the K_d and ΔH values observed. Several observations are apparent. First, for DHF binding, the addition of 1 Q67H mutation has a large, immediate effect on the first K_d value, while for NADPH binding, it takes 3 mutations to show any advance towards the tighter binding previously observed in the Q67H homotetramer (*1*). Second, the various double mutants show different binding patterns, particularly for DHF, indicating they present different arrangements of the Q67H mutations. This implies that the Quad 3 parent protein has been locked into a single topology (ABCD) and that the effect of two Q67H mutations is a function of how they are arranged with respect to each other. Third, the cooperativity between ligands (monitored by K_{d2} / K_{d1}) shows large variations, particularly for binding of DHF. These issues are discussed more fully below.

Since $NADP^+$ binding gets progressively tighter with the successive addition of Q67H mutations, a straightforward result for binding of NADPH would have been a

Table 4. Results of binding studies at pH 8.0 using isothermal titration calorimetry.

Complex	K_d (μM)	ΔH (cal/mol)	K_{d2} / K_{d1}
Quad 3 with NADPH	4.0 ± 0.3 37.1 ± 3.0	-3000 ± 26 -9400 ± 83	9.3
Q67H:1 with NADPH	3.6 ± 0.8 53.5 ± 6.5	-5800 ± 95 -9830 ± 160	15
Q67H:1+2 with NADPH	2.7 ± 0.1 15.0 ± 0.4	-5030 ± 28 -3530 ± 32	5.6
Q67H:1+3 with NADPH	8.7 ± 0.5 51.1 ± 3.2	-8650 ± 59 -5030 ± 91	5.9
Q67H:1+4 with NADPH	17.7 ± 0.8 16.1 ± 0.5	-8540 ± 100 -14,000 ± 165	0.91
Q67H:1+2+3 with NADPH	0.21 ± 0.01 3.5 ± 0.07	-3740 ± 20 -2900 ± 75	17
Q67H R67 DHFR with NADPH[a]	0.054 ± 0.016 0.31 ± 0.06	-4800 ± 100 -2500 ± 400	5.7
Quad 3 with DHF	46 ± 0.7 2.0 ± 0.02	-8420 ± 110 -3750 ± 39	0.043
Q67H:1 with DHF	0.88 ± 0.06 2.0 ± 0.05	-6340 ± 46 -5770 ± 74	2.3
Q67H:1+2 with DHF	0.97 ± 0.04 1.1 ± 0.02	-6250 ± 44 -5740 ± 45	1.1
Q67H:1+3 with DHF	1.5 ± 0.05 20 ± 0.6	-8500 ± 260 -1100 ± 33	13
Q67H:1+4 with DHF	0.93 ± 0.03 320 ± 16	-7340 ± 31 -3360 ± 23	340
Q67H:1+2+3 with DHF	0.21 ± 0.1 0.64 ± 0.1	-7350 ± 76 -7270 ± 82	3.0
Q67H R67 DHFR with DHF[a]	0.040 ± 0.008	-8000 ± 100	identical sites

[a] Results from reference 1.

similar trend. Instead, addition of 1 Q67H mutation has a minimal effect on NADPH binding. Addition of two mutations has observable effects on binding, particularly for the Q67H:1+4 configuration, but tight binding is not observed. Only when three Q67H mutations are introduced does tighter binding begin to appear. While we would expect the Q67H:1+2+3+4 mutant to mimic the Q67H homotetramer and display 100 fold lower K_d values, we are unable to confirm this prediction due to protein aggregation.

The non-linearity between the number of Q67H mutations and the corresponding NADPH K_d values suggests conformational changes may occur. These changes could describe altered interactions between either the wild type Q67 and mutant Q67H residues and/or between the 2 ligands. The first alternative appears feasible as the Q67 residues occur very near the 222 symmetry operator and each Q67 residue interacts with its symmetry related partner. Therefore it would not be surprising if introduction of a Q67H mutation alters the position of the other member of the pair. Another possibility to explain the binding data is that the cooperativity between the 2 NADPH molecules is altered. One measure of the interligand cooperativity is given by the ratio of K_{d2}/K_{d1}. As seen in Table 4, this ratio varies from a low of 0.91 to a high of 17 depending on the number of mutations introduced as well as the positioning of the double mutants. We previously observed that this ratio varies less than 2 fold when studying NADPH binding to various homotetrameric R67 DHFR mutants (Q67H, I68L, Y69F; refs 1,7). This minimal variance of the K_{d2} to K_{d1} ratio was striking as the K_d values themselves varied over 3 orders of magnitude! From those studies, we concluded that interligand cooperativity is important in binding and catalysis in R67 DHFR and must be linked to the symmetry of the active site pore. Therefore the data given in Table 4 are the first

examples of varying levels of cooperativity associated with NADPH binding to R67 DHFR. We also find support for interligand cooperativity modulating the nonlinear effects of the asymmetric Q67H mutations on NADPH binding as the transition from a relatively linear relationship between the number of mutations and log K_d to a clearly non-linear relationship occurs as the binding stoichiometry goes from one ($NADP^+$) to two (NADPH). This difference suggests the conformational changes could also arise from ligand-ligand interactions. The main differences between $NADP^+$ and NADPH are the positive charge and aromaticity of the nicotinamide ring in $NADP^+$.

In contrast to the above results with NADPH, binding of DHF shows a clear effect upon addition of one Q67H mutation. Binding is tightened to the first DHF molecule by a factor of 52, suggesting a direct interaction between the Q67H mutation and DHF. The second K_d is also tight. Since the remaining residues are wt, this result suggests positive cooperativity remains between the two DHF molecules. Addition of 2 mutations shows varying results, depending on the configuration of the Q67H residues. For the Q67H:1+2 double mutant, both K_d values are relatively tight, suggesting either that each DHF is responding to the presence of the Q67H and Q167H mutations at the "floor and ceiling" of the pore, or that positive cooperativity remains between the two DHF molecules. For the Q67H:1+3 and Q67H:1+4 double mutants, positive cooperativity between the DHF molecules clearly does not occur and 2 possibilities can be envisioned to explain the binding pattern. Either the two DHF molecules now bind differently enough so that negative cooperativity occurs between them *or* binding of the first DHF molecule is tight due to the presence of the Q67H mutations while binding of the second DHF molecule remains weak due to the interactions with the wt Q67 residues.

For the latter, minimal to no DHF-DHF interactions would be expected. Alternatively, conformational changes associated with the mutations may be occurring as the K_ds for the Q67H:1 mutant are different from the Q67H:1+4 mutant. In these mutants, either 1 or 2 mutations occur at one interface while the other interface possesses only wt residues. If the second DHF binding event was responding only to the wt Q167-Q267 residues, then similar values would be expected for these K_ds. This is not observed. Finally, the introduction of 3 Q67H mutations also tightens binding to both DHF sites, although the effect is not as dramatic as for NADPH binding. That 3 mutations can continue to affect the first K_d also supports a model where conformational changes are occurring, either via altered interactions between the wild type Q67 and mutant Q67H residues and/or between the 2 ligands. The latter model where ligand-ligand interactions influence the binding behavior remains feasible, as positive cooperativity between DHF molecules is observed in Quad 3 while no to negative cooperativity patterns are detected for the various Q67H asymmetric mutants.

Addition of DHF to R67 DHFR•$NADP^+$ to form a ternary complex was additionally monitored by ITC methods. The K_d values are given in Table 5. Only minor variations are observed, indicating the affinity of DHF for R67 DHFR•$NADP^+$ remains fairly constant throughout this series. To monitor interligand cooperativity between DHF and $NADP^+$, we have continued to use a ratio of the K_d for the second binding event divided by the K_d for the first binding event. In this case, the ratio is the K_d of DHF binding to R67 DHFR•$NADP^+$ divided by the K_d for $NADP^+$ binding to R67 DHFR. The cooperativity values remain mostly constant and indicate positive cooperativity between

Table 5. Ternary complex formation monitored by ITC.

Complex	K_d (μM)	ΔH (cal/mol)	stoichiometry	$K_{d\ (DHF\ ternary)}$/ $K_{d\ (NADP^+\ binary)}$
Quad 3 • $NADP^+$ with DHF	4.9 ± 0.1	-11500 ± 800	0.99 ± 0.01	0.16
Q67H:1 • $NADP^+$ with DHF	2.2 ± 0.05	-11400 ± 940	1.0 ± 0.01	0.11
Q67H:1+2 • $NADP^+$ with DHF	4.5 ± 0.1	-9400 ± 400	0.94 ± 0.01	0.34
Q67H:1+3 • $NADP^+$ with DHF	4.8 ± 0.1	-9400 ± 600	1.07 ± 0.01	0.31
Q67H:1+4 • $NADP^+$ with DHF	2.0 ± 0.05	-10000 ± 370	1.03 ± 0.01	0.18
Q67H:1+2+3 • $NADP^+$ with DHF	6.6 ± 0.2	-8500 ± 590	1.01 ± 0.03	1.6
Q67H R67 DHFR • $NADP^+$ with DHF[a]	6.7 ± 0.3	-9000 ± 450	0.82 ± 0.04	2.0

[a] Results from reference 1.

the ligands, except for the Q67H:1+2+3 mutant, which indicates negligible or a slight negative cooperativity.

Steady state kinetics of asymmetric mutants

The asymmetric mutants were additionally evaluated by steady state kinetic analysis. The values were readily determined for Q67H:1 using SAS to globally fit all the data to the Michaelis Menton equation describing bisubstrate kinetics. The data and a 3D representation of the fit are shown in Figure 4a; best fit values are given in Table 1. Each grid line on the 3D plot corresponds to a constant first ligand concentration with varying second ligand concentrations (and vice versa). The K_m values both decrease ~1.5 fold and k_{cat} decreases 3 fold. These values agree with those determined by data linearization, followed by secondary replots (*22, 23*).

Analysis of the kinetic data for the other mutants is less straightforward as they display various levels of substrate and cofactor inhibition. Therefore a rate equation (eq 1) was derived for the mechanism describing inhibition associated with formation of the 2 non-productive complexes, NADPH•NADPH or DHF•DHF (*4*). The steady state kinetic data were then fit globally using SAS; the K_d values obtained by ITC were entered as constraints. Since the mechanism predicts formation of the NADPH•NADPH or DHF•DHF complexes as well as the productive NADPH•DHF complex, this fitting method requires data to cover a wide range of substrate/cofactor "space" describing catalysis as well as inhibition. Therefore >130 but <370 data points were used in these fits.

Figure 4. Steady state kinetic data for various R67 DHFRs. Panel A describes the Q67H:1 R67 DHFR, which was fit to the Michaelis-Menton equation describing bisubstrate kinetics using SAS. Data points above and below the calculated 3D plot are filled and hollow stars respectively. Panel B describes the Q67H homotetramer data (Park et al., 1997a). This representation reverses the axes for [DHF] and [NADPH] to accentuate a "ridgeline" of maximal activity. Nonlinear fitting was performed by SAS to equation 1 and Table 1 gives the best fit values. K_d values derived from ITC data were used as constraints in fitting with 2-3 fold variations accepted if the ITC data could be reasonably refit with these values. Panel C describes the Q67H:1+2 data as well as its accompanying 3D fit. The plots for the Q67H:1+3 and Q67H:1+4 double mutants are given as supplementary information in the appendix.

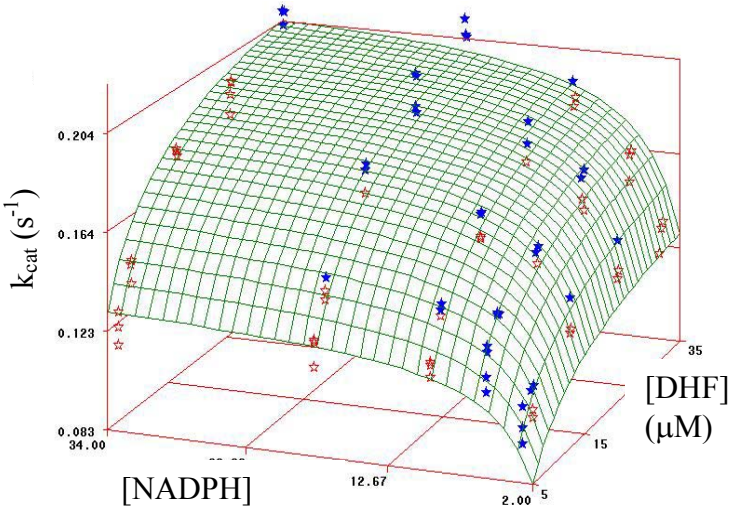
A
k_{cat} (s^{-1})
0.204
0.164
0.123
0.083
34.00
12.67
2.00
[NADPH]
35
15
5
[DHF] (μM)

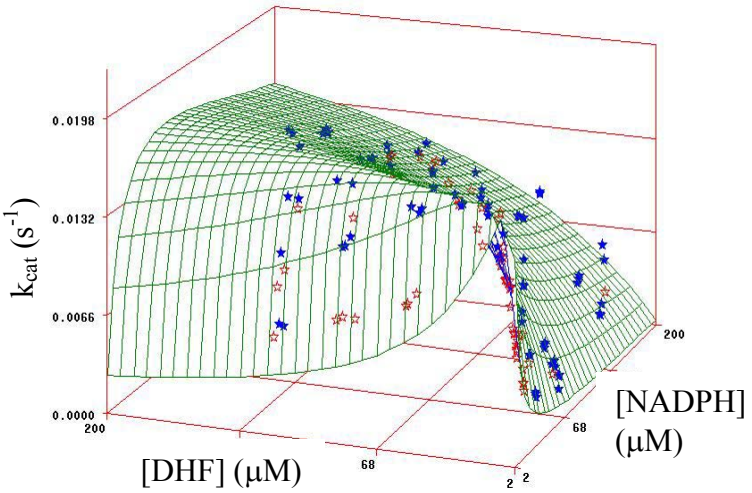
B
k_{cat} (s^{-1})
0.0198
0.0132
0.0066
0.0000
200
68
2
[DHF] (μM)
200
68
2
[NADPH] (μM)

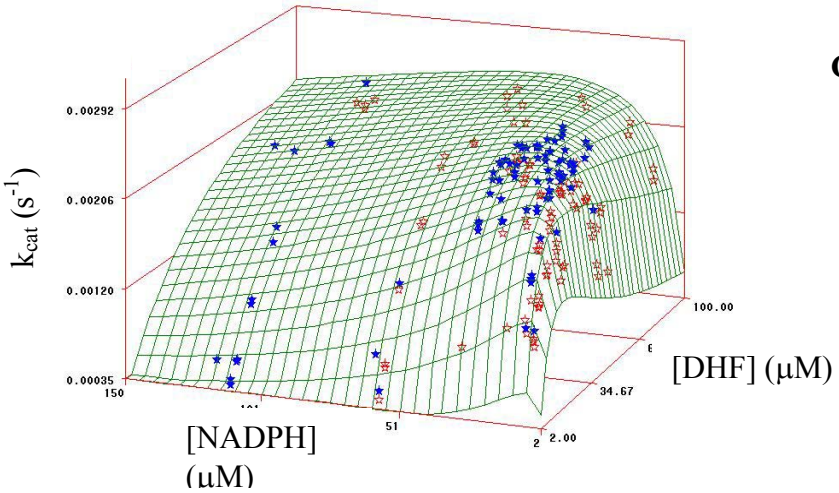
C
k_{cat} (s^{-1})
0.00292
0.00206
0.00120
0.00035
150
51
2
[NADPH] (μM)
100.00
34.67
2.00
[DHF] (μM)

Since global nonlinear SAS analysis of steady state kinetic data to a complicated rate equation is a new approach, we first confirmed its ability to fit the Q67H homotetramer data that had previously been analyzed with the computer program, FITSIM (*1,31*). Our FITSIM analysis at that time indicated the Q67H homotetramer data could not be fit well without varying the ITC K_d values 2-3 fold. These alterations arose as NADPH was observed to be more inhibitory than DHF, even though the K_d values were similar. To fit the kinetic data, both NADPH K_d values were decreased 3 fold and both DHF K_d values were increased 2 fold. In this scenario, NADPH binds more tightly than DHF, providing more inhibition. SAS was able to identify this solution. In addition, SAS identified a second possibility where the cooperativity patterns were altered. In this solution, neither K_{d1} for NADPH or DHF were altered, but reduced negative cooperativity was proposed between the two NADPH molecules as well as the introduction of negative cooperativity between the two DHF molecules. In this second model, the NADPH•NADPH complex forms more easily than expected as its K_d values are closer, while it is harder to form the DHF•DHF complex as its K_d values are farther apart. A comparison of the correlation coefficient (R^2) for these 2 different fits supports the first SAS solution. Figure 4b shows the data overlaid on a 3D representation of the fit for the Q67H homotetramer. A good fit is observed with a R^2 value of 91%; best fit values are given in Table 1. This analysis clearly validates the SAS global fitting approach.

Analysis of the steady state kinetic data for the other asymmetric mutants was therefore performed using SAS. The data set for the Q67H:1+2 mutant as well as a 3D representation of the fit are given in Figure 4c. The data and 3D plots show

substrate/cofactor inhibition at low second ligand concentrations. The fit values for this asymmetric mutant as well as the others are given in Table 1.

Each double mutant displays different kinetic behavior, indicating the various topologies generate different responses. The Q67H:1+2 double mutant displays obvious cofactor inhibition, its k_{cat} value decreases ~3 fold and K_m values decrease ~16 and 2 fold for NADPH and DHF respectively, leading to a 4 fold increase in $k_{cat}/K_{m\ (NADPH)}$. The next double mutant, Q67H:1+3, exhibits cofactor and substrate inhibition (particularly at low second ligand concentration) as well as a ~4 fold decrease in k_{cat}, a 2.5 fold decrease in $K_{m\ (NADPH)}$ and a slight (1.6 fold) *increase* in $K_{m\ (DHF)}$. The Q67H:1+4 double mutant displays no obvious substrate or cofactor inhibition and is readily saturated. While k_{cat} decreases ~6 fold, $K_{m\ (NADPH)}$ decreases 5 fold, yielding an approximately equal $k_{cat}/K_{m\ (NADPH)}$ value to that of Quad 3. $K_{m\ (DHF)}$ decreases approximately 3 fold. The Q67H:1+2 double mutant is the most functional with respect to $k_{cat}/K_{m\ (NADPH)}$ values while the Q67H:1+4 double mutant maintains its catalytic efficiency with no obvious substrate/cofactor inhibition. In fact, a fit of the Q67H:1+4 data to the bisubstrate kinetics equation provides very similar fit values.

The triple mutant shows more obvious NADPH and DHF inhibition, and the corresponding fit indicates a further decrease in k_{cat}, and K_m values that remain within the range of the double mutants. The quadruple mutant displays increasing levels of NADPH and DHF inhibition, similar to that of the Q67H homotetramer (*1*). The data set for the Q67H:1+2+3+4 mutant was fit using the ITC K_d values measured for the Q67H homotetramer as constraints; the values were allowed to deviate up to 4 fold (within range of the Q67H:1+2+3 mutant). For the quadruple mutant, k_{cat} decreases 8 fold with

respect to Quad 3, while $K_{m\,(NADPH)}$ decreases 170 fold and $K_{m\,(DHF)}$ decreases 48 fold. This leads to a 21 fold increase in $k_{cat} / K_{m\,(NADPH)}$ which is accompanied by tighter binding of NADPH and DHF at symmetry related sites, resulting in severe cofactor/substrate inhibition. The similarity between kinetic values suggests the Q67H:1+2+3+4 quadruple mutant mimics the Q67H homotetramer reasonably well.

To deal with fitting the kinetic data, SAS varied the K_d constraints by various combinations of 2 approaches: by either maintaining the cooperativity but changing the overall K_d values 2-3 fold (the Q67H:1+2+3, Q67H:1+2+3+4 and Q67H homotetramer data sets) and/or by altering the cooperativity between ligands. For example, in the Q67H:1+2 data set, negative cooperativity between NADPH molecules was weakened (8 fold) while negative cooperativity between the two DHF molecules was enhanced (2 fold). For the Q67H:1+3 data set, cooperativity between NADPH molecules was maintained while binding was strengthened (3 fold), but the negative cooperativity between DHF molecules was enhanced (6 fold). For the Q67H:1+4 data set, negative cooperativity was enhanced between NADPH molecules (9 fold, ie a 3 fold tighter binding of the first NADPH and a 3 fold weaker binding of the second NADPH), while negative cooperativity was weakened between DHF molecules (7 fold). To fit the kinetic data with reasonable R^2 values required changes in the ITC constraints. Two to three fold changes in K_d values were tolerated by the ITC refits reasonably well.

Effects of the mutations on protein structure

To confirm that all the Quad 3 protein variants are monomeric, gel filtration studies were performed to assess how the oligomeric state varies as a function of pH. All measurements confirm the protein is a monomer at both pHs 5 and 8 (data not shown).

We further assessed the level of structural change by monitoring the equilibrium between "closed" and "open" forms of the quadruplicated gene product (which correspond to the tetrameric and dimeric forms in wt R67 DHFR) using protein fluorescence. This titration monitors the pK_a of the symmetry related H62 residues (of which 3 remain in Quad 3 as it contains a complementing S59A and H362L pair) by the fluorescence of nearby W38 residues (*11,12*). The behavior of Quad 3 continues to mimic that of Quad 1 while the Q67H mutations slightly destabilize the "closed" structure (see Figure 8 and Table 6 in the appendix). All proteins are in the active ("closed") form for activity measurements at pH 7 and ITC measurements at pH 8.

Since the non-additive nature of the kinetic and binding data suggest either a conformational change in the protein or alterations in the ligand-ligand interactions, we assessed the effect of the mutations on protein structure by CD measurements. There is some variation in the CD signal (not shown). The largest change is observed in the Q67H:1+2+3+4 mutant, however this signal change correlates with that previously seen for the Q67H homotetramer (*1*). While these spectral changes may reflect some degree of conformational change, they also could arise from the proximity of the Q67H mutation to W38 (~3.7-4A), as Woody (*32*) indicates aromatic side changes can make detectable contributions to the far-UV CD signal.

Discussion

The Q67H homotetramer has been observed to bind both NADPH and DHF more tightly ($\geq$100 fold) than wild type R67 DHFR (*1*). Linked to this behavior was a 6.8 fold decrease in k_{cat}, resulting in a 3.6 fold enhancement in $k_{cat}/K_{m\ (NADPH)}$. However the ability of the Q67H mutant to reach its transition state was compromised by tighter

binding of a second identical ligand at a symmetry related site, leading to substantial cofactor and substrate inhibition. Therefore the symmetry in the active site pore imposes a balance between catalysis and inhibition. Introduction of asymmetric mutations was pursued to determine if tight binding of the transition state could be uncoupled from inhibition. We reasoned if addition of 1-2 mutations was sufficient to tighten binding at one binding surface, the remaining wildtype residues at the other binding surface might not invoke tight binding and inhibition could be blocked. We address these linked issues by discussing the interligand cooperativities as measured by ITC, followed by steady state kinetic analysis.

What is the role of interligand cooperativity in R67 DHFR?

Our previous mutations at Q67, I68 and Y69 in the context of the homotetramer (i.e. 4 mutations per active site pore) show minimal to no changes in NADPH cooperativity over a 1000 fold change in binding affinity (*1,7*). We previously interpreted this result as indicating either changes in affinity occur at all symmetry related sites leading to similar effects and/or that interligand cooperativity is quite important in ligand binding/catalysis. This is the first case where significant changes in NADPH cooperativities have been observed in R67 DHFR. Essentially no cooperativity between 2 NADPH molecules is observed for the Q67H:1+4 double mutant while a 17 fold difference exists between the K_d values for the Q67H:1+2+3 mutant. Further the DHF•DHF interaction varies dramatically with Quad 3 displaying positive cooperativity and the Q67H:1+4 mutant possessing either independent sites or negative cooperativity. The range of K_{d2}/K_{d1} for DHF binding varies from 0.043 to 340, a 7,900 fold effect. Formation of the $NADP^+$•DHF ternary complex also shows effects over a 10 fold range.

That the cooperativity between $NADP^+$ and DHF is least affected suggests a preference for the hetero-ligand complex, a catalytic advantage that R67 DHFR utilizes.

Figure 5 compares the cooperativities between the various 2 ligand complexes, where cooperativity measures the K_d for binding of the second ligand divided by the K_d for binding the first ligand. Quad 3 shows negative cooperativity between the 2 NADPH molecules, positive cooperativity between the two DHF molecules and positive cooperativity between $NADP^+$ and DHF, i.e. ternary complex formation. To increase catalytic efficiency, these traits should either be enhanced or alternately, the strong positive cooperativity between the two DHF molecules could theoretically be replaced by a strong negative cooperativity. Negative cooperativity patterns are observed for the Q67H:1+3 and Q67H:1+4 double mutants. How does this translate into steady state kinetic behavior? Also the cooperativity ratios for the triple mutant show the most convergence. Does this correlate with an inability to discriminate between the various complexes?

Patterns of steady state kinetic behavior

As discussed above, 2 issues arise in R67 DHFR catalysis. The first is stabilization of the productive ternary complex leading to the transition state. The second issue arising from the 222 symmetry of the active site pore is competing formation of inhibitory complexes. To express this in an energy landscape perspective, R67 DHFR binds 3 complexes, DHF•DHF, NADPH•NADPH or NADPH•DHF. To enhance catalysis, R67 DHFR can either stabilize the NADPH•DHF complex and/or destabilize

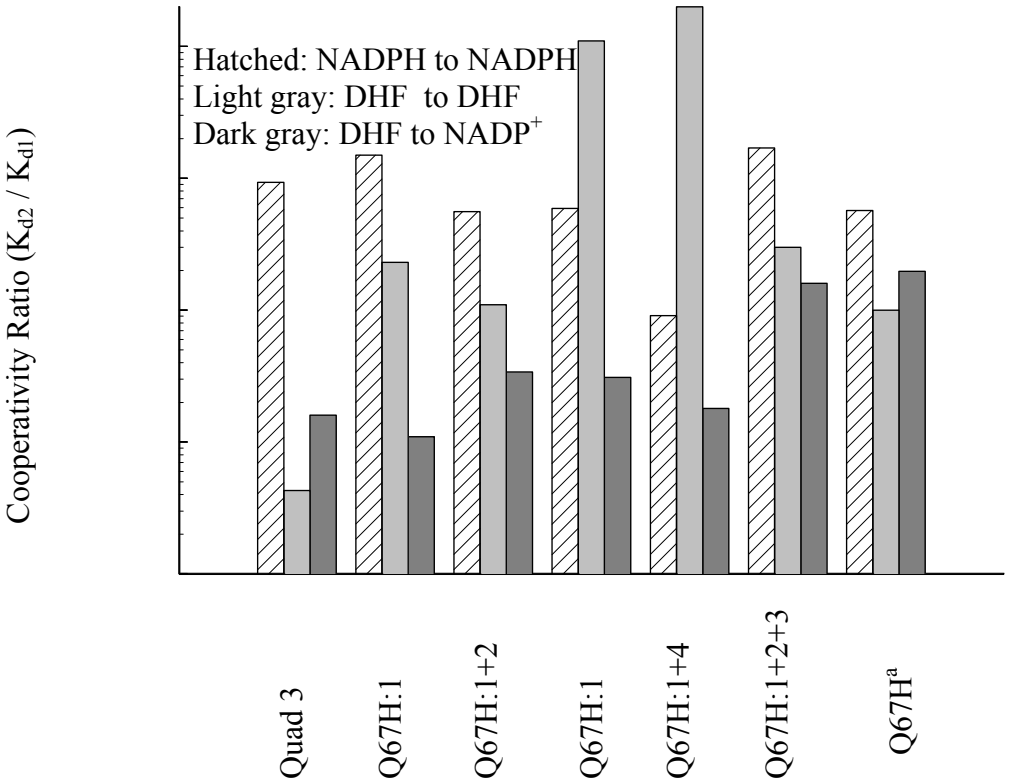

Figure 5. A bar graph comparing cooperativity ratios for the various protein constructs. The cooperativity between the first and second bound NADPH molecules (hatched bar) is described by K_{d2} / K_{d1} (see Table 4). The cooperativity between the DHF molecules (light gray bar) is given by K_{d2} / K_{d1} (see Table 4). The cooperativity between $NADP^+$ and DHF (dark gray bar) is given by $K_{d\ DHF\ ternary} / K_{d\ NADP+\ binary}$ (see Table 5). Data for the Q67H homotetramer were from reference 1.

the NADPH•NADPH and DHF•DHF complexes. The latter approach is termed negative design (*33-35*).

This second issue arises when considering the steady state kinetic behavior of the Q67H mutation series. Increasing levels of substrate/cofactor inhibition are noted as the number of mutations increases, with Quad 3 showing no evidence of inhibition in the assay concentrations used (6-121μM NADPH, 4-112 μM DHF), the double mutants exhibiting zero to moderate levels of inhibition and the triple and quadruple mutants displaying severe inhibition. Quad 3 appears to have evolved a reasonable binding surface that achieves a low free energy state for the NADPH•DHF complex coupled with a large free energy difference between productive and non-productive complexes. While addition of Q67H mutations slightly alters binding to the NADPH•DHF complex, a large energy difference between the NADPH•DHF complex and the NADPH•NADPH and DHF•DHF states is no longer maintained, resulting in increasing levels of inhibition.

The competition between the three ligation states can clearly be seen in the 3D plots describing bisubstrate kinetics. We begin this discussion considering the simple 3D plot for Q67H:1 which shows no inhibition at the concentrations shown (figure 4a). Hyperbolic (2D) plots can be seen on all 4 vertical edges of the cube and a plateau can be seen at the upper back corner of the cube as Q67H:1 approaches its k_{cat} value (0.23 sec^{-1}) at a 1:1 ratio of DHF to NADPH. In contrast, the Q67H homotetramer (Figure 4b) shows that at low levels of DHF, addition of NADPH is inhibitory due to formation of the NADPH•NADPH complex (2D plot on right face of cube). At high concentrations of NADPH, addition of DHF displays hyperbolic kinetics (back face of cube), but since the

enzyme is strongly inhibited due to formation of the NADPH•NADPH complex, the only possibility is for the activity to rise. This curve does not reach k_{cat} (0.025 sec^{-1}) as there is always some level of inhibition present. At low levels of NADPH, addition of DHF is inhibitory due to formation of the DHF•DHF complex (front face of cube). At high concentrations of DHF, addition of NADPH shows initial hyperbolic kinetics followed by inhibition (left face of cube). Again since the enzyme is strongly inhibited under these high DHF conditions, the activity can only increase. The rate increases until the NADPH concentration becomes high enough to be inhibitory and the NADPH•NADPH complex forms (back corner of cube). The k_{cat} is never reached anywhere on the surface of this 3D plot. A "ridgeline" that describes maximal activity can be clearly seen. The "ridgeline" appears to correspond to a 1:1 ratio of DHF to NADPH, modified by the relative inhibitory capacities of the DHF•DHF to the NADPH•NADPH complexes.

Another way to consider the kinetic results is that the cooperativity patterns for the various double mutants vary substantially, yet k_{cat} is barely affected. This behavior indicates the cooperativity associated with reaching the productive ternary complex state has not changed dramatically (see Table 5). What has changed is the ability of the NADPH•NADPH and/or DHF•DHF complexes to compete favorably for formation. When these dead-end complexes readily form, the ability of the mutant enzyme to reach k_{cat} decreases. This is clearly shown in Figure 4b for the Q67H homotetramer.

Role of Q67H in interligand interactions?

Gene duplication followed by divergence is commonly proposed as a mechanism of enzyme evolution. In this study, we quadruplicated the gene for R67 DHFR and

introduced various combinations of Q67H mutations. While addition of the Q67H mutation in the homotetramer tightens binding to both ligands by a factor of 100, this effect does not appear in an additive fashion as increasing numbers of Q67H mutations are added asymmetrically to the quadruplicated gene product. This study of gradually breaking the symmetry of the binding surface suggests one consequence of the symmetry is overdetermination of the binding interactions, particularly for the heteroligand complex. While addition of a single Q67H mutation might be expected to provide one mutation has minimal effects on catalysis. For example while similar K_d values for tight binding interaction that would enhance binding, we find introduction of a single binding two DHF molecules leads to the prediction of DHF inhibition in the Q67H:1 variant, none is observed. This suggests the remaining wt sites maintain their function and are strongly preferred during catalysis. If a pair of Q67 residues need to interact to provide one tight binding surface, then the Q67H:1+4 double mutant would be expected to enhance binding as these mutations form a pairwise interaction. This double mutant shows larger effects on ligand binding, but minimal effects on k_{cat}, again suggesting an overdetermination of the binding sites with a preference for wt sites. As 3-4 mutations are added, increasing effects on catalysis are noted, with the ability of the enzyme to discriminate between the productive ternary complex and nonproductive homoligand complexes becoming compromised. While the 222 symmetry in R67 DHFR imposes numerous deleterious effects on binding and catalysis, overdetermination of the binding site suggests an evolutionary advantage for symmetry as asymmetric mutations are introduced.

An alternate, but linked, point of view suggests that while protein interactions are important, the symmetry in R67 DHFR has selected for a strong influence arising from hetero-ligand interactions. While the $NADP^+$•DHF complex is not the catalytic species, it provides a reasonable mimic. The ternary complex K_d values (Table 5) as well as the k_{cat} values (Table 1) suggest that the hetero-ligand interactions are maintained (for the most part) in all the asymmetric mutants and perhaps drive binding. Additional support for this point of view comes from an *ab initio* quantum mechanical calculation that predicts the *endo* transition state (where the nicotinamide ring overlaps the more bulky side of the pteridine ring) is 2-8 kcal/mol more stable than the *exo* transition state (with minimal overlap of the pteridine and nicotinamide rings; *36,37*). Interligand NOE NMR data also favor R67 DHFR using an *endo* transition state (*5*) as do our docking studies focused on generating a ternary complex model (*6*). Some degree of ring stacking may allow R67 DHFR to partition binding towards the ternary complex.

While Q67 appears to play a minimal role in formation of the NADPH•DHF complex, it appears more active in discriminating against formation of the NADPH•NADPH and DHF•DHF complexes. To describe how the Q67H mutations affect the 2DHF and 2NADPH complexes will require better models of these complexes. From the crystal structure of R67 DHFR•folate•folate, the N1 and N3 containing rings of the pteridine moieties overlap (*3*). More recent studies monitoring interligand NOEs (ILOEs) in R67 DHFR (*5*) describe a folate•2-deamino-2-methyl-5,8-dideazafolate complex with a similar overlap of the N1, N3 containing rings of the pteridines. In contrast, no structural information is available about the NADPH•NADPH complex.

How does R67 DHFR differentiate between these various complexes? Perhaps a clue comes from our ITC studies that measure the enthalpies associated with ligand binding.

Figure 6 shows a plot of ΔH vs. $T\Delta S$ for the various complexes. Binding can be altered in mutant enzymes by different degrees of hydrogen bonding and van der Waals contacts which in turn can alter the degrees of freedom of the ligand and amino acid side chain (*38,39*). The former would affect ΔH, the latter, $T\Delta S$. Solvent re-organization may be involved in the effects of different ligands and mutant enzymes on ΔH and $T\Delta S$ (*40,41*). Finally any proton exchange between enzyme and buffer to which ligand binding may be coupled could also be perturbed by use of a different mutant and result in a concomitant change in the thermodynamics of ligand binding. With these caveats in mind, it is worth noting that all the asymmetric proteins in this series show binding of DHF to the R67 DHFR•$NADP^+$ complex is enthalpy driven. When trends within an enzyme variant are considered, most of the binary binding interactions for Quad 3 are enthalpy driven as are those for the Q67H:1+4 mutant. In contrast, binding in the other mutants is driven by both thermodynamic components (enthalpy and entropy).

Calderone & Williams (*42*) suggest structural tightness displays a positive correlation with the exothermicity of the binding interaction. Maintaining enthalpy-driven formation of the ternary complex in these Q67H asymmetric mutants suggests a strong role for enthalpy in catalysis. Our studies support recent reports of catalytic function that suggest a strong role for enthalpy (*43-51*).

To conclude, formation of the R67 DHFR•DHF•$NADP^+$ ternary complex is enthalpy driven, and introduction of Q67H mutations does not drastically affect its

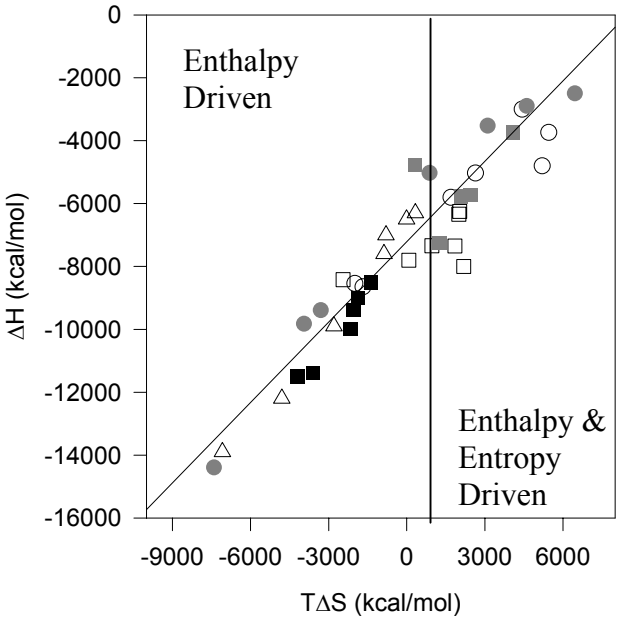

Figure 6. A plot of entropy (TΔS) versus enthalpy (ΔH) for various mutants and ligands. Binding data from Quad 3, Q67H:1, Q67H:1+2, Q67H:1+3, Q67H:1+4, Q67H:1+2+3 and the Q67H homotetramer proteins (1) are included. Values for binding the first and second NADPH molecules are given by ○ and gray filled circles. Values for binding the first and second DHF molecules are given by □ and gray filled squares. Values for binding $NADP^+$ are shown by △ and values for DHF binding to R67 DHFR•$NADP^+$ are given by ■ points. The slope of the line is 0.85 and the correlation coefficient is 0.87. A plot of ΔH versus ΔG shows no correlation (not shown).

formation. This result suggests a strong role for interligand ($NADP^+$ to DHF) interactions in complex formation. (Presumably interligand interactions would be important in the NADPH•DHF complex as well). Further, addition of increasing numbers of Q67H mutations results in the inability of the enzyme to discriminate between the productive and nonproductive complexes. These results support a role for Q67 in minimizing formation of the NADPH•NADPH and DHF•DHF complexes.

The Q67H:1+4 double mutant remains an interesting mutant as it displays minimal NADPH and DHF inhibition and it tightly binds the productive ternary complex (ΔH in table 5 as well as maintains its $k_{cat}/K_{m\ (NADPH)}$ value). This mutant may serve as a stepping stone for addition of other asymmetric mutations, leading to design of an alternate active site constellation with half the pore preferentially binding DHF and the other half binding NADPH. Further, we anticipate addition of asymmetric mutations at positions further away from the 222 symmetry operator will allow ready analysis of their effects as these substitutions will not be involved in the pairwise interactions that occur at the unusual position at the center of the pore.

Acknowledgment

We thank Cynthia Peterson for helpful advice and comments on the manuscript.

Supporting Information Available

Steady state kinetic data for Q67H:1+3 and Q67H:1+4 R67 DHFRs (Figure 7), a series of fluorescence titration curves monitoring the equilibrium between open and closed forms of Quad 3 and its mutants (Figure 8), and a table (Table 6) of pK_a values

describing the titration of Quad 3 variants from a closed to an open form are available free of charge via the Internet at http:://pubs.acs.org and are included in the appendix.

References

1. Park, H., Bradrick, T.D., and Howell, E.E. (1997) *Protein Engineering 10,* 1415-1424.
2. Brisson, N. and Hohn, T. (1984) *Gene 28,* 271-275.
3. Narayana, N., Matthews, D. A., Howell, E.E., and Xuong, N.H-. (1995) *Nature Structural Biology 2,* 1018-1025.
4. Bradrick, T.D., Beechem, J. M., and Howell, E.E. (1996) *Biochemistry 35,* 11414-11424.
5. Li, D., Levy, L.A., Gabel, S.A., Lebetkin, M.S., DeRose, E.F., Wall, M.J., Howell, E.E., and London, R.E. (2001) *Biochemistry 40,* 4242-4252.
6. Howell, E.E., Shukla, U., Hicks, S.N., Smiley, R.D., Kuhn, L.A., and Zavodszky, M.I. (2001) *J. Applied Computer-Aided Molecular Design 15,* 1035-1052.
7. Strader, M.B., Smiley, R.D., Stinnett, L., VerBerkmoes, N.C. & Howell, E.E. (2001) *Biochemistry 40*, 11344-11352.
8. Park, H., Zhuang, P., Nichols, R., and Howell, E. E. (1997) *J. Biol. Chem. 272,* 2252-2258.
9. Deng, H., Callender, R., and Howell, E.E. (2001) *J. Biol. Chem. 276,* 48956-48960.
10. Maharaj, G., Selinsky, B.S., Appleman, J.R., Perlman, M., London, R.E., and Blakley, R.L. (1990) *Biochemistry 29,* 4554-4560.
11. Nichols, R., Weaver, C.D., Eisenstein, E., Blakley, R.L., Huang, T-H., Huang, F-Y., and Howell, E.E. (1993) *Biochemistry 32,* 1695-1706.

12. Bradrick, T.D., Shattuck, C., Strader, M.B., Wicker, C., Eisenstein, E., and Howell, E.E. (1996b) *J. Biol. Chem. 271,* 28031-28037.

13. Brocchierei, L., and Karlin, S. (1994) *Proc. Natl. Acad. Sci. 91,* 9297-9301.

14. Hakoshima, T. -I., Itoh, T., Tomita, K. -I., Goda, K., Nishikawa, S., Morioka, H., Uesugi, S. -I., Ohtsuka, E., and Ihehara, M. (1992) *J. Mol. Biol. 223,* 1013-1028.

15. Sapse, A. M., Schweitzer, B. S., Diker, A. P., Bertino, J. R. and Frecer, V. (1992) *Int. J. Pept. Res. 39,* 18-23.

16. Reece, L.J., Nichols, R., Ogden, R.C., and Howell, E.E. (1991) *Biochemistry 30,* 10895-10904.

17. Strader, M.B. and Howell, E.E. (1997) *Gibco-BRL Focus 19,* 24-25

18. Wiseman,T., Williston, S., Brandts, J.F., and Lin, L.-N. (1989) *Anal. Biochem. 179,* 131-137.

19. Ellis, K.J., and Morrison, J.F. (1982) *Methods Enzymol. 87,* 405-426.

20. Howell, E.E., Warren, M.S., Booth, C.L.J., Villafranca, J.E., and Kraut, J. (1987) Biochemistry 26, 8591-8598.

21. Segel, I.H. (1975) *Enzyme Kinetics,* John Wiley and Sons, New York.

22. Cleland, W.W. (1963*) Biochim. Biophs. Acta 67,* 104-137.

23. Smiley, R.D., Hicks, S.N., Stinnett, L.G., Howell, E.E., & Saxton, A.M., (2002) *Anal. Biochem. 301,* 153-156.

24. Gornall, A.G., Bardawill, C.J., and David, M.M. (1949) *J. Biol. Chem. 177,* 751-766.

25. Blakley, R.L. (1960) *Nature 188,* 231-232.

26. Horecker, B.L., and Kornberg, A. (1948) *J. Biol. Chem. 175,* 325-390.

27. Baccanari, D., Phillips, A., Smith, S., Sinski, D., and Burchall, J. (1975) *Biochemistry 14,* 5267-5273.

28. Flensburg, J. and Steen, R. (1986) *Nucleic Acids Res. 14,* 5933.

29. Dam, J., Rose, T., Goldberg, M.E, and Blondel, A. (2000) *J. Mol. Biol. 302,* 235-250.

30. Wells, J.A. (1990) *Biochemistry 29,* 8509-8517.

31. Zimmerle, C.T., and Frieden, C. (1989) *Biochem. J. 258,* 381-387.

32. Woody, R.W. (1995) *Methods Enzymol. 246,* 34-71.

33. Richardson, J.S. and Richardson, D. C. (2002) *Proc Natl Acad Sci 99,* 2754-2759.

34. Hellinga, H. (1998) *J. Amer. Chem. Soc., 120,* 10055-10066.

35. Hecht, M.H., Richardson, J.S., Richardson, D.C. and Ogden, R.C. (1990) *Science 249,* 884-891.

36. Andres, J., Moliner, V., Safont, V.S., Domingo, L.R., Picher, M.T., and Krechl J. (1996) Bioorg. Chem. 24, 10-18.

37. Castillo, R., Andres, J., and Moliner, V. (1999) *J. Am. Chem. Soc. 121,* 12140-12147.

38. Gilli, P., Ferretti, V., Gilli, G., and Borea, P.A. (1994) *J. Phys. Chem. 98,* 1515-1518.

39. Dunitz, J.D. (1995) *Chem. Biol. 2,* 709-712.

40. Chervenak, M.C., and Toone, E.J. (1994) *J. Am. Chem. Soc. 116,* 10533-10539.

41. Grunwald, E. and Steel, C. (1995) *J. Am. Chem. Soc. 117,* 5687-5692.

42. Calderone, C.T., and Williams, D.H. (2001) *J. Amer. Chem. Soc. 123,* 6262-6267.

43. Bruice, T.C. (2001) *Acc. Chem. Research 35,* 139-148.

44. Bruice, T.C. and Benkovic, S.J. (2000) *Biochemistry 3,* 6267-6274.

45. Bruice, T.C. and Lightstone, F.C. (1999) *Acc. Chem. Research 32,* 127-136.

46. Shurki, A., Strajbl, M., Villa, J., and Warshel, A. (2002) *J. Amer. Chem. Soc. 124,* 4097-4107.

47. Snider, M.J., Gaunitz, S., Ridgway, C., Short, S.A. and Wolfenden R. (2000) *Biochemistry 39,* 9746-9743.

48. Snider, M.J., Lazarevic, D., and Wolfenden, R. (2002) *Biochemistry 41,* 3925-30

49. Villa, J., Strajbl, M., Glennon, T.M., Sham, Y.Y., Chu, Z.T., and Warshel, A. (2000) *Proc. Natl. Acad. Sci.* 97, 11899-11904.

50. Wolfenden, R., Snider, M., Ridgway, C. and Miller, B. (1999) *J. Amer. Chem. Soc. 121,* 7419-7420.

51. Wolfenden, R., and Snider, M. (2001) *Acc. Chem. Res. 34,* 938-945.

52. Cantor, C.R., and Schimmel, P.R. (1980) Biophysical Chemistry Part II, The Behavior of *Biological Macromolecules,* W.H. Freeman & Co., San Francisco.

Appendix

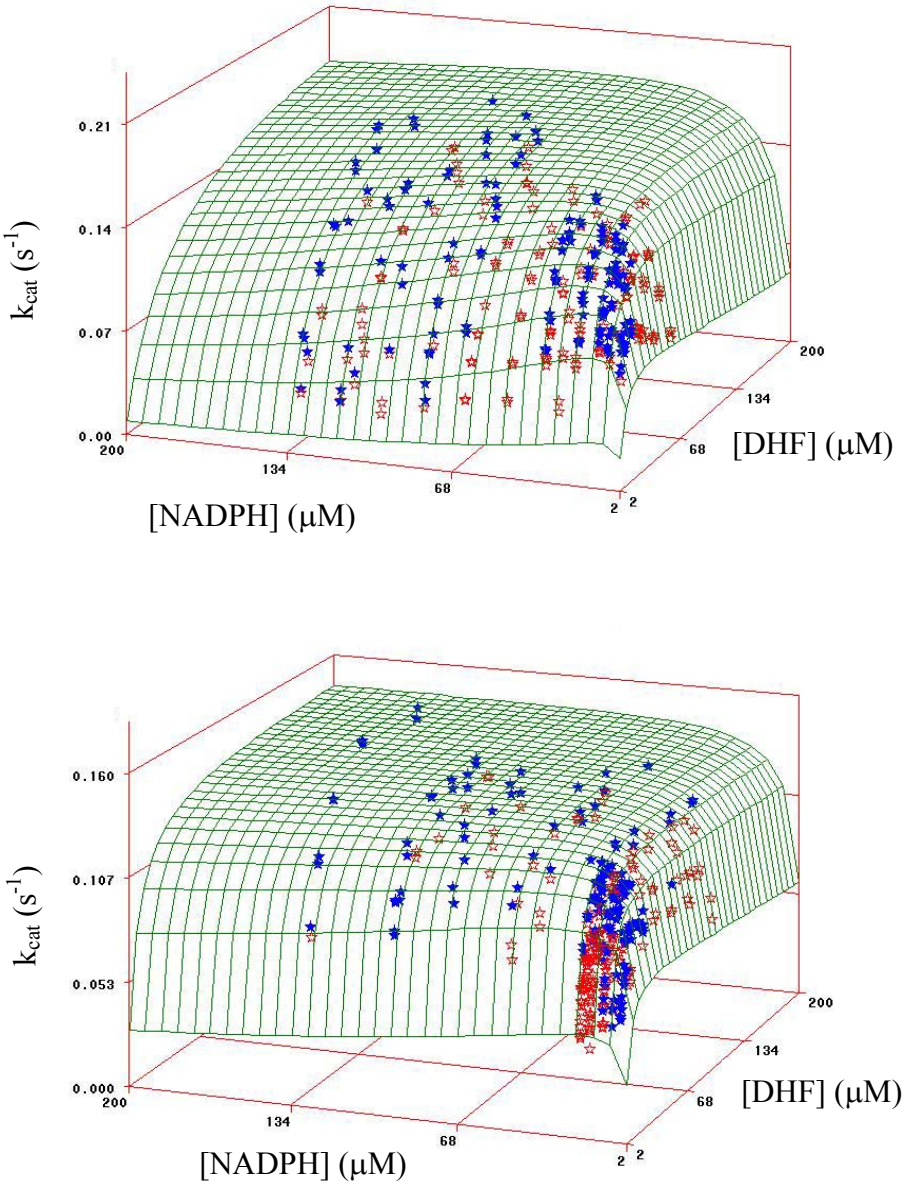

Figure 7. Steady state kinetic data for Q67H:1+3 (top panel) and Q67H:1+4 R67 DHFRs (bottom panel). Nonlinear fitting to equation 1 was performed using SAS and Table 1 gives the best fit values. Data points above and below the calculated 3D plot are filled and hollow stars respectively. K_d values derived from ITC data were used as constraints in fitting with 2-3 fold variations accepted if the ITC data could be reasonably refit with these values.

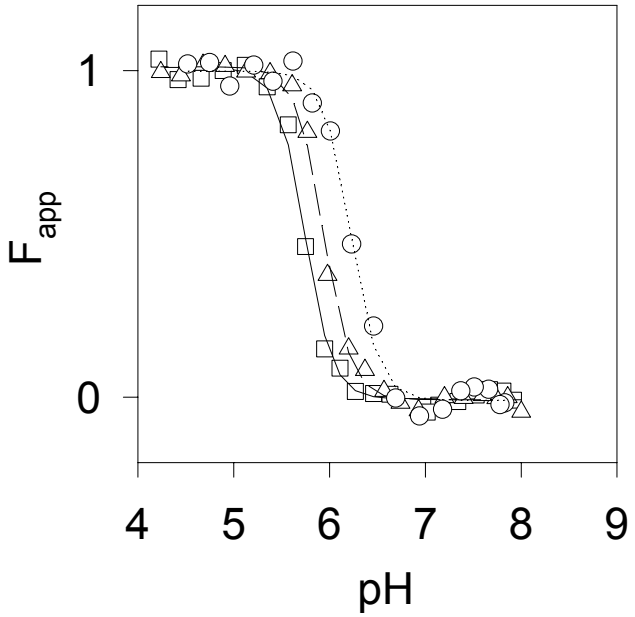

Figure 8. A series of fluorescence titration curves monitoring the equilibrium between "open" and "closed" forms of Quad 3 and its mutants. This equilibrium corresponds to titration of H62 residues. In wt R67 DHFR, titration of H62 is linked to a tetramer to 2 dimers equilibrium (*11-12*). Fluorescence data were converted to a fraction to aid comparison. The □ points and solid line correspond to the Quad 3 protein; the Δ points and the dashed line correspond to the Q67H:1 mutant; the ○ points and dotted line correspond to the Q67H:1+2 double mutant. The other 4 proteins are not shown for clarity. Best fit pK_a values associated with the titrations are given in the Table 6.

Table 6. A comparison of pK_a values describing titration of Quad 3 variants from a "closed" to an "open" form as monitored by fluorescence.

DHFR Variant	pK_a
Quad 1[a]	5.5
Quad 3	5.74 ± 0.01
Q67H:1	5.92 ± 0.02
Q67H:1+2	6.22 ± 0.02
Q67H:1+3	6.02 ± 0.03
Q67H:1+4	6.00 ± 0.02
Q67H:1+2+3	6.11 ± 0.03
Q67H:1+2+3+4	6.06 ± 0.07

[a] Value from reference 12.

Part III: Determining the Role of Symmetry Related Y69 Residues in Ligand Binding and Catalysis in R67 Dihydrofolate Reductase

The section is being submitted to the *Journal of Biological Chemistry*:

Lori G. Stinnett, R. Derike Smiley, Stephanie N. Hicks, and Elizabeth E. Howell. (submitted). **Determining the Role of Symmetry Related Y69 Residues in Ligand Binding and Catalysis in R67 Dihydrofolate Reductase.** *Journal of Biological Chemistry.*

This author contributed the following to the manuscript: (1) protein expression and purification, (2) protein extinction coefficients, (3) isothermal titration calorimetry data, (4) steady state kinetic data, (5) circular discroism spectroscopy data, (6) pH titration data, (7) manuscript preparation. This work was supported by NSF grant MCB-0131394 (to E.E.H)

Abstract

R67 dihydrofolate reductase reduces dihydrofolate to tetrahydrofolate where the cofactor, NADPH, is required for the hydride transfer reaction. The homotetrameric enzyme provides a unique environment for catalysis as both ligands bind within a single active site pore. Mutation of one active site residue results in concurrent mutation of three additional symmetry related residues, and large effects on binding of both ligands as well as catalysis. For example, mutation of symmetry related tyrosine 69 to phenylalanine (Y69F), results in large increases in K_m values for *both* ligands and a two fold rise in the k_{cat} for the reaction [Strader, M. B. et al. (2001) *Biochemistry 40*, 11344-11352]. To understand the interactions between specific Y69 residues and each ligand, asymmetric Y69F mutants were generated which contain one, two, three, or four Y69F mutations. A general trend observed from isothermal titration calorimetry and steady-state kinetic studies of these asymmetric mutants is that increasing the number of Y69F mutations results in an increase in the K_d and K_m values. In addition, a comparison of steady state kinetic values suggests that *two* Y69 residues on one side of the active site pore are necessary for NADPH to exhibit a wild-type K_m value. A tyrosine 69 to leucine

(Y69L) R67 DHFR homotetrameric mutant was also generated to approach the *type(s)* of interaction(s) occurring between Y69 residues and the ligands. These studies suggest that the hydroxyl group of Y69 is important for interactions with NADPH while both the hydroxyl group and benzene ring of the Y69 residues are necessary for proper interactions with dihydrofolate.

Introduction

Dihydrofolate reductase (DHFR) catalyzes the reduction of dihydrofolate (DHF) to tetrahydrofolate (THF) via hydride transfer from its cofactor NADPH. DHFR is necessary for cell survival as THF is involved in pathways leading to the synthesis of purine nucleosides and other metabolites (*1*). The chromosomal (*E. coli*) form of DHFR is inhibited by trimethoprim. However, R67 DHFR, a plasmid encoded DHFR, has been found to provides resistance to the antibiotic ((*2*) and references therein). The plasmid encoded DHFR is unique in that it shows no structural (*3*, *4*) or genetic (*2*) homology to chromosomal DHFR.

R67 DHFR[1], shown in Figure 1, is composed of four identical monomers that associate to form the apoenzyme. Each monomer is made up of 78 amino acids that form five β-barrel strands oriented antiparallel to one another. The tetramer is classified as a D_2 symmetric enzyme that possesses 222 symmetry (*3*). Crystallographic data have indicated that a pore, 25 Å long, extends through the center of the enzyme. The size of

[1] The monomers of R67 DHFR are labeled ABDC going in a clockwise orientation in the crystal structure (1VIE and 1VIF in the Protein Data Bank). The residues in monomer A are labeled 1-78, while those in monomers B, C, and D are designated 101-178, 201-278, and 301-378, respectively. All four symmetry related residues are implied when one residue of the homotetramer is described. The corresponding domains in Quad 3 are relabeled 1234.

Figure 1. A ribbon structure of R67 DHFR (protein data bank file 1VIE). Panel A shows a front view of the R67 DHFR structure, where the active site pore corresponds to the "doughnut hole" in the center. Monomers are relabeled clockwise as 1, 2, 3, and 4 (green, yellow, magenta and cyan) respectively. Each monomer corresponds to a domain in the Quad 3 construct. The protein crystallized had its 16 N-terminal residues removed by chymotrypsin treatment *(2, 21)*. Y69 residues are indicated by CPK surfaces. Panels B-D illustrate the topologies associated with the various double mutants. These views are related to that in panel A by a 90^{o} rotation along the y-axis. Wild-type Y69 residues are shown as CPK surfaces while Y69F mutants are shown as ball-and-stick structures. Panels B and D represent the Y69F: 1+2 and Y69F: 1+4 mutants where each half of the pore contains one Y69 and one Y69F residue. Panel C shows the Y69F: 1+3 mutant where one half of the pore contains two 69 residues and one half of the pore contains two Y69F residues. Panel E shows a reverse image of the active site pore generated by DOCK (*13*, *24-25*). Each white sphere corresponds to a potential atom position used by the docking program. This sphere cluster was generated from panel A by a 90^{o} rotation around the x and y axes. The reverse image compares to panels B-D by a 90^{o} rotation along the x axis. The position of a docked NADPH molecule that meets the NMR constraints is shown in red and the position of the highest scoring docked folate molecule is shown in orange (*13*). Stacking between the nicotinamide ring of cofactor and pteridine ring of folate is predicted near the center of the pore. The positions of the 4 symmetry related Y69 residues in the surrounding protein are colored and numbered as described above. The rest of the protein is not shown for simplicity.

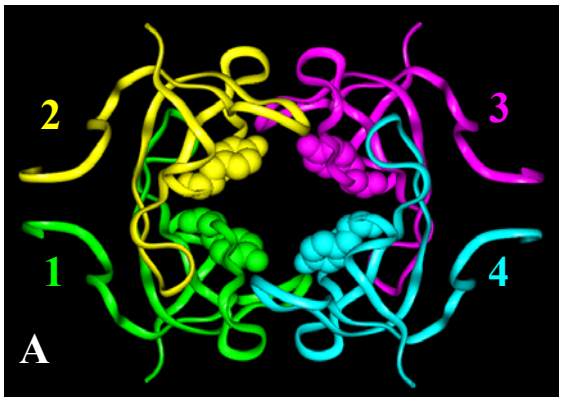
2
3
1
4
A

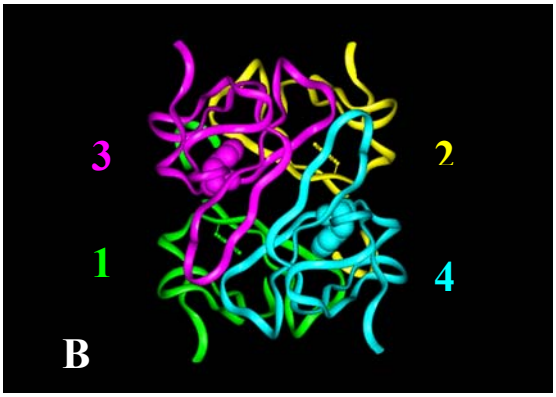
3
2
1
4
B

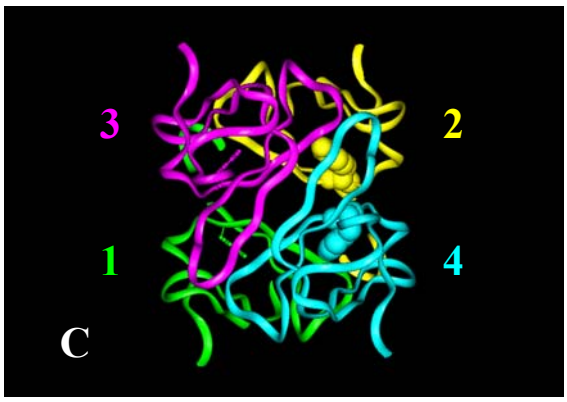
3
2
1
4
C

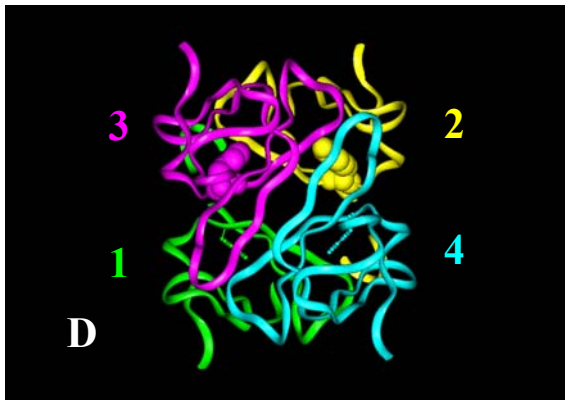
3
2
1
4
D

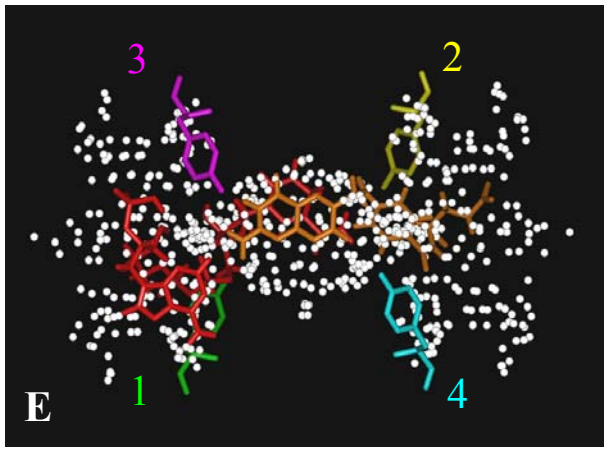
3
2
1
4
E

the pore decreases towards the center of the enzyme due to interactions between symmetrically related glutamine residues (Q67). Hydrogen bonding interactions between these residues to create "a floor and ceiling" in the pore and a proposed area for binding of substrate (DHF)[2] and cofactor (NADPH) (*3*).

In addition to the structure for the apoenzyme, a crystal structure for a binary enzyme-folate complex has also been solved (*3*). In this crystal structure, the largest accumulation of electron density for folate is observed near the pore's center. This electron density is most consistent with two folate molecules binding in the pore in slightly different orientations. Specifically, FolI is proposed to bind in the pore in an orientation where its *si* face is available for hydride transfer from NADPH. In contrast, FolII is bound such that its *si* face cannot be accessed (*3*). NMR studies previously conducted on a variant of R388 DHFR, a homolog of R67 DHFR, indicate that the pro-R hydrogen is transferred from NADPH to the same face of DHF during the reaction (*5*). Thus, only FolI is in the proper orientation to accept a hydride during catalysis (*3*).

In contrast to folate, attempts at generating co-crystals for NADPH or $NADP^+$ have to date proven unsuccessful. However, NMR studies indicate that the nicotinamide of the cofactor also interacts with the pteridine ring of folate in the pore's center as

---

[2] Abbreviations: DHFR, dihydrofolate reductase; TMP, trimethoprim; DHF, dihydrofolate; THF, tetrahydrofolate; NMNH, reduced nicotinamide mononucleotide; NADP(+/H), oxidized/reduced nicotinamide adenine dinucleotide phosphate; PABA-glutamic acid tail, para-aminobenzoyl glutamic acid region of dihydrofolate/folate; ITC, isothermal titration calorimetry; CD, circular dichroism; and Quad 3, the protein product of a tandem array of four in-frame R67 DHFR genes. Mutations are indicated by listing the wild-type residue and its location in the amino acid sequence followed by the residue to which it is mutated. For example, mutation of tyrosine at position 69 to phenylalanine will be represented as Y69F.

interligand NOEs were observed between $NADP^+$ and a folate analog (*6*). Chemical shifts upon ligand binding also suggest that numerous residues comprising the active site pore are involved in interactions with $NADP^+$ (*7*).

This present series of experiments examines the means by which NADPH and DHF interact with R67 DHFR. Since limited structural evidence is available, we have approached this problem by mutagenesis of specific residues within the active site that are proposed to facilitate ligand binding and/or catalysis. Site-directed mutagenesis of most of the residues proposed to comprise the active site surface has been performed (*8-10*). Because R67 DHFR is composed of 4 symmetry-related monomers, mutation of one residue results in 4 symmetry related mutations which often have large effects on kinetic and thermodynamic parameters (*9*). Therefore, our goal has been to generate a system by which we can control the number and location of the mutation(s) by building asymmetric mutants where only defined subunits of the tetramer are mutated (*11*, *10*, *12*). To approach this goal, Bradrick et al. (*12*) constructed "quadruple R67 DHFR". The gene coding for quadruple R67 DHFR contains four in-frame copies of the DNA encoding wild-type R67 DHFR. Transcription and translation yield a monomeric protein mimicking the wild-type protein. Each domain in quadruple R67 DHFR equates to a monomer in the homotetramer. Unique restriction enzyme sites, flanking the tandem gene copies, were later engineered into the construct, allowing for removal of the DNA coding for a specific domain followed by its replacement with DNA containing the specified mutation(s). Each of the asymmetric mutants described below were generated in the Quad 3 construct, which has been previously described (*11*).

These present experiments explore the role of symmetry related tyrosine 69 residues in ligand binding and catalysis. Docking studies suggest that these symmetry related residues may play a role in binding both the substrate and cofactor (*13*). Two symmetry-related tyrosine 69 residues are proposed to form contacts with the pyrophosphate bridge of NADPH as well as with the adenine ribose. Docking studies also predict a possible interaction between the tyrosine hydroxyl and the glutamic acid tail of folate (*13*). Kinetic studies of the homotetrameric Y69F mutant also support the hypothesis that Y69 interacts with both DHF and NADPH, as the K_m values for DHF and NADPH are 11 and 17 fold weaker respectively than those for wild-type R67 DHFR (*9*). In addition, the k_{cat} for the reaction is two fold greater than the k_{cat} for wild-type R67 DHFR. These data indicate that although binding of both substrate and cofactor is weaker, the rate at which the reaction proceeds is faster (*9*).

Our approach to understanding the role of symmetry related tyrosine 69 residues in ligand binding and catalysis is two-fold. First, we generated a series of asymmetric Y69F mutants including a single mutant (containing one Y69F mutation), three double mutants (each containing two Y69F mutations), a triple mutant (containing three Y69F mutations), and a quadruple mutant (containing four Y69F mutations) to better understand the specificity of the interactions between Y69 and both DHF and NADPH. This approach allows us to determine if there is a preference for NADPH and/or DHF to interact with wild-type tyrosine 69 residues. Our second approach involved site-directed mutagenesis of tyrosine 69 residues within the homotetrameric enzyme in order to better understand the *type(s)* of interaction(s) occurring between symmetry related tyrosine 69 and the ligands and how these interactions are involved in catalysis.

Materials and Methods

Construction of asymmetric Y69 mutants:

Asymmetric Y69F mutants were generated by PCR based site-directed mutagenesis as previously described (*11*) using the following primer:

Y69F forward: 5′ - GGCTCAGTACAGATC**TTC**CCTGTTGCGGCG - 3′

Correct mutations were confirmed using ABI Prism Automated Sequencing at the University of Tennessee DNA sequencing laboratory. DNA containing the appropriate mutations was transformed into *E. coli* STBLII cells (*14*). Cells were grown overnight at 30°C on Luria broth agar plates containing 200 μg/ml ampicillin and 20 μg/ml trimethoprim to assay for trimethoprim resistance. All six Y69F asymmetric mutants provided resistance to trimethoprim as evidenced by their ability to allow host *E. coli* to grow on LB plates containing 20μg/ml of trimethoprim.

Y69T, Y69K, Y69Q, and Y69L homotetrameric mutants were generated by PCR based site-directed mutagenesis using the following primers:

Y69T forward: 5′ - GGCTCAGTACAGATC**ACT**CCTGTTGCGGCG - 3′

Y69K forward: 5′ - GGCTCAGTACAGATC**AAA**CCTGTTGCGGCG - 3′

Y69Q forward: 5′ - GGCTCAGTACAGATC**CAG**CCTGTTGCGGCG - 3′

Y69L forward: 5′ - GGCTCAGTACAGATC**CTT**CCTGTTGCGGCG - 3′

None of the cell lines transformed with these Y69 mutants were able to grow in the presence of TMP. Therefore, only the Y69L mutant was pursued.

Protein expression and purification

For Y69F asymmetric mutant protein expression, STBLII cells were grown at 30°C in TB media (*15*) containing 200μg/ml ampicillin and 20μg/ml trimethoprim for approximately 60 hours. Cells were lysed by sonication, and protein was precipitated with 55% ammonium sulfate. Proteins were purified (as determined by SDS-PAGE) using a variety of chromatography columns as described previously (*1*). PEG_{3350} (0.1g/L) was added to the buffer to decrease aggregation and is present in most experimental conditions (*16*). Extinction coefficients for the asymmetric mutants were determined by biuret analysis (*17*).

Steady-state kinetics

Steady-state kinetics were performed for each of the mutants to determine the corresponding K_m and k_{cat} values. Experiments were performed at 30°C on a Perkin-Elmer Lambda 3B UV/Vis spectrophotometer using UVSL3 software. Experiments were conducted in MTH buffer (50 mM Mes, 100 mM Tris and 50 mM acetic acid with 10 mM β-mercaptoethanol) at pH 7.0. Data were collected for five sub-saturating concentrations of NADPH and five sub-saturating concentrations of DHF. The data were analyzed using SAS as described previously (*11*) using global, non-linear least squares fit to a bi-substrate mechanism (*18*). This software is available on the internet at: http://www.agriculture.utk.edu/ansci/faculty/saxton_software.html.

Isothermal titration calorimetry (ITC)

Isotherms were generated for substrate or cofactor binding to each asymmetric mutant on a Microcal VP isothermal titration calorimeter at 28°C. Mes-Tris-acetic acid

buffer at pH 8 was used for NADPH binding studies while 10 mM Tris + 1 mM EDTA buffer pH 8 was used for DHF binding studies. As DHF is a weak acid, the pH of the DHF solution was titrated with NaOH to ~ pH 8 prior to ligand binding studies. The data for NADPH binding to each of the Y69F asymmetric mutants were analyzed by Origin software (Version 5.0) using both the single sites model and the sequential sites model where the stoichiometry was set to two.

Circular dichroism

To determine whether the Y69F asymmetric mutations in Quad 3 and/or the Y69L mutations in homotetrameric R67 DHFR had affected the overall secondary structure of the protein, circular dichroism (CD) experiments were performed on an AVIV 202 circular dichroism spectrophotometer at 22°C in phosphate buffer at pH 8. Data were collected for 10μM protein samples between 190 and 300nm at 2 or 3nm steps (*9*).

pH titrations

Homotetrameric R67 DHFR dissociates into dimers upon titration with acid due to protonation of symmetry related histidine 62 residues (*19*, *20*). This dissociation process can be monitored by a change in fluorescence of symmetry related tryptophan residues which become solvent exposed upon dissociation of the tetramer (*19-21*). In order to determine if Y69L mutations in the homotetramer had affected this equilibrium, pH versus fluorescence intensity profiles were generated. Data were fit as described previously by non-linear regression using SAS (*9*, *19*, *20*). Although the Y69F asymmetric mutants are unable to undergo a dimer to tetramer equilibrium as the domains are covalently linked, it is possible for the domains to "open up" or "splay apart" upon titration of symmetry related histidine 62 residues (*11*, *12*). This process can also

be monitored as a change in tryptophan fluorescence as pH is decreased. To determine whether Y69F asymmetric mutations had affected this process, pH versus fluorescence intensity profiles were generated. Data were fit to a simple ionization equation using Sigmaplot (*22*).

Results

Nomenclature

The following nomenclature will be used to describe each of the asymmetric mutants. The residue, residue number, and mutation will be listed first followed by a colon. The asymmetric location of the particular mutations will be indicated numerically where 1 refers to domain 1, 2 refers to domain 2, etc. This is illustrated using the crystal structure for homotetrameric R67 DHFR in Figure 1 where each monomer would correspond to a domain in Quad 3 (*3*, *23*) The four domains are labeled in a clockwise fashion where domain 1 is located at the bottom, left position. For example, the Y69F: 1+3 mutant contains two mutations: tyrosine 69 in domain 1 has been mutated to a phenylalanine residue, as has tyrosine 69 located in domain 3. Figure 1 also compares the different topologies of the three double mutants. For the Y69F: 1+3 mutant, one side of the pore contains wild-type Y69 residues while the opposite side of the pore contains mutant Y69F residues (panel C). In contrast, both the Y69F: 1+2 and Y69F: 1+4 mutants contain one Y69 and one Y69F residue on each side of the pore (panels B and D), although with different distances between the mutations. Because Y69 residues are located further away from the center of symmetry, these residues likely interact with the ADP-ribose and/or the PABA-glutamic acid tails of NADPH and DHF, respectively (*3*, *13*). Figure 1E displays the relative positions of the Y69 residues with respect to a

docked ternary complex model that incorporates NMR and X-ray crystallography information (*3, 6*, *7*, *13*).

In addition to Y69F asymmetric mutants, the effects of Y69L mutations in the homotetrameric enzyme were also assessed. This construct will be referred to as Y69L R67 DHFR and contains four symmetry-related Y69L mutations. For clarity, the data for the Y69F asymmetric mutants will be discussed first, followed by that for Y69L R67 DHFR.

Steady-state kinetics

In order to gain a better understanding of the effects of Y69 mutations on catalysis, steady-state kinetic data were collected for each of the asymmetric Y69F mutants. The kinetic results are presented in Table 1. In general, the K_m values for NADPH and DHF as well as the k_{cat} display a trend contingent upon the location and number of Y69F mutations. A wild-type $K_{m\,(NADPH)}$ value is observed for both the Y69F: 1 and Y69F: 1+3 mutants, while the $K_{m\,(NADPH)}$ for the Y69F: 1+2 and Y69F: 1+4 mutants is ~3-4 fold weaker. The $K_{m\,(NADPH)}$ for the triple mutant (Y69F: 1+2+3) continues to rise as does the $K_{m\,(NADPH)}$ for the quadruple mutant (Y69F: 1+2+3+4). The kinetic parameters for the Y69F: 1+2+3+4 mutant are similar to those for Y69F R67 DHFR. Thus, for NADPH binding interactions in the productive, ternary complex, as the number of mutations is increased, $K_{m\,(NADPH)}$ is increased. The two exceptions to this trend are the Y69F: 1 and Y69F: 1+3 mutants. However, these two mutants are similar in that they are the only mutants in which an entire "side" of the pore is wild-type. This suggests that for NADPH to bind in a manner similar to that of the wild-type enzyme, it is necessary for one side or half of the pore to remain wild-type.

Table 1. A comparison of kinetic parameters for wild-type R67 DHFR, Quad 3 DHFR, Y69F asymmetric mutants, Y69L R67 DHFR, and Y69F R67 DHFR at pH 7.0.

Enzyme Variant	k_{cat} (sec^{-1})	$K_{m\ (NADPH)}$ (μM)	$K_{m\ (DHF)}$ (μM)
WT R67 DHFR[a]	1.3 ± 0.073	3.0 ± 0.060	5.8 ± 0.015
Quad 3 DHFR[b]	0.81 ± 0.02	4.4 ± 0.4	6.7 ± 0.4
Y69F: 1 DHFR	0.98 ± 0.06	6.4 ± 0.6	21 ± 2
Y69F: 1+2 DHFR	0.96 ± 0.01	14 ± 0.8	20 ± 0.9
Y69F: 1+3 DHFR	0.56 ± 0.01	3.1 ± 0.4	20 ± 2
Y69F: 1+4 DHFR	1.9 ± 0.08	14 ± 0.7	28 ± 2
Y69F: 1+2+3 DHFR	1.4 ± 0.04	21 ± 0.9	35 ± 2
Y69F: 1+2+3+4 DHFR	1.4 ± 0.04	40 ± 3	54 ± 3
Y69F R67 DHFR[c]	2.9 ± 0.1	69 ± 3	68 ± 4
Y69L R67 DHFR	0.16 ± 0.01	68 ± 3	180 ±11

[a] Taken from (*23*).
[b] Taken from (*11*).
[c] Refit from (*9*) using the non-linear, global SAS fit described in (*11*).

Similar to NADPH interactions in the ternary complex, $K_{m\,(DHF)}$ values also tend to increase as the number of mutations is increased. Specifically, the $K_{m\,(DHF)}$ for the single and all the double mutants is ~2-3 fold weaker than the $K_{m\,(DHF)}$ for Quad 3. In addition, the $K_{m\,(DHF)}$ for the Y69F: 1+2+3 mutant continues the trend of increasing as additional mutations are added, up to the limit associated with the Y69F: 1+2+3+4 mutant.

Although binding of both NADPH and DHF in the Michaelis complex is, in general, weakened as the number of Y69F mutations is increased, the k_{cat} value is increased. The k_{cat} values vary over an approximately 2 fold range. A trend is noted where the k_{cat} increases when two Y69F mutations occur in either the "ceiling" and or the "floor" of the active site pore as occurs in the Y69F: 1+4, Y69F: 1+2+3 and Y69F: 1+2+3+4 mutants, suggesting this topology may be preferred in the transition state.

Isothermal titration calorimetry

Although steady-state kinetics provide important insight into interactions between ligands in the Michaelis complex, these K_m values do not necessarily correspond to dissociation constants (K_ds) as other events can contribute to the observed K_m values (22). Isothermal titration calorimetry provides a direct measure of the heat exchange upon ligand binding as well as a direct measure of the dissociation constant for the ligand of interest (26, 27). In order to determine the effects of the asymmetric Y69F mutations on NADPH and DHF binding, isothermal titration calorimetry experiments were performed for the binary complexes where either two NADPH molecules or two DHF molecules interact with the enzyme. Data for NADPH binding to the Y69F asymmetric mutants are summarized in Table 2. These data were analyzed using both the single sites

Table 2. Comparison of NADPH binding constants for Y69F asymmetric mutants and Y69L R67 DHFR as determined by isothermal titration calorimetry. Data reported were fit using the single sites model. Each value is an average of at least two different experiments (except Y69F R67 DHFR).

Complex	K_d (μM)	ΔH (cal/mol)	Stoichiometry
Quad 3 DHFR	8 ± 0.3	-7600 ± 260	0.83 ± 0.01
Y69F: 1 DHFR	10 ± 1	-6200 ± 120	0.88 ± 0.003
Y69F: 1+2 DHFR	25 ± 2	-4900 ± 170	0.69 ± 0.02
Y69F: 1+3 DHFR	15 ± 1	-5200 ± 390	0.72 ± 0.01
Y69F: 1+4 DHFR	9 ± 1	-7500 ± 490	0.84 ± 0.02
Y69F: 1+2+3 DHFR	25± 2	-5000 ± 120	0.75 ± 0.03
Y69F: 1+2+3+4 DHFR	52 ± 5	-2400 ± 210	0.95 ± 0.11
Y69F R67 DHFR[a]	65 ± 6	-2200 ± 170	1.1 ± 0.1
Y69L R67 DHFR	75 ± 0.4	-2800 ± 40	1.1 ± 0.1

[a] Refit from (*9*) to a single sites model.

model and the sequential sites model where the stoichiometry was set to two. The K_d and ΔH values for the first NADPH binding event were similar regardless of the model used to describe the data. However the K_{d2} and ΔH_2 values generated using the sequential sites model varied, most likely since the K_{d2} values are high and fall outside of the detection window afforded by the calorimeter. For accurate results, the c value, where c is defined as [protein]*K_a, should occur within a range of 1 and 1000 (*26*, *27*). Therefore, only the values for the first NADPH binding event are reported.

In general, the effects of the Y69F mutation(s) on NADPH binding to the single and double mutants are minor, with the Y69F: 1+2 configuration having the most dramatic effect. However, as the number of mutations is increased in the triple and quadruple mutants, the K_d values also increase. The enthalpy change for NADPH binding to the Y69F: 1 and Y69F: 1+4 mutants is similar to that for Quad 3, while the ΔH becomes less negative as the number of mutations is increased in the Y69F: 1+2+3 and Y69F: 1+2+3+4 mutants.

Isothermal titration calorimetry experiments were also performed to determine the effects of asymmetric Y69F mutations on interactions with DHF. Previously, isotherms generated for DHF binding to wild-type R67 DHFR were fit to an interacting sites model as isotherms displayed a hook reflecting positive cooperativity between bound DHF molecules (*28*). New calorimeters have increased sensitivity to minor changes in solution pH during the titration. Close attention to the pH of both the ligand and protein solution indicated that the prominence of the hook is related to changes in pH of the protein solution upon injection of ligand into the solution. Additional studies indicate that the presence of the hook is affected by the ionic strength of the buffering solution (data not

shown). This effect is likely due to disruption of electrostatic interactions between symmetry related lysine 32 residues and DHF (*8*). The sensitivity of DHF binding to R67 DHFR may also be related to previous NMR studies that found DHF dimerizes in solution and this dimerization is affected by ligand concentration (where dissociation constants for dimerization are in the mM range), pH as well as ionic strength (*29, 30*).

Due to the characteristics of the isotherms generated for DHF binding to the Y69F asymmetric mutants, we are unable to consistently fit the data using the Origin software provided by MicroCal. In particular, if there are only a few points in the hook, the Origin software does not provide a strong weighting to those points and the fit line does not go through them. Therefore, for comparative purposes, we have overlaid the raw data for DHF binding to each of the asymmetric mutants in Figure 2. Based on the raw data, a trend is observed in both the shape of the curve and the initial heat released upon ligand binding as well as in the prominence of the hook. Specifically, there appears to be a trend in the DHF concentration required to reach saturation for the asymmetric mutants. The signal for Quad 3 increases most dramatically as the DHF concentration is increased; this behavior is expected when tight binding occurs. The steepness of the slope in the titrations decreases as the number of mutations is increased. This suggests that as the number of mutations is increased, more ligand is required to reach saturation and thus binding interactions are weaker. In addition, the enthalpy change upon ligand binding appears to decrease from ~ -9000 cal/mole for Quad 3 to ~ -6000 cal/mole for the Y69F: 1+2+3+4 mutant. Finally, an increase in the prominence of the "hook" in the isotherms is

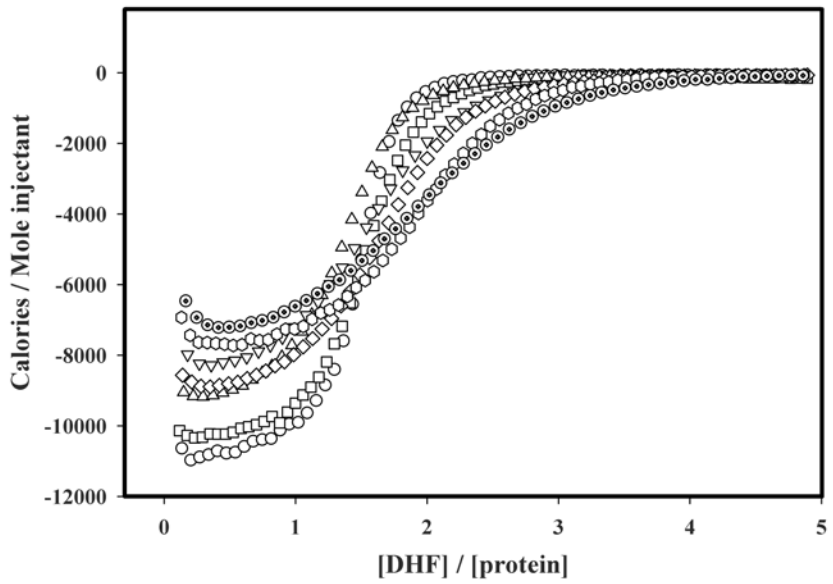

Figure 2. Isotherms for DHF binding to Y69F asymmetric mutants generated by isothermal titration calorimetry. Data for Quad 3 (○), Y69F: 1 (□), Y69F: 1+2 (Δ), Y69F: 1+3 (∇), Y69F: 1+4 (◊), Y69F: 1+2+3 (hexagon), and Y69F: 1+2+3+4 (circle with dot) mutants are overlaid for comparative purposes.

observed as the number of mutations increases, with Quad 3 displaying a minimal hook and the Y69F: 1+2+3 and Y69F 1+2+3+4 mutants displaying the most dramatic hooks.

Physical studies

One possible effect of engineered mutations is a change in protein conformation. Therefore, circular dichroism spectroscopy was used to determine whether Y69F asymmetric mutations cause major secondary structural changes in the Quad 3 construct. As shown in Figure 3, slight to moderate variations in the CD signals are observed for the Y69F asymmetric mutants and are in the range of those previously observed for other mutants (*9*, *11*). It seems most likely these variations are due to minor changes in local protein structure and/or to effects of aromatic residues on the CD signal (*9*, *11*, *31*).

Additionally, pH titrations were performed to determine whether the Y69F asymmetric mutations affected the structure by altering the transition between the "open" and "closed" conformations of Quad 3 mutants. This equilibrium describes protonation of symmetry-related histidine 62 residues upon titration with acid (*19*, *20*). As the proteins are titrated with acid, symmetry-related tryptophan residues become solvent exposed allowing the pK_a for histidine-62 residues to be determined from the titration (*11*, *19-21*). Figure 4 shows an overlay of several representative titrations for the Y69F aymmetric mutants. The pK_a values for each of the Y69F asymmetric mutants are shown in Table 3 and are within 0.09 pH units of each other, consistent with minimal structural perturbations.

Homotetrameric Y69L R67 DHFR

In order to gain a better understanding of the *type(s)* of interaction(s) formed between Y69 and the ligands, DHF and NADPH, site-directed mutagenesis of

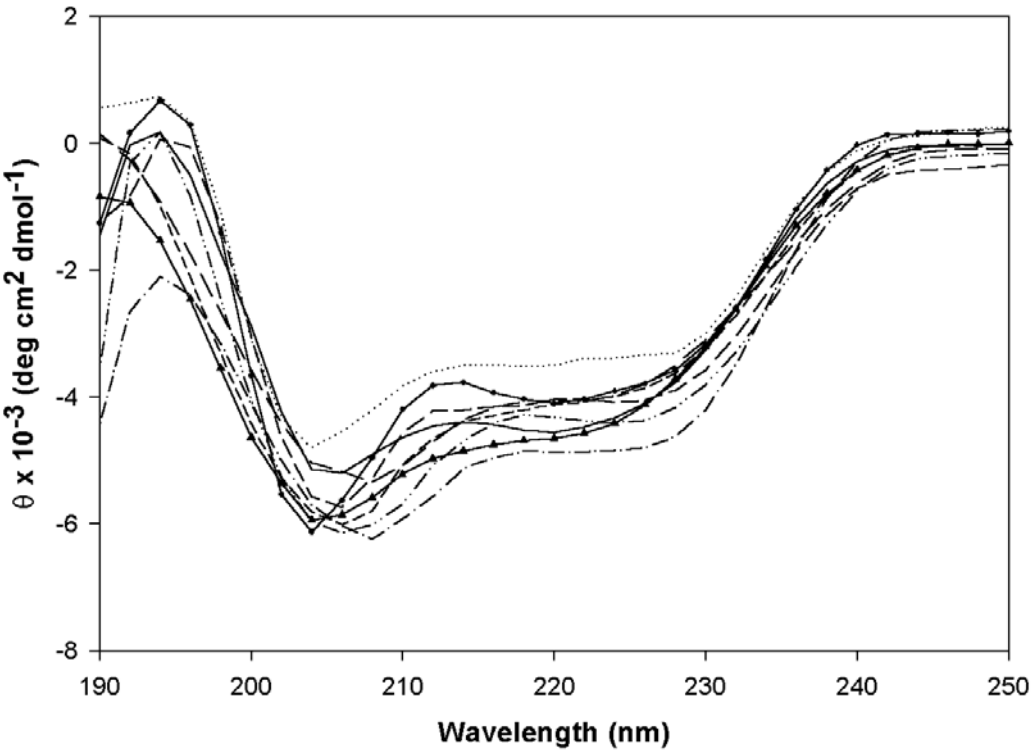

Figure 3. Comparison of CD spectra for Y69 mutants. Wild-type R67 DHFR (solid circle with line through circle), Quad 3 (solid line), Y69F: 1 DHFR (long dash), Y69F: 1+2 DFHR (dotted), Y69F: 1+3 DHFR (medium dash), Y69F: 1+4 (short dash), Y69F: 1+2+3 DHFR (dash-single dot), Y69F: 1+2+3+4 DHFR (dash-two dots), and Y69L R67 DHFR (solid triangle with line through triangle) spectra are overlaid for comparative purposes.

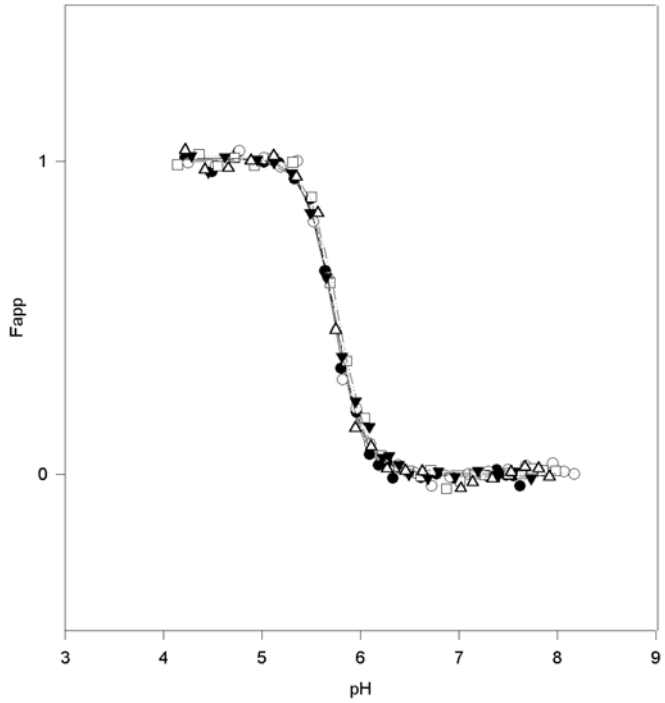

Figure 4. pH titrations for select Y69F asymmetric mutants. Data are plotted as pH versus $F_{apparent}$. Actual data are indicated with symbols while lines through the data represent the best fit line through the data when H=3 (three his62 residues are protonated causing the protein to splay open). Quad 3 data (Δ) and best fit line (short dash), the Y69F:1 data (•) and best fit line (solid line), Y69F: 1+2 data (O) and best fit line (dotted), Y69F: 1+4 data (□) and best fit line (dash-dot), and Y69F: 1+2+3 data (▼) and best fit line (medium dash) are overlaid as representative examples of titrations for the Y69F asymmetric mutants.

Table 3. Comparison of pK_a values for Y69F asymmetric mutants. Values represent the pKa of symmetry-related his62 residues which become protonated upon titration with acid.

Complex	pKa
Quad3 DHFR[a]	5.74 ± 0.01
Y69F: 1 DHFR	5.73 ± 0.01
Y69F: 1+2 DHFR	5.73 ± 0.01
Y69F: 1+3 DHFR	5.75 ± 0.01
Y69F: 1+4 DHFR	5.78 ± 0.01
Y69F: 1+2+3 DHFR	5.74 ± 0.01
Y69F: 1+2+3+4 DHFR	5.81 ± 0.01

[a] Taken from (*11*)

homotetrameric Y69 to alternative residues including leucine, lysine, threonine, and glutamine was performed. These mutations all resulted in the same phenotype (TMP sensitive host *E. coli* cells), therefore only one mutant, Y69L R67 DHFR, was further characterized.

Similar to the effects of Y69F mutations in homotetrameric R67 DHFR (*9*), mutation of symmetry related tyrosine 69 residues to non-conservative leucine residues also affects both ligand binding and catalysis. As indicated in Table 1, the $K_{m\ (NADPH)}$ values are similar between Y69F and Y69L R67 DHFRs as are the $K_{d\ (NADPH)}$ values shown in Table 2. In contrast, the $K_{m\ (DHF)}$ value is ~2.5 fold weaker for Y69L as compared to Y69F R67 DHFR. In addition, a clear reduction in k_{cat} for Y69L R67 DHFR is observed as compared to both Y69F R67 DHFR and wild-type R67 DHFR.

Circular dichroism studies, shown in Figure 3, were again performed to ensure that the Y69L mutations do not cause a large change in the protein structure. Although changes in the CD signal for Y69L and wild-type R67 DHFRs are observed, these variations are similar to those observed previously for mutations in the homotetrameric enzyme and are likely due to local changes in structure brought about by the non-conservative mutations (*9*).

Titrations of Y69L R67 DHFR with hydrochloric acid were also performed to ensure that the mutations do not affect the dimer-tetramer equilibrium that occurs upon protonation of symmetry-related histidine 62 residues (*19*, *20*). The $K_{overall}$ value (defined as K_d^{2n}/K_a) for Y69L R67 DHFR differs from that of the wild-type enzyme (data not shown) suggesting that mutations do have an affect on this equilibrium.

Discussion

This study investigates the role of Y69 in the binding and catalysis of R67 DHFR. Since specific contacts involving Y69 with the ligands have not been delineated by NMR and X-ray crystallography, a mutagenesis approach was used.

Steady-state kinetic and isothermal titration calorimetry studies were performed on the various Y69F asymmetric mutants. Previous studies suggest that R67 DHFR follows a random mechanism, but because of the interligand cooperativity patterns, NADPH binding followed by DHF binding is the preferred pathway (*28*). Therefore, when possible, NADPH should bind the enzyme first and preferentially interact with the tightest binding site available. This site, presumably, should contain the wild-type Y69 residue(s). DHF should bind next to the enzyme•NADPH complex and its pterin ring would be expected to stack with the nicotinamide ring of NADPH in the center of the pore. The PABA-glutamic acid tail would then be forced to interact with the amino acid residue available at position 69, either wild-type or mutant, depending on the configuration.

NADPH Binding Interactions in the Binary and Michaelis Complexes

Comparisons of steady-state kinetic values for the asymmetric Y69F mutants suggest that for NADPH to display a wild-type K_m value, *two* Y69 residues are required and these *two* residues must be located on the same side of the pore. Only two of the Y69F asymmetric mutants meet this criterion: Y69F: 1 and Y69F: 1+3. For these mutants, NADPH likely continues to bind first and prefers the wild-type side of the pore, thus exhibiting a wild-type K_m value as indicated in Table 1. However, when one half of the pore contains one Y69 and one Y69F residue (Y69F: 1+2, Y69F: 1+4, and Y69F:

1+2+3), the K_m for NADPH might be expected to be weaker if one Y69-NADPH interaction has been disrupted. As shown in Table 1, the $K_{m\,(NADPH)}$ values for the Y69F: 1+2 and Y69F: 1+4 mutants are increased 3 fold while the $K_{m\,(NADPH)}$ value for the Y69F: 1+2+3 mutant is increased 5 fold. This latter increase may be a kinetic effect due to interligand interactions between NADPH and DHF in the Michaelis complex as DHF presumably binds to the half pore possessing two Y69F mutations. Finally, the $K_{m\,(NADPH)}$ value for Y69F: 1+2+3+4 continues to increase and mimics the $K_{m\,(NADPH)}$ for homotetrameric Y69F R67 DHFR.

Why is it necessary that both tyrosine 69 residues be located on one side of the pore for NADPH to bind with a wild-type K_m? One possibility is that two tyrosine 69 residues located in different domains on the same side of the pore form interactions with NADPH. Support for this proposal comes from a computational model of the ternary complex. From this model, contacts are proposed between Y69 in monomer A of the homotetramer and the pyrophosphate bridge of NADPH as well as contacts between Y69 in monomer D of the homotetramer and the adenine ribose of NADPH (*3*). Monomer A corresponds to domain 1 of the Quad 3 construct while monomer D corresponds to domain 3. As illustrated in Figure 1C, both of these residues have been mutated to phenylalanine residues in the Y69F: 1+3 mutant. However, due to the symmetry of the protein, the same contacts proposed in the docking model can also occur between Y69 residues in domains 2 and 4 and NADPH.

Since a direct interaction(s) between the -OH of Y69 and NADPH was not predicted, either the ternary complex model requires revision or water mediated interactions could be occurring. Alternatively, since the contacts predicted by DOCK

betweenY69 residues and NADPH largely involve the ring edge of the tyrosine residue (*8*), it is possible that a dipole-charge interaction(s) may be present ($1/r^2$ distance dependence; (*32*)). Since the phenylalanine sidechain lacks the -OH group of tyrosine, this dipole moment would be diminished in the Y69F mutant.

Do the K_d data also support the model that suggests two Y69 residues are involved in NADPH binding? In general, the K_d values for NADPH binding obtained by ITC correspond to the K_m values and exhibit a similar trend in that the K_d values increase as the number of mutations is increased. The ΔH values also become less negative as the number of mutations is increased. If the K_d values were to exactly mimic the K_m behavior, the $K_{d\,(NADPH)}$ for the Y69F: 1+3 mutant should be wild-type and the $K_{d\,(NADPH)}$ for the Y69F: 1+4 mutant would be weaker. Instead, the K_d and ΔH values for the Y69F: 1+4 mutant are more similar to Quad 3 values than those for the Y69F: 1+3 mutant. However, some differences may occur as these two techniques monitor different complexes, the Michaelis complex for steady-state kinetics and a binary complex where two NADPH molecules bind for isothermal titration calorimetry. Since interactions between two NADPH molecules versus one DHF and one NADPH molecule are likely different, it is possible that these differences are reflected in the values obtained by the two techniques.

DHF binding interactions in the binary and Michaelis complexes

Interligand Overhauser effects suggest that NADPH and DHF bind on opposite halves of the pore, allowing only the rings of the ligands to interact at the pore's center (*6*). This model is supported by steady-state kinetics data for the Y69F: 1 and Y69F: 1+3 mutants which suggest that NADPH interacts with the wild-type side of the pore, thus

forcing DHF to bind to the other half pore which contains a mutation(s). Therefore for these mutants, a wild-type $K_{m\,(NADPH)}$ is observed coupled with a weaker $K_{m\,(DHF)}$ value. Also, similar $K_{m\,(DHF)}$ values are observed for the Y69F: 1+2 and Y69F: 1+4 mutants as both halves of the pore possess a mutation. The $K_{m\,(DHF)}$ value for Y69F: 1+2+3 is weaker than that of the single and double mutants as the second half of the pore now contains two mutations. The $K_{m\,(DHF)}$ for Y69F: 1+3 is tighter than expected since the half pore with which DHF is proposed to interact also has two mutated Y69 residues. However, previous studies suggest the importance of interligand interactions in ligand binding (*28*). Specifically, positive cooperativity between enzyme bound NADPH and the second ligand, DHF, is proposed to facilitate binding of DHF (*28*). Since NADPH is proposed to bind in a wild-type orientation in Y69F: 1+3 DHFR, it is possible that interligand interactions between bound NADPH and DHF partially account for the tighter $K_{m\,(DHF)}$ observed in this mutant.

Support for this model is also provided in the ternary complex model where folate was docked into a DHFR•NMNH complex. (NMNH is a fragment of NADPH that contains only the nicotinamide ring, ribose ring, and a single phosphate group.) From the docking studies, the highest scoring folate conformer is predicted to form a hydrogen bond between the –OH of Y69 (in monomer C which corresponds to domain 4 of Quad 3) and the α-carboxylate of the folate tail. However, other high scoring folate conformers are also predicted with alternate positions for the PABA-glutamic acid tail of DHF (*13*). Mobility in the tail region has additionally been observed in both X-ray crystallography and NMR studies (*3*, *6*). It is therefore possible that interactions occurring between Y69

and folate (or DHF) are weak and/or transient, hence, interligand interactions between enzyme bound NADPH and folate/DHF play an important role in DHF binding.

Do these trends continue in the DHF binary complex data? Although we are unable to quantify differences in binding affinity of the Y69F symmetric mutants for DHF, we can draw qualitative conclusions based on variations in isotherm shape for the asymmetric mutants. First, increasing the number of Y69F mutations weakens the binding affinity for DHF as increasing DHF concentrations are required to reach saturation. Interestingly, as the number of Y69F mutations is increased, a more prominent hook is observed in the isotherms, suggesting changes in inter-ligand interactions between the two DHF molecules and/or different enthalpies associated with the two binding events.

What role does Y69 play in catalysis?

Mutation of tyr 69 to phe in R67 DHFR facilitates catalysis as the k_{cat} value for the mutant reaction increases (*9*). Comparison of the k_{cat} values for Quad 3 and the Y69F: 1+2+3+4 mutant reveals an approximately 2 fold increase in the k_{cat} upon addition of the mutations. This increase is comparable to the increase observed in Y69F R67 DHFR as compared to wild-type R67 DHFR. That the k_{cat} for the Y69F: 1+2+3+4 mutant is less than that of Y69F R67 DHFR is not unreasonable since the k_{cat} for Quad 3 is also less than the k_{cat} for wild-type R67 DHFR (*11*). In addition, an increase in k_{cat} is not observed until two Y69F mutations are present in the Y69F: 1+4 mutant. The k_{cat} values for the Y69F: 1+2+3 and Y69F: 1+2+3+4 mutants are similar to that of the Y69F: 1+4 mutant indicating that increasing the number of Y69F mutations to 3 or 4 does not result in additional increases in k_{cat}. These three mutants are similar in that they each

contain two mutations along either the ceiling and/or floor of the active site pore. It is therefore tempting to suggest that loss of interactions between these residues and NADPH and/or DHF facilitate the reaction.

Based on steady-state kinetic analyses of Y69F R67 DHFR and the Y69F asymmetric mutant series, one possible role for Y69 is in ground-state binding. This is supported by steady-state kinetic data where the K_m values for NADPH and DHF binding are increased as the number of mutations is increased. However, these data also suggest that in order to reach the transition state, it is necessary for at least one Y69 interaction to be disrupted. This is supported by increasing k_{cat} values as Y69 residues are mutated to phenylalanine in the Y69F: 1+4, Y69F: 1+2+3, and Y69F: 1+2+3+4 mutants. These data continue to support the model (*9*) that Y69F mutations in the homotetramer destabilize binding in the ground state to a greater extent than binding in the transition state. Further, the model can be extended such that the Y69F: 1+4 double mutant topology appears to provide the least perturbation to ground-state binding coupled with the best match to the transition state configuration.

What types of interactions occur between the ligands and Y69?

Another goal of this mutagenesis series has been to determine the *type(s)* of interaction(s) that occur between Y69 and both NADPH and DHF. We have approached this goal via site-directed mutagenesis of symmetry-related Y69 residues to both conservative and non-conservative amino acid residues. With the exception of the Y69F enzyme variants, site-directed mutagenesis of Y69 to other amino acid residues has been complicated by trimethoprim sensitivity in cells containing the mutagenized plasmids. The importance of Y69 in catalysis is, therefore, emphasized in that most mutations at

this position are not tolerated without a loss of TMP resistance which usually correlates with large decreases in protein yield and/or k_{cat}/K_m.

Comparisons of the kinetic parameters observed for Y69F R67 DHFR, Y69L R67 DHFR, and wild-type R67 DHFR yield interesting information regarding the involvement of Y69 in both ligand binding and catalysis. Analysis of Y69F R67 DHFR suggests the importance of tyrosine's hydroxyl group as its removal results in a 20 fold increase in $K_{m\,(NADPH)}$ and a 10 fold increase in $K_{m\,(DHF)}$ (*9*). Hence, the hydroxyl group is necessary for binding interactions with NADPH and DHF. However, removal of the hydroxyl group appears to facilitate catalysis as the k_{cat} for Y69F R67 DHFR is increased ~ 2 fold in comparison to the wild-type enzyme (*9*). Similar to Y69F R67 DHFR, the steady state kinetic parameters are also affected in Y69L R67 DHFR. The $K_{m\,(DHF)}$ for Y69L R67 DHFR is > 20 fold weaker than the $K_{m\,(DHF)}$ for wild-type R67 DHFR and is ~2.5 fold greater than the $K_{m\,(DHF)}$ for Y69F R67 DHFR suggesting that the aromatic ring of Y69 as well as the hydroxyl group are important for interactions with DHF. Although the $K_{m\,(NADPH)}$ is also increased in Y69L R67 DHFR as compared to the wild-type enzyme, the value is similar to that obtained for Y69F R67 DHFR suggesting that the hydroxyl moiety is most important for interactions with NADPH. This is supported by the similar K_d values obtained for NADPH binding to Y69L R67 DHFR and Y69F R67 DHFR. The aromatic ring also appears to play an important role in catalysis as is evidenced by the 4 fold decrease in k_{cat} in Y69L R67 DHFR. Whether the hydroxyl and aromatic regions of tyrosine 69 are directly involved in interactions with both DHF and NADPH or are mediated through water is not clear. Direct assessment of the type of

interaction afforded by tyrosine 69 and the ligands requires more structural based studies such as NMR and x-ray crystallography, which are currently in progress.

What general trends are observed for Quad 3 asymmetric mutants?

We have previously constructed asymmetric mutant series involving Q67H (*1*) as well as K32M substitutions (Hicks et al., manuscript in preparation). From these studies, as well as the present experiments, several general trends are noted. (K32, Q67, I68 and Y69 have been identified as the most important residues in binding and catalysis from a series of site directed mutagenesis experiments probing the residues in the active site pore ((*2*, *9*), Strader et al., manuscript submitted,). The first pattern finds the single asymmetric mutant behaves similarly to Quad 3, indicating a single mutation is well tolerated. Conversely, to produce a substantial effect and begin to mimic the mutation in a homotetrameric context, three mutations are usually required. (This could not be accomplished with the K32M asymmetric mutants as this mutation affects the dimer-dimer interface, hence only single and double K32M mutants were constructed (Hicks et al., manuscript submitted)). Second, the 1+2 and 1+4 double mutants (Y69F and K32M series) show similar steady state kinetic behavior. For these mutants, an initial expectation was that if the docked model for the ternary complex described how the molecules were arranged in the ground state, then minimal effects on k_{cat} and K_m would be expected for the asymmetric mutant that matches this predicted, productive topology (1+2), with larger effects on the non-preferred topology (1+4). However the observed similar kinetic behavior for the 1+2 and 1+4 mutants indicates that both topologies allow comparable interactions with the PABA-glutamic acid tail of DHF. This behavior correlates with the disorder observed for the glutamate tail of bound folate in the crystal

structure (*6*) as well as NMR studies that find the glu tail is mobile (*3*). Further, docking of DHF into an R67 DHFR•NMNH complex predicts various orientations for the *p*-aminobenzoic acid (PABA)-glu tail (*13*).

A third, general pattern observed for the K32M and Y69F asymmetric mutant series is that the 1+3 double mutants show minimal perturbation of NADPH binding. This pattern supports initial binding of NADPH into the "wild type half-pore" followed by DHF being forced to bind in the "mutant side." Consequently greater effects on DHF binding are observed in these mutants. Fourth, mutations at the center of the pore (Q67H) produce different effects than mutations further out on the pore surface (K32M and Y69F). For example, the Q67H mutations are associated with tighter binding of all complexes and result in severe NADPH and DHF inhibition. This observation is consistent with the crystallographic R67 DHFR•folate•folate binary complex and the docked ternary complex model that point to the hourglass center of the pore being associated with ring stacking and helping to establish interligand cooperativity patterns. In contrast, mutations further out the pore surface do not display substrate/cofactor inhibition, but rather are most consistent with alternative binding modes associated with the DHF tail being tolerated.

To conclude, these trends all support the general model whereby NADPH and folate enter the active site pore from either end, meeting at the center where catalysis occurs. NADPH likely binds first, with a preference for the least perturbed side of the pore. The nicotinamide ring then provides an interaction surface for binding the pteridine ring of DHF. A "one site fits both" strategy must be employed because the homotetramer possesses only a single active site pore coupled with the need to bind two ligands. This

"catch-22" situation appears to lead to symmetry related residues that aid ligand binding, but provide too much ground state stabilization. To reach the transition state, some of these interactions likely need to break. Thus construction of asymmetric mutants has begun to provide clues to unravel how R67 DHFR works as an enzyme.

Acknowledgements

Authors thank Jun Wu for purification of Y69L R67 DHFR and preliminary steady-state kinetic experiments and Dr. Cynthia Peterson for review of this manuscript.

References

1. Matthews, C. K., and van Holde, K. E. (1996) *Biochemistry*, The Benjamin/Cummings Publishing Company, Inc., New York.
2. Stone, D., and Smith, S. L. (1979) *J Biol Chem 254*, 10857-10861.
3. Narayana, N., Matthews, D. A., Howell, E. E., and Nguyen-huu, X. (1995) *Nat Struct Biol 2*, 1018-1025.
4. Matthews, D. A., Smith, S. L., Baccanari, D. P., Burchall, J. J., Oatley, S. J., and Kraut, J. (1986) *Biochemistry 25*, 4194-4204.
5. Brito, R. M., Reddick, R., Bennett, G. N., Rudolph, F. B., and Rosevear, P. R. (1990) *Biochemistry 29*, 9825-9831.
6. Li, D., Levy, L. A., Gabel, S. A., Lebetkin, M. S., DeRose, E. F., Wall, M. J., Howell, E. E., and London, R. E. (2001) *Biochemistry 40*, 4242-4252.
7. Pitcher, W. H., 3rd, DeRose, E. F., Mueller, G. A., Howell, E. E., and London, R. E. (2003) *Biochemistry 42*, 11150-11160.
8. Hicks, S. N., Smiley, R. D., Hamilton, J. B., and Howell, E. E. (2003) *Biochemistry 42*, 10569-10578.
9. Strader, M. B., Smiley, R. D., Stinnett, L. G., VerBerkmoes, N. C., and Howell, E. E. (2001) *Biochemistry 40*, 11344-11352.
10. Park, H., Bradrick, T. D., and Howell, E. E. (1997) *Protein Eng 10*, 1415-1424.
11. Smiley, R. D., Stinnett, L. G., Saxton, A. M., and Howell, E. E. (2002) *Biochemistry 41*, 15664-15675.
12. Bradrick, T. D., Shattuck, C., Strader, M. B., Wicker, C., Eisenstein, E., and Howell, E. E. (1996) *J Biol Chem 271*, 28031-28037.

13. Howell, E. E., Shukla, U., Hicks, S. N., Smiley, R. D., Kuhn, L. A., and Zavodszky, M. I. (2001) *J Comput Aided Mol Des 15*, 1035-1052.

14. Strader, M. B., and Howell, E. E. (1997) *Gibco-BRL Focus 19*, 24-25.

15. Tartof, K. D., and Hobbs, C.A. (1987) *BRL Focus 9*, 12.

16. de Bernandez Clark, E., Schwartz, E., and Rudolph, R. (1999) *Methods Enzymol. 309*, 217-235.

17. Gornall, A. G., Bardawill, C.J., and David, M. M. (1949) *Journal of Biological Chemistry 177*, 751-766.

18. Segel, I. H. (1975) *Enzyme Kinetics*, John WIley & Sons, Inc., New York.

19. Park, H., Zhuang, P., Nichols, R., and Howell, E. E. (1997) *J Biol Chem 272*, 2252-2258.

20. Nichols, R., Weaver, C. D., Eisenstein, E., Blakley, R. L., Appleman, J., Huang, T. H., Huang, F. Y., and Howell, E. E. (1993) *Biochemistry 32*, 1695-1706.

21. West, F. W., Seo, H. S., Bradrick, T. D., and Howell, E. E. (2000) *Biochemistry 39*, 3678-3689.

22. Fersht, A. (1999) *Structure and Mechanism in Protein Science*, W.H. Freeman and Company, New York.

23. Reece, L. J., Nichols, R., Ogden, R. C., and Howell, E. E. (1991) *Biochemistry 30*, 10895-10904.

24. Kuntz, I. D., Blaney, J. M., Oatley, S. J., Langridge, R., and Ferrin, T. E. (1982) *J. Mol. Biol. 161*, 269-288.

25. Shoichet, B. K., and Kuntz, I. D. (1993) *Protein Eng 6*, 723-732.

26. Wiseman, T., Williston, S., Brandts, J.F., and Lin, L.N. (1989) *Analytical Biochemistry 179*, 131-137.

27. Leavitt, S., and Freire, E. (2001) *Current Opinion in Structural Biology 11*, 560-566.

28. Bradrick, T. D., Beechem, J. M., and Howell, E. E. (1996) *Biochemistry 35*, 11414-11424.

29. Poe, M. (1973) *Journal of Biological Chemistry 248*, 7025-7032.

30. Khaled, M. A., and Krumdieck, C. L. (1985) *Biochem Biophys Res Commun 130*, 1273-1280.

31. Woody, R. W. (1995) *Methods of Enzymology 246*, 34-71.

32. Burley, S. K., and Petsko, G. A. (1988) *Adv Prot Chem 39*, 125-189.

Part IV: R67 DHFR and Quad 3 DHFR, A Global Perspective

Catalytic Efficiency

R67 dihydrofolate reductase provides a unique approach to catalysis as a 25Å pore serves as the binding site for both ligands, DHF and NADPH (*2*). Compared to other enzymes, however, R67 DHFR is rather inefficient. Enzyme efficiency is defined by k_{cat}/K_m. For the most efficient enzymes, such as acetylcholinesterase, the k_{cat}/K_m values are on the order of 10^8 $s^{-1}M^{-1}$(*3*). In these enzymes, the rate-determining step for the reaction approximates the rate of encounter of the enzyme and substrate which is diffusion-limited (*3*). In contrast, lower $k_{cat}/K_{m(NADPH)}$ and $k_{cat}/K_{m(DHF)}$ values of $1.8•10^5$ $s^{-1}M^{-1}$and $1.2•10^5$ $s^{-1}M^{-1}$, respectively are observed for R67 DHFR, yielding a less efficient enzyme (*4*).

One of the goals of asymmetrically mutating R67 DHFR has been to artificially generate a more efficient enzyme (*5*). This goal was first approached by generating asymmetric Q67H mutants (*1*). Interestingly, Q67H R67 DHFR is a more efficient enzyme than wild-type R67 DHFR as its $k_{cat}/K_{m(NADPH)}$ value is 10 fold greater than the wild-type enzyme, while the $k_{cat}/K_{m(DHF)}$ value is also slightly increased (1.2 fold) (*5*). The increase in catalytic efficiency for the Q67H R67 DHFR mutant is largely due to the increase in binding affinity for both NADPH and DHF (~200 and ~40 fold, respectively) as the k_{cat} for the reaction actually decreases ~50 fold (*5*). With this increase in binding affinity, however, an increase in non-productive binding is observed for Q67H R67 DHFR where both substrate and cofactor become inhibitory (*5*). Therefore, our goal in generating the asymmetric Q67H mutants was to generate an efficient enzyme which maintains tight binding but disfavors formation of inhibitory complexes (*1, 5*).

Table 1 compares the k_{cat}/K_m values for the Q67H asymmetric mutants. As indicated in the table, none of the k_{cat}/K_m values for the asymmetric mutants is increased greater than that of the Q67H: 1+2+3+4 asymmetric mutant which corresponds to Q67H R67 DHFR, except the $k_{cat}/K_{m(NADPH)}$ value for the Q67H:1+2 mutant which is increased ~2 fold compared to the quadruple mutant. The binding and catalysis constants for the Q67H: 1+2+3+4 mutant are similar to those for Q67H R67 DHFR (*1*). Unfortunately, rather noticeable inhibition, similar to that observed for Q67H R67 DHFR, is also observed for this mutant. Although the Q67H: 1+2 mutant also has an obvious increase in the $k_{cat}/K_{m(NADPH)}$, cofactor inhibition is noticeable in this mutant as well. The only Q67H asymmetric mutants which lack clear substrate and/or cofactor inhibition are the Q67H: 1 and Q67H: 1+4 mutants (*1*). However, the catalytic efficiency of these mutants is not increased relative to the Quad 3 control. In fact, the $k_{cat}/K_{m(DHF)}$ values are actually decreased ~ 2 fold. We were, therefore, unable to engineer a more efficient enzyme lacking substrate and cofactor inhibition with this series of asymmetric mutants.

One issue associated with the Q67H asymmetric mutants is the location of Q67 residues in the center of the active site pore (*1*). These residues form the "ceiling" and "floor" of the pore as they form hydrogen bonds with their symmetry related residues across the dimer-dimer interface of the enzyme (*2*). We, therefore, proposed that introduction of histidine residues asymmetrically at these locations may affect local packing interactions as the hydrogen bonding network may be disrupted when one histidine is introduced along the dimer-dimer interface (i.e. in the Q67H: 1+3 mutant) (*1*). This problem diminishes when the mutated residues occur further from the center of symmetry. As shown in Figure 1, symmetry related tyrosine 69 residues occur further

Table 1. Comparison of catalytic efficiencies for Q67H, Y69F, and K32M asymmetric mutants of Quad 3 DHFR.

Complex	$k_{cat}/K_{m(NADPH)}$ ($s^{-1}M^{-1}$)	$k_{cat}/K_{m(DHF)}$ ($s^{-1}M^{-1}$)
Quad3 DHFR[a]	$1.8*10^5$	$1.2*10^5$
Q67H: 1 DHFR[b]	$1.8*10^5$	$6.0*10^4$
Q67H: 1+2 DHFR[b]	$7.5*10^5$	$6.0*10^4$
Q67H: 1+3 DHFR[b]	$1.3*10^5$	$2.0*10^4$
Q67H: 1+4 DHFR[b]	$1.6*10^5$	$6.0*10^4$
Q67H: 1+2+3 DHFR[b]	$2.0*10^5$	$1.0*10^4$
Q67H: 1+2+3+4 DHFR[b]	$3.8*10^6$	$7.7*10^5$
Y69F: 1 DHFR[c]	$1.5*10^5$	$5.0*10^4$
Y69F: 1+2 DHFR[c]	$7.0*10^4$	$5.0*10^4$
Y69F: 1+3 DHFR[c]	$1.8*10^5$	$3.0*10^4$
Y69F: 1+4 DHFR[c]	$1.4*10^5$	$7.0*10^4$
Y69F: 1+2+3 DHFR[c]	$7.0*10^4$	$4.0*10^4$
Y69F: 1+2+3+4 DHFR[c]	$4.0*10^4$	$3.0*10^4$
K32M: 1 DHFR[a]	$1.6*10^5$	$9.0*10^4$
K32M: 1+2 DHFR[a]	$1.0*10^4$	$7.0*10^4$
K32M: 1+3 DHFR[a]	$2.0*10^4$	$1.0*10^4$
K32M: 1+4 DHFR[a]	$2.0*10^4$	$1.0*10^4$

[a] Taken from (Hicks et al., manuscript in preparation).
[b] Taken from (*1*).
[c] Taken from (Stinnett et al., manuscript in preparation).

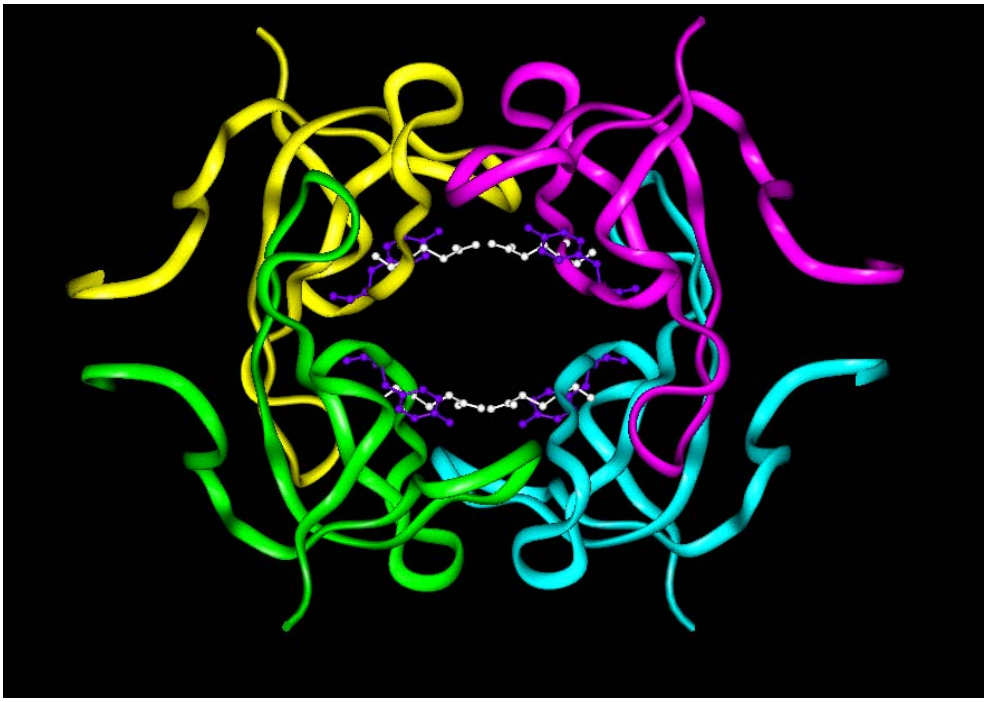

Figure 1. Ribbon diagram of R67 DHFR (protein data bank 1VIE) with Y69 residues shown as purple balls-and-sticks, while Q67 residues are shown as white balls-and-sticks. Monomer 1 is green, while monomers 2, 3, and 4 are yellow, pink, and cyan, respectively.

from the center of symmetry than symmetry related glutamine 67 residues. The tyrosine 69 residues are also sufficiently separated that they are unable to hydrogen bond with their symmetry related partners (*2, 6*). In addition, the k_{cat} for the Y69F R67 DHFR mutant is increased ~2 fold in respect to the wild-type enzyme while the $K_{m(NADPH)}$ and $K_{m(DHF)}$ values are increased ~15 and ~10 fold, respectively (*6*). It was, therefore, possible that a more efficient enzyme could be generated in the Y69F asymmetric mutant series where the k_{cat} for the reaction is increased but the K_m values are unaffected.

Catalytic efficiencies for each of the Y69F asymmetric mutants are outlined in Table 1. None of the k_{cat}/K_m values for these mutants is increased relative to the Quad 3 control. In fact, in most cases, these mutants are less efficient than the Quad 3 control. This is likely due to the disparate effects of the mutations on both the k_{cat} and K_m values. For example, the Y69F: 1 and Y69F: 1+3 mutants are the only mutants where the $K_{m(NADPH)}$ values are unaffected. However, for these mutants, the k_{cat} values are also affected minimally (Stinnett et al., manuscript in preparation). Hence, the $k_{cat}/K_{m(NADPH)}$ values for these mutants are similar to the Quad 3 control. In addition, the $K_{m(DHF)}$ values for the remainder of the asymmetric Y69F mutants are weakened in respect to the Quad 3 control, thus resulting in lower $k_{cat}/K_{m(DHF)}$ values (Stinnett et al., manuscript in preparation). Although it was proposed that a more efficient enzyme could be generated where the K_m values were unaffected and the k_{cat} values were increased, for the Y69F asymmetric mutant series, an increase in k_{cat} was observed only when K_m values were also increased (Stinnett et al., manuscript in preparation). Therefore, none of the Y69F asymmetric mutants were more efficient enzymes than the Quad 3 control.

Asymmetric mutants of symmetry related K32 residues have also been generated and analyzed (Hicks et al., manuscript in preparation). Similar to Y69, K32 residues are also located further away from the center of symmetry of the active site (*2*). In contrast to Y69, however, mutation of K32 residues to methionine residues in the homotetrameric enzyme results in a dimeric form of the enzyme (*7*). Since docking studies suggest that these residues interact with both ligands of R67 DHFR (*8*), an alternate approach involving salt effects was employed to determine the role of these residues in ligand binding and catalysis (*7*).

Lysine residues, being positively charged in water at pH values around neutrality, are capable of forming ionic contacts with negatively charged ligands which include the ligands for DHFR. Therefore, it is possible for lysine 32 residues to interact with both NADPH and DHF electrostatically. Since mutagenesis of K32 residues to non-polar methionine residues affects the stability of the enzyme, the interactions between K32 residues and the ligands were evaluated by adding increasing concentrations of salt into the reaction solution. From these studies, it was determined that symmetry related K32 residues are involved in interactions with both NADPH and DHF (*7*).

Similar to studies of Y69F R67 DHFR, disruption of electrostatic interactions between symmetry related K32 residues and the substrate and cofactor yields an increased rate of catalysis for the reaction while resulting in weaker K_m values for both ligands (*7*). Therefore, generation of a more efficient enzyme could again be possible by building asymmetric K32M mutants where the K_m values are minimally perturbed but k_{cat} is increased. In addition, it was proposed that adding only one or two K32M mutations to the enzyme would be less destabilizing than adding all four mutations to the enzyme (as

occurs in K32M R67 DHFR). Therefore, the following K32M asymmetric mutants were generated and analyzed: K32M: 1, K32M: 1+2, K32M: 1+3, and K32M: 1+4 (Hicks et al., manuscript in preparation).

The catalytic efficiencies of each of the K32M asymmetric mutants are shown in Table 1. The k_{cat}/K_m values for the K32M: 1 mutant are similar to Quad 3 as would be expected since the k_{cat} and K_m values are affected minimally in this mutant (Hicks et al., manuscript in preparation). Each of the k_{cat}/K_m values for the double mutants is decreased with respect to Quad 3. However, the cause of this decrease differs for the K32M: 1+2 and K32M: 1+4 mutants as compared to the K32M: 1+3 mutant. For the K32M: 1+2 and K32M: 1+4 mutants, the decrease in k_{cat}/K_m values is largely related to the effect of these mutations on k_{cat} (Hicks et al., manuscript in preparation). For both mutants, the rate of the reaction is slower, while the K_m values are either not affected or are increased no more than four-fold (Hicks et al., manuscript in preparation). These effects combine to yield decreases in k_{cat}/K_m. In contrast, the rate of catalysis for the K32M: 1+3 mutant is increased ~ 4.5 fold. However, the K_m values for NADPH and DHF are increased ~ 35 fold and ~50 fold, respectively. Although an increase in k_{cat} is observed, greater increases in the K_m values result in decreases in k_{cat}/K_m. Again, in no K32M asymmetric mutant was the catalytic efficiency increased as none of the mutations resulted in increasing k_{cat} values with minimal effects on K_m (Hicks et al., manuscript in preparation).

Interestingly, none of our mutagenesis strategies, including mutations in the homotetramer and asymmetric mutations, has generated a more efficient enzyme that does not also yield substrate and cofactor inhibition. Is it possible that this enzyme is

optimized for the greatest possible efficiency without substrate and cofactor inhibition? While this possibility exists, we have yet to test the effects of generating asymmetric mutants which contain different amino acid mutations such as asymmetric mutants containing both Q67H and Y69F or Q67H and K32M mutations.

Why generate mutants with both Q67H and Y69F or K32M asymmetric mutations? Q67H asymmetric mutations result in decreases in K_m values and k_{cat} values (*1*), while certain Y69F asymmetric mutations result in increases in K_m and k_{cat} values (Stinnett et al., manuscript in preparation) as does the K32M: 1+3 mutant (Hicks et al., manuscript in preparation). It is therefore possible that building an asymmetric mutant containing both Q67H and Y69F or K32M mutations may result in decreased K_m values and an increase in k_{cat} values yielding a more efficient enzyme.

Of the possible Y69F/Q67H asymmetric mutant combinations, which combination would likely result in the most efficient enzyme which is not inhibited at high concentrations of substrate and cofactor? In order to approach this question, it is first necessary to understand which mutations result in tighter K_m values and which facilitate k_{cat}. A single Q67H mutation results in an ~ 4 fold decrease in k_{cat} with little affect on the K_m values. This effect may be related to disruption of hydrogen bonding interactions between symmetry-related Q67 residues which could affect local packing interactions (*1*). To minimize this possibility, both glutamine residues along one dimer-dimer interface should be mutated to histidine residues. This occurs in the Q67H: 1+4 mutant. For this mutant, the $K_{m(NADPH)}$ is ~4.5 fold tighter than the Quad 3 control while the $K_{m(DHF)}$ is only ~ 2.5 fold tighter than the Quad 3 control. In addition, no noticeable DHF or NADPH inhibition is observed for this mutant making it an ideal template on

which to add Y69F mutations (*1*). Of the Y69F double mutants, only one results in a noticeable increase in k_{cat} for the reaction, the Y69F: 1+4 mutant. This mutant contains two Y69F mutations, both located along the "floor" of the active site. It was therefore proposed that mutation of two Y69 residues along the dimer-dimer interface may facilitate transition state binding (Stinnett et al., manuscript in preparation). The $K_{m(NADPH)}$ and $K_{m(DHF)}$ values for this mutant are increased ~2.5 fold and ~ 4 fold, respectively, while the k_{cat} is increased ~ 2 fold (Stinnett et al., manuscript in preparation). Based on this information, we propose that the combination of Y69F: 1+4/Q67H: 1+4 mutations may result in a more efficient enzyme (compared to the Quad 3 control) as the Q67H mutations will drive tighter binding and the Y69F mutations will facilitate catalysis. We also expect that this mutant will not be inhibited at high concentrations of substrate and cofactor as the Q67H: 1+4 mutation and the Y69F: 1+4 mutation do not cause noticeable DHF and NADPH inhibition ((*1*), Stinnett et al., manuscript in preparation).

What K32M/Q67H asymmetric combinations may increase catalytic efficiency? In this case, we propose use of the Q67H: 1+2+3+4 mutant as a template as the $K_{m(NADPH)}$ and $K_{m(DHF)}$ values for this mutant are ~ 170 and ~ 50 fold tighter, respectively, than those of the Quad 3 control (*1*). Of the possible K32M asymmetric mutants, we propose addition of K32M mutations to domains 1 and 3 of the Q67H: 1+2+3+4 template. These mutations are chosen as they include the only K32M asymmetric mutations which result in an increase in k_{cat} for the reaction (Hicks et al., manuscript in preparation). For the Q67H: 1+2+3+4/K32M: 1+3 mutant, we expect that NADPH will bind first to the enzyme and its nicotinamide ring will interact with the Q67H residues along either the

"floor" or "ceiling" of the active site. The tail of NADPH will interact with wild-type K32 residues (in domains 2 and 4) on one half of the enzyme. DHF will bind following NADPH and interact with both the nicotiname ring (through interligand contacts) and the residues available on the opposite side of the pore, specifically with the Q67H residues located on the "floor" or "ceiling" (which are not tied up forming contacts with NADPH). The k_{cat} for the reaction will be increased as these studies suggest that a K32 interaction with DHF must be disrupted to approach the transition state, and this requirement is fulfilled in the K32M: 1+3 mutant where no wild-type K32 residues are available to interact with DHF (Hicks et al., manuscript in preparation). Therefore, we propose that generation of a Q67H: 1+2+3+4/K32M: 1+3 mutant may yield an increase in catalytic efficiency as the Q67H mutations will drive tight binding through ring stacking interactions while the K32M mutations will facilitate catalysis. Some inhibition, however, is possible in this construct as noticeable inhibition is observed for the Q67H: 1+2+3+4 mutant (*1, 5*).

Ligand Specificity

In addition to attempts at generating a more efficient enzyme, another goal of building asymmetric mutants is to engineer specificity into the active site such that NADPH and DHF each bind at a specific location rather than having the option of interacting at four positions (*1*). Steady-state kinetic analyses of certain Y69F (Stinnett et al., manuscript in preparation) and K32M (Hicks et al., manuscript submitted) asymmetric mutants suggest that this has been accomplished for NADPH. For the Y69F: 1 and Y69F: 1+3 mutants, a wild-type $K_{m(NADPH)}$ value is observed while a weaker $K_{m(DHF)}$ occurs (Stinnett et al., manuscript in preparation). In addition, the $K_{d(NADPH)}$ for

the K32M: 1 and K32M: 1+3 mutants is affected to a lesser extent by the mutations than the K32M: 1+2 and K32M: 1+4 mutants (Hicks et al., manuscript in preparation). These data suggest that NADPH interacts first with the enzyme preferentially forming contacts with the wild-type side of the pore. DHF then interacts with the residues available on the other side of the pore (Stinnett et al., manuscript in preparation, Hicks et al., manuscript in preparation). This is supported by the Q67H asymmetric mutant studies. In these studies, four Q67H mutations were necessary to yield a greater than 3 fold decrease in the $K_{m(DHF)}$ value (*1*).

Although evidence suggests that NADPH binding specificity has been engineered into the enzyme through generation of certain asymmetric Y69F and K32M mutants, DHF specificity has not been achieved as DHF interacts with the site available following NAPDH binding. Weaker $K_{m(DHF)}$ values have therefore been observed as DHF is required to interact with a least one mutant residue on the opposite side of the active site pore (Stinnett et al., manuscript in preparation, Hicks et al., manuscript in preparation). How then can DHF specificity be engineered into R67 DHFR? Can we "rescue" DHF binding by engineering the opposite side of the pore with residues that will drive DHF binding.

One possible means to generate DHF specificity is to again build asymmetric mutants which contain mutations of different amino acid residues such as K32 and Y69. Structural based studies, including NMR and x-ray crystallography, as well as docking studies, predict mobility of the glutamic acid tail of DHF/folate (*2, 8, 9*). In addition, studies involving asymmetric K32M (Hicks et al., manuscript in preparation) and Y69F (Stinnett et al., manuscript in preparation) mutants suggest that interactions between these

residues on one side of the pore are weak allowing mobility of the tail between both domains. One means to provide greater specificity for DHF would therefore be to provide additional contacts for the DHF tail on a single domain of one half of the active site limiting mobility of the tail region. Several studies also suggest that NADPH may participate in DHF binding through interligand interactions (*9, 10*). Thus, optimal DHF binding would be provided by tight binding of the nicotinamide ring of NADPH which, through interligand interactions, may tighten DHF binding. In addition, specificity for DHF binding may be generated by providing additional contacts to the tail of DHF.

What asymmetric mutations could tighten NADPH binding and through interligand contacts tighten DHF binding while providing contacts with the tail of DHF to limit its mobility? The Q67H: 1+4 mutant provides a tighter binding site for NADPH which likely tightens DHF binding through interligand interactions (*1*). Therefore, this mutant may provide a template for addition of other mutations to provide specificity for DHF (*1*). Additional mutations must be built into this construct which preferentially provide contacts with the tail of DHF in contrast to the tail of NADPH. Mutation of a Y69 residue to a lysine residue may provide such a contact. Docking studies suggest that a hydrogen bond may form between the hydroxyl group of tyrosine 69 in domain 4 and the glutamate tail of DHF (*8*) which could, in theory, be replaced by ionic interactions between a lysine residue and the glutamate tail. However, most contacts proposed between Y69 and NADPH are through the ring edge of tyrosine (*8*). Mutation of the residue to lysine would result in disruption of these interactions. Therefore, a Q67H: 1+4/Y69K: 4 mutant could provide tight binding of NADPH through ring stacking interactions between the histidine residues and the nicotinamide ring. Interligand

interactions between NADPH and DHF would facilitate DHF binding. In addition, the tail of DHF should interact preferentially with the Y69K residue in domain 4 thereby limiting its mobility and rendering greater affinity. The tail of NADPH would be disfavored from interacting with this residue as it lacks the ring edge dipolar contacts provided by the tyrosine residue (Stinnett et al., manuscript in preparation).

Selection of the Productive Ternary Complex

Another aspect of ligand binding in R67 DHFR that has become apparent through studies of these asymmetric mutants is the ability or inability of certain mutants to select for the productive ternary complex over the non-productive 2NADPH/2DHF binding modes. Of the asymmetric mutants that have been analyzed, one series of mutants is particularly limited in its ability to select for the productive ternary complex, the Q67H series (*1*). While moderate to severe substrate and/or cofactor inhibition is observed for most of the Q67H asymmetric mutants (*1*), no DHF and/or NADPH inhibition has been observed for any of the other asymmetric mutants (Stinnett et al., manuscript in preparation, Hicks et al., manuscript in preparation). What characteristics of these mutants render them unable to select for the productive ternary complex?

In contrast to Y69 and K32, Q67 residues are located in the center of the active site pore (*2*) allowing them to form contacts with the pteridine ring of DHF (*2*) and the nicotinamide ring of NADPH (*9*) which are also proposed to interact in the pore's center. Mutation of these residues to histidine residues tightens binding for each ligand of R67 DHFR (*1, 5*). It has been suggested that this increase in binding affinity is related to stacking interactions between the rings of symmetry related histidine side chains and both the pteridine and nicotinamide rings (*1, 5*). Structural evidence also suggests that the

NADPH and DHF tails are pointed away from the center of the enzyme's active site. Thus, interligand interactions between DHF and NADPH occur mainly between the pteridine and nicotinamide rings. Q67H mutations increase the binding affinity for both DHF and NADPH (*9*). This increase in binding affinity likely alters the interligand cooperativity patterns between the 2DHF and 2NADPH non-productive binding modes in addition to the interligand interactions between the productive binding mode. Specifically, the productive binding mode has been altered in these mutants as the k_{cat} for the reaction decreases as the number of mutations is increased. This suggests that the nicotinamide and/or pteridine ring orientations are altered to some extent in these mutants as a result of ring stacking interactions. As the rings must be juxtaposed in an optimal orientation for hydride transfer, it is likely that interactions with the histidine residues alter this juxtaposition (*1*). It has been proposed that the nicotinamide and pteridine rings of R67 DHF are likely oriented in an *endo* conformation in the transition state (*9*). These ring stacking interactions likely hinder formation of the *endo* transition state thus causing a decrease in the k_{cat} for the reaction (*1*).

What prevents Y69 and K32 mutations from displaying substrate and/or cofactor inhibition? First, no such inhibition is observed in the wild-type enzyme (*4*). Second, mutations of both of these residues weaken rather than tighten interactions with NADPH and DHF ((*11*), Stinnett et al., manuscript in preparation, Hicks et al., manuscript in preparation). Third, these residues are located less near the center of the active site (*2*) and as such primarily interact with the tail regions of NADPH and DHF (*8*). As interligand interactions occur mainly between the pteridine and nicotinamide rings (*9*),

Y69 and K32 residues have only an indirect affect on these interactions as they form contacts with only the tail regions of the molecules (*8*).

Quad 3 as a Template for Understanding Ligand Binding and Catalysis in R67 DHFR

The Quad 3 construct has proved valuable in gaining insight into ligand binding and catalysis in R67 DHFR. With this construct, we have been able to control the number and location of specific mutations within the active site and determine the effects of these mutations (*1*). Analyses of the asymmetric Y69F and K32M mutants have provided support for a model in which residues on one side of the pore, consisting of 2 domains (or monomers in the wild-type enzyme), form contacts with NADPH (Stinnett et al., manuscript in preparation, Hicks et al., manuscript in preparation). In addition, results from the Y69F, K32M, and Q67H asymmetric mutant studies support a model (*10*) in which catalysis follows a preferred pathway where NADPH interacts with the enzyme first allowing it to form contacts with the tightest binding site available and allowing DHF bind to the enzyme-NADPH complex. These studies have also pointed to the importance of interligand interactions in DHF binding (Stinnett et al., manuscript in preparation, Hicks et al., manuscript in preparation, (*1*)). Finally, the Q67H: 1+4 mutant will likely prove valuable as a template for engineering asymmetric mutations as its binding affinity towards NADPH is increased in the absence of noticeable DHF and/or NADPH inhibition (*1*).

R67 DHFR as a Template for "Evolving" an Enzyme Active Site

Our goal in these research projects has been to determine the mechanisms of ligand binding and catalysis in R67 DHFR. Our approach has therefore been to perform site-directed mutagenesis studies that will provide a better understanding of the R67

DHFR catalyzed reaction. However, these studies have largely focused on understanding the R67 DHFR reaction and its mechanisms involved in catalysis. How, then, can we broaden the scope of our research to gain a better understanding of enzyme catalysis in general using R67 DHFR as a template?

Based on the understanding we have gained regarding the R67 DHFR catalyzed reaction using several biochemical and biophysical approaches, we propose R67 DHFR as an ideal template for "evolving" or modifying an enzyme's active site. Penning and Jez (*12*) review the methodologies commonly used to modify or alter enzyme active sites. In general, there are two approaches to this objective. The first, enzyme redesign, is also referred to as a "rational" approach as specific mutations are generated in the enzyme active site which are expected to yield predicted results. For redesigning an active site, structural information is critical in order to be able to predict the effects of specific mutations. Two different types of redesign are common, site-directed mutagenesis and domain switching. In the former, single amino acid residues are mutated while in the latter, an entire domain of the enzyme is changed. The second approach, directed evolution, is "irrational" as random mutants of the active sites are generated and selected on the basis of their having a particular characteristic or function. In contrast to enzyme redesign, directed evolution does not require extensive structural information since mutations are added randomly. One common means of directed evolution is phage display.

Penning and Jez (*12*) review the use of enzyme redesign and directed evolution to approach five questions involving ligand binding and catalysis which include the following. (1) Can an enzyme's preference for substrate be changed with minimal effects

on catalytic efficiency using the same mechanism? (2) Can an enzyme be designed to recognize a cofactor other than its natural cofactor? (3) Can the stereochemistry of an enzyme's ligands be altered? (4) Can an enzyme catalyze a reaction other than its natural reaction? (5) Can a *protein* be engineered such that it is able to catalyze a reaction? Our discussion will focus on answering three of the questions using R67 DHFR as question 3 is not straightforward without additional structural information and question 5 is not applicable. For the purposes of this dissertation, we will focus only on redesign.

The first question that can be approached by enzyme redesign involves modification of an enzyme's active site in order to accommodate different substrates (*12*). This has been accomplished for lactate dehydrogenase where specificity for oxaloacetic acid over pyruvate is achieved. In these studies, the active site was "redesigned" by first comparing the crystal structures for malate and lactate dehydrogenases in order to predict residues in the substrate binding site of lactate dehydrogenase that should be mutated for selection of oxaloacetic acid. From these predictions, three single mutants of lactate dehydrogenase were generated, including mutations of Q102, D197, and T246 to arginine, asparagine, and glycine, respectively. For each single mutant, the catalytic efficiency for the alternative ligand, oxaloacetic acid, was increased. It should be noted that lactate dehydrogenase is capable of using oxaloacetic acid as a substrate; however, the catalytic efficiency for oxaloacetic acid is 1000 fold less than that for pyruvate. Hence, the active site of lactate dehydrogenase was "evolved" to recognize oxaloacetic acid as a substrate over pyruvate (*12, 13*).

Can R67 DHFR be modified such that it recognizes an alternate substrate and catalyzes its reduction? As a first approach to this objective, Howell and Chopra

(unpublished data) focused on the PTR1 catalyzed reaction. PTR1 catalyzes the reduction of biopterin to dihydrobiopterin and dihydrobiopterin to tetrahydrobiopterin (*14-16*). Interestingly, however, the enzyme is also capable of reducing folate to dihydrofolate and dihydrofolate to tetrahydrofolate (*14-16*). In fact, the enzyme is proposed to be the cause of unsuccessful attempts at inhibiting DHFR using anti-folate drugs in clinical settings as the enzyme is able to catalyze the same reaction as DHFR without being inhibited by anti-folate inhibitors (*17-19*).

Comparisons of the PTR1 structure to that of R67 DHFR by Howell and Chopra yielded interesting results. First, both enzymes are active as homotetramers possessing 222 symmetry (*2, 14*). Similar to the model proposed for R67 DHFR (*1, 9, 10*), NADPH comprises a major portion of the substrate binding site for PTR1 (*14*). In fact, co-crystals of the complex PTR1-NADPH-MTX (methotrexate, a folate analog) indicate that "interactions between MTX and PTR1-NADPH occur principally at the pterin end of the drug and involve direct hydrogen bonds with the cofactor" (*14*). This compares to NMR and X-ray crystallography studies for R67 DHFR which suggest that the rings of NADPH and DHF interact in the pore's center (*2, 9*). In contrast to R67 DHFR, however, two active sites are present in PTR1(*14*).

Based on the similarities between PTR1 and R67 DHFR and their substrates, Howell and Chopra asked the following question. Is it possible to redesign R67 DHFR to catalyze the reduction of dihydrobiopterin using NADPH as its cofactor? Preliminary experiments, performed by S. Chopra using the Quad 3 construct, suggest that R67 DHFR can catalyze the reduction of dihydrobiopterin without the addition of point mutations. Although this alternate activity is at present rather inefficient, point mutations

may be added to increase the efficiency of the reaction as was observed for the lactate dehydrogenase reaction (*13*). The "hot spot" binding site of R67 DHFR (*8*) may be particularly suited for optimizing recognition of alternative ligands.

Another question that can be addressed by enzyme redesign involves modification of the enzyme's preference for cofactor, specifically NADPH for NADH (*12*). Again, this objective is greatly facilitated by structural information (*12*) and has been accomplished for glutathione reductase (*20*). This enzyme recognizes NADPH as a cofactor. Comparisons of glutathione reductase from two organisms indicated similar contacts between the two enzymes and NADPH. Following addition of seven point mutations, preference for binding the alternate cofactor, NADH, was increased ~18000 fold with respect to NADPH binding. In these experiments, researchers generated mutations that would not only disfavor recognition of NADPH but would also favor recognition of NADH (*12, 20*).

Can cofactor preference for R67 DHFR be modified? R67 DHFR uses NADPH as a cofactor but can also catalyze the conversion of DHF to THF when NADH is supplied as the cofactor although the k_{cat}/K_m values for NAD(P)H and DHF are decreased ~ 50 fold and ~ 18 fold respectively when NADH is added as the cofactor (*7*). Since R67 can use NADH as a cofactor, albeit inefficiently, we propose that the active site of R67 DHFR may be "evolved" to select for NADH rather than NADPH.

Salt studies on R67 DHFR suggest that K32 may be involved in an electrostatic contact with the 2′ phosphate of NADPH. This interaction is likely involved in selection of NADPH over NADH (*7*). Therefore, to alter the cofactor preference of R67 DHFR, it would be necessary to mutate K32 to a residue not capable of forming such interactions

with the 2′ phosphate. As has been demonstrated previously, this solution is complicated by the symmetry of R67 DHFR in that mutation of each of the four K32 residues yields an inactive dimer (*7*). In addition, generation of asymmetric K32M mutants still provides at least one wild-type K32 residue with which the cofactor may interact depending on the location of the mutations (Hicks et al., manuscript in preparation). Therefore, to accomplish this goal it may be necessary to engineer the active site pore such that NADPH recognizes only one side of the pore. Specifically, mutation of residues other than K32 on one side of the pore may be necessary in order to drive DHF binding to that side of the pore and NADPH binding to the opposite side of the pore. Asymmetric mutagenesis of K32 residues only on the side of the pore with which NADPH would interact would then decrease the affinity of NADPH for the enzyme.

Although it may be possible to decrease the affinity of NADPH through mutagenesis of specific K32 residues, in order to alter cofactor preference, it is necessary to simultaneously increase affinity for NADH. Penning and Jez (*12*) maintain that "in nearly all cases elimination or introduction of basic residues that interact with the 2′-phosphate of AMP of NADP(H) often in combination with additional mutations leads to successful conversion of cofactor preference" (*12*). However, choosing the "additional mutations" for R67 DHFR where limited structural information defining cofactor interactions is available is complex.

Docking studies suggest that, in addition to K32, Y69 may also play a role in providing contacts for the adenine ribose. Specifically, the ring edge of Y69 is predicted to form contacts with one of the phosphate oxygens of the adenine ribose (*8*). Mutagenesis studies suggest that this interaction may be a charge-dipole interaction that

is decreased by mutagenesis of the tyrosine to phenylalanine (Stinnett et al., manuscript in preparation). Could mutation of a Y69 residue(s) to a residue(s) capable of accepting a hydrogen bond facilitate selection for NADH over NADPH? Again, this mutagenesis strategy is complicated by the symmetry of the enzyme. Prior to mutating Y69 residues, it is likely necessary that additional residues be mutated such that one side of the pore prefers NADPH and the opposite side of the pore prefers DHF. Both Y69 residues on the side of the pore selecting NADPH could then be mutated to residues capable of accepting a hydrogen bond. Since the contact is between the ring edge of tyrosine 69 and the adenine ribose, a smaller hydrogen bond acceptor such as threonine may be capable of interacting with the 2′ hydroxyl group of NADH while disfavoring interactions with the 2′-phosphate of NADPH. As threonine has a smaller van der Waals volume than tyrosine, it is however possible that these mutations may disrupt packing interactions. Additional (or other) mutations may be engineered to select for NADH as more structural information regarding NADPH binding is obtained using NMR.

A final question that may be approached using redesign of R67 DHFR is modifying the enzyme to catalyze other reactions (*12*). One means by which to accomplish this is by "unmasking" additional activities catalyzed by the enzyme. It has been suggested that several enzymes are capable of catalyzing other reactions. However, the efficiency with which they do so is beyond that which is physiologically relevant (*12, 21*). When these alternate activities are observed, mutations can be engineered into the enzyme that promote catalysis of an alternate reaction (*12*). This has been accomplished for the adenine glycosylase, MutY. Mutation of a single serine residue in this enzyme to a lysine provides the enzyme with both glycosylase and lyase activities (*12, 22*).

Can R67 DHFR be redesigned to catalyze alternate reactions? Interestingly, NMR studies performed to gain a better understanding of NADPH interactions in the active site revealed two additional activities catalyzed by the enzyme, a phosphatase activity and a transhydrogenase activity (*23*). The first activity was observed as the time dependent appearance two resonances in the downfield portion of the NMR spectrum when $NADP^+$ was incubated with the enzyme. These resonances were most consistent with those of NAD^+ suggesting a possible phosphatase activity for R67 DHFR. In addition, chemical shift data also suggest that R67 DHFR is able to catalyze the transfer of a hydride ion from NADPH to an analog of $NADP^+$, $ADADP^+$ (3-acetylpyridine adenine dinucleotide phosphate). The authors propose that K32 is involved in the former reaction but do not propose residues for involvement in the latter (*23*). Without more structural information regarding the contacts between the ligands and the active site, proposing mutagenesis studies to redesign R67 DHFR to better catalyze these activities is not straightforward. However, as more structural evidence is obtained via x-ray crystallography and NMR, the ability to redesign R67 DHFR to better catalyze these reactions is feasible.

Due to its "hot spot" binding site (*8*), ability to use NADH as a cofactor (*7*), and ability to catalyze alternative reactions (*23*), we propose R67 DHFR as an ideal enzyme for redesign of an active site. This is supported by evidence from Matsumura and Ellington (*24*) who observed a "non-specific intermediate" with "broadened specificity" during their attempts to change the activity of the enzyme, beta-glucuronidase. However, successive rounds of mutagenesis and selection yielded an enzyme with specificity for the alternate ligand (*24*). Based on the characteristics of R67 DHFR, it may be possible

to envision the enzyme as a type of "non-specific intermediate" in that it employs a "hot spot" binding mechanism (*8*) and can use NADH as a cofactor (*7*). Therefore, with the appropriate mutagenesis strategies, it may be possible to alter the properties of R67 DHFR such that it is able to recognize alternate ligands and catalyze other reactions.

How will these studies be important to the field of enzymology? First, they will provide a greater understanding of the means by which enzymes catalyze reactions. Specifically, they will provide more information regarding the types of scaffolds that are necessary for recognition of alternate substrates and catalysis of new reactions. In addition, these experiments are important from a pharmaceutical and industrial perspective as enzymes are redesigned to catalyze novel reactions (*12*).

References

1. Smiley, R. D., Stinnett, L. G., Saxton, A. M., and Howell, E. E. (2002) *Biochemistry 41*, 15664-75.
2. Narayana, N., Matthews, D. A., Howell, E. E., and Nguyen-huu, X. (1995) *Nat Struct Biol 2*, 1018-25.
3. Fersht, A. (1999) *Structure and Mechanism in Protein Science*, W.H. Freeman and Company, New York.
4. Reece, L. J., Nichols, R., Ogden, R. C., and Howell, E. E. (1991) *Biochemistry 30*, 10895-904.
5. Park, H., Bradrick, T. D., and Howell, E. E. (1997) *Protein Eng 10*, 1415-24.
6. Strader, M. B., Smiley, R. D., Stinnett, L. G., VerBerkmoes, N. C., and Howell, E. E. (2001) *Biochemistry 40*, 11344-52.
7. Hicks, S. N., Smiley, R. D., Hamilton, J. B., and Howell, E. E. (2003) *Biochemistry 42*, 10569-78.
8. Howell, E. E., Shukla, U., Hicks, S. N., Smiley, R. D., Kuhn, L. A., and Zavodszky, M. I. (2001) *J Comput Aided Mol Des 15*, 1035-52.
9. Li, D., Levy, L. A., Gabel, S. A., Lebetkin, M. S., DeRose, E. F., Wall, M. J., Howell, E. E., and London, R. E. (2001) *Biochemistry 40*, 4242-52.
10. Bradrick, T. D., Beechem, J. M., and Howell, E. E. (1996) *Biochemistry 35*, 11414-24.
11. Strader, M. B., Stinnett, L. G., Hicks, S. N., Smiley, R. D., and Howell, E. E. (2003) in *18th Annual Enzyme Mechanisms Conference*, Galveston Island, TX.
12. Penning, T. M., and Jez, J. M. (2001) *Chem Rev 101*, 3027-3046.

13. Wilks, H. M., Hart, K. W., Feeney, R.,. Dunn, C. R., Muirhead, H., Chia, W. M., Barstow, D. A., Atkinson, T., Clarke, A. R., and Holbrok, J. J. (1988) *Science 242*, 1541-4.

14. Gourley, D. G., Schuttelkopf, A. W., Leonard, G. A., Luba, J., Hardy, L. W., Beverley, S. M., and Hunter, W. N. (2001) *Nat Struct Biol 8*, 521-5.

15. Nare, B., Hardy, L. W., and Beverley, S. M. (1997) *J Biol Chem 272*, 13883-91.

16. Papadopoulou, B., Roy, G., and Ouelette, M. (1992) *Embo J 11*, 3601-3608.

17. Nare, B., Luba, J., Hardy, L. W., and Beverley, S. (1997) *Parasitology 114 Suppl*, S101-10.

18. Hardy, L. W., Matthews, W., Nare, B., and Beverley, S. M. (1997) *Exp Parasitol 87*, 158-70.

19. Luba, J., Nare, B., Liang, P., Anderson, K. S., Beverley, S. M., and Hardy, L. W. (1998) *Biochemistry 37*, 4093-4104.

20. Scrutton, N. S., Berry, A., and Perham, R. N. (1990) *Nature 343*, 38-43.

21. Jensen, T. A. (1976) *Annu Rev Microbiol 30*, 409-25.

22. Williams, S. D., and David, S. S. (2000) *Biochemsitry 39*, 10098-109.

23. Pitcher, W. H., 3rd, DeRose, E. F., Mueller, G. A., Howell, E. E., and London, R. E. (2003) *Biochemistry 42*, 11150-60.

24. Matsumura, I., and Ellington, A. D. (2001) *J Mol Biol 305*, 331-339.

Vita

Lori Gail Stinnett was born on December 4, 1976 in Knoxville, Tennessee. She graduated from Sevier County High School in 1995. She received her B.A. degree from Maryville College where she majored in biology and minored in chemistry. Following college, she continued her education at the University of Tennessee at Knoxville in the Biochemistry and Cellular and Molecular Biology Department. Her graduate research training is as a protein chemist. After receiving her Ph.D. in May, 2004, she plans to continue her career as a scientist by working as a postdoctoral fellow at the University of North Carolina at Chapel Hill in the Nutrition department. Lori's long-term goal is to teach biochemistry at a small liberal arts college.